Moisture Response of Wall Assemblies of Cross-Laminated Timber Construction in Cold Canadian Climates

by

Robert T.M. Lepage

A thesis

presented to the University of Waterloo

in fulfilment of the

thesis requirement for the degree of

Master of Applied Science

in

Civil Engineering

Waterloo, Ontario, Canada, 2012

Author's Declaration

I hereby declare that I am the sole author of this thesis. This is a true copy of the thesis, including any required final revisions, as accepted by my examiners.

I understand that my thesis may be made electronically available to the public.

Robert T.M. Lepage

Abstract

Wood is a highly versatile renewable material (with carbon sequestering properties), that is light in weight, has good strength properties in both tension and compression while providing good rigidity and toughness, and good insulating properties (relative to typical structural materials). Engineered wood products combine the benefits of wood with engineering knowledge to create optimized structural elements. Cross-laminated timber (CLT), as one such engineered wood product, is an emerging engineering material which provides great opportunities for the building industry.

While building with wood has many benefits, there are also some concerns, particularly decay. Should wood be exposed to elevated amounts of moisture, rots and moulds may damage the product or even risk the health of the occupants. As CLT panels are a relatively new engineered wood product, the moisture characteristics have yet to be properly assessed. Consequently, the amount of decay risk for CLT in building applications is unknown, and recommended protective actions during design construction and operation have yet to be determined.

The goal of this research was to determine the moisture durability of CLT panels in wall assemblies and address concerns related to built-in construction moisture. The approach used to address the problem was to first determine select moisture properties of CLT panels through experimental approaches, and then use the results to calibrate a hygrothermal model to quantify the risks of wall assemblies. The wall assemblies were simulated in six different cities across Canada, representing a range of climates: Vancouver, B.C., Edmonton, A.B., Winnipeg, M.B., Ottawa, O.N., Québec City, Q.C., and St. John, New-Brunswick. The risks associated with moisture exposure during construction are also considered in the simulations.

The experimental phase of the research was limited to moisture uptake tests. These tests were utilized to determine the liquid water absorption coefficient for four different types of full scale panels (2'x2') and 12 clear wood samples. The panels were either made of 5-ply of Western-SPF, Eastern-SPF, Hemlock-Fir, or 3-ply of a generic softwood provided by a European CLT manufacturer; the clear samples were all cut from the same nominal 2x6 SPF-grade lumber. The panels were installed in a drying rack and gravimetrically tracked to assess the drying rates of the panels. Finite resources precluded more thorough material testing, but a parametric study was conducted to determine the relative impact of the missing material data on the final simulation results.

In the hygrothermal simulations, four main wall assembly types were considered- those with either exterior or interior insulation, and those using either vapour permeable or impermeable air-water barriers. Various types of insulation and vapour control were also modelled. The simulations were run for a variety of interior relative humidities. The metric for comparison between the simulations was the water content of a 4mm thin layer on the extreme lamina of a CLT panel system.

The results of the simulation suggest that vapour impermeable membranes, when install on dry CLT panels (less than 14% M.C.) do not pose moisture risks in any of the climates considered. However, when high levels of construction moisture is considered, only vapour permeable membranes controlled moisture risks by allowing the CLT panel to dry both to the interior and to the exterior.

Acknowledgements

Firstly, I am deeply thankful for the guidance from Dr. John Straube. You have been an incredible mentor and not only a great help on the composition of this thesis, but a good guide in revealing to me a deeper understandings of the intricacies and *mysteries* of building science.

I also owe a debt of gratitude to Chris Schumacher for helping with some problem solving, providing industry input, and whose thesis was of tremendous help and guidance. A thanks must also be extended to Jonathan Smegal, who smuggled me some of the weather data files for my hygrothermal simulations.

I also extend my thanks for the help and friendship of Emily Vance, a fellow BEG-er. She helped with managing and running my side-experiments (which were surprisingly fundamental towards the core of my research). Similarly, I owe a great deal of my sanity to the friendship of Luke Yaraskavitch- a fellow commiserator on the stresses and anxiety of research and the writing of a thesis.

Lastly, I'd like to thank my mom and dad for helping me throughout my entire career as a student- without your support, I would not have succeeded to the degree that I have.

Contents

List of Figures

List of Tables

Chapter 1- Introduction

1.1. Introduction

Wood is a material of great importance to mankind. Concerns related to environmental pollution, global warming, and sustainability have led to increased consideration for novel uses of wood as a building material. Wood is a highly versatile material, light in weight that has good strength properties in both tension and compression while providing good rigidity, toughness and insulating properties (Hutcheon & Jenkins, 1963). Furthermore, it is widely available, renewable, low cost and easily worked and shaped. However, as wood is an inhomogeneous, orthotropic, and natural material, its properties vary widely based on the source tree species, growing conditions, etc. Wood is susceptible to decay mechanisms via fungal growth, and its dimensional, thermal, and structural properties vary with temperature and relative humidity. Consequently, the environmental conditions under which wood will or could be exposed during service must be carefully considered such that the desired properties remain within the accepted limits.

Some of the problems and limitations associated with wood can be compensated through processing. Engineered wood products, such as oriented strandboard (OSB), plywood, laminated veneer lumber (LVL), and glue laminated structural members (glulam), attempt to do so by combining wood with adhesives, waxes, and other additives to control dimensional stability and decay resistance while providing increased structural capacities in desired orientations. Cross laminated timber (CLT) panels were designed to provide strong structural capacities in both longitudinal and transverse loading while minimizing dimensional changes due to moisture and temperature changes (FP Innovations, 2011). CLT panels are intended to be used as environmentally conscious substitutes for steel and concrete structural assemblies.

1.2. Objectives

The research in this thesis was part of the research requirements for the multi-disciplinary NSERC strategic research **N**etwork for **E**ngineered **W**ood-based **Build**ing **S**ystems (NEWBuildS). The work, as part of Task Group 4, was related to uncertainty about the moisture durability of CLT when exposed to construction moisture- predominantly from exposure of unprotected CLT panels to precipitation. The objectives for this task group are to quantify the sub-assembly moisture characteristics of the CLT panels and to provide recommendations to resolve the aforementioned problems, if any. However, as the research progressed, it was found that a more holistic approach towards CLT construction was required.

The objectives of this research reported herein are to determine salient moisture transport properties of CLT panels required to assess the moisture-related response of CLT in a multitude of climates in various wall assembly systems. The objectives of this thesis are to document and summarize the results from the research and to present the information such a way that it is relevant and useful to designers, builders, and other researchers.

1.3. Approach

To answer the concerns about moisture durability of CLT panels, a two-pronged approach was utilized. An experimental component was used to identify and determine the important moisture-related properties of CLT panels. A modelling strategy was used to extrapolate the collected data and infer durability performance of CLT panels in wall systems across Canada.

The experimental component was approached by collecting water absorption and redistribution coefficients by testing a small sample size of CLT panels. The mass of these panels were measured through the tests to gauge the mass gain by wetting absorption and loss by drying over a period of time using diffusion-based calculation methods. The associated material values are determined through correlation of mass loss with respect to the square root of time.

After the empirical testing was conducted, the salient values were used to calibrate WUFI, a hygrothermal numerical simulation program by the Oak Ridges National Laboratory and the Fraunhofer Institute of Building Physics. The parameters were modified to obtain a range which mimics the empirical results. Then, typical wall assemblies for residential and commercial construction are replicated in the software and are exposed to various climatic conditions which may be reasonably encountered in buildings constructed with CLT walls.

1.4. Scope

Several limitations were imposed on the research. Due to time and facility limitations, only a limited number of CLT samples could be tested. This small sample size limits the accuracy of the tests. Further, standardized tests could not be used in the testing of the CLT panels. Standardized tests, such as those by ASTM, were designed for material testing. CLT panels are a sub-assembly level material- the method of construction of these panels result in intrinsic qualities in which the standardized tests cannot appropriately accommodate. Nonetheless, the approach taken towards acquiring CLT moisture properties are inspired by the standardized tests, with some modifications made, as required, to accommodate the samples.

Two experiments were designed to aid in the determination of the moisture response of the CLT samples. First, a clear sample tests was devised to better understand the behaviour of wood with respect to moisture uptake. The results of this test provide a first-order assessment on the anticipated behaviour of CLT panels. Finally, the CLT panels were subjected to similar testing conditions as the clear sample test. Variations in the results provide a good indication in the variability between the material test and the sub-assembly material test.

As this research forms part of a greater research effort (part of a multi-year, multi-organization research project), other researchers are currently studying such material properties as suction isotherms, vapour permeability, and sorption isotherms of CLT panels. At the time of the publication of this document, the data were not available. Further, full functional material properties are difficult to obtain and are resource exhaustive. Estimates and parametric studies can be conducted to determine the relative impact from the missing data. Consequently, the research required to determine these properties was not conducted. Engineering judgment was utilized to determine appropriate values, when required.

Data, if unavailable, were inferred from literature of existing engineered wood products. A parametric study was conducted to define upper and lower boundaries for most CLT properties.

The modelling aspect of the research was limited to a few representative cities for the various climate zones across Canada. A total of six cities and four wall types were modelled with interior climates representative of their respective climates. The metric for comparison is the total moisture content of a thin outer layer of the CLT panels above temperatures of 4°C.

Chapter 2- Cross-Laminated Timber and the Building Enclosure

This chapter discusses the background of CLT panels, as well as the role that it fills within the requirements and functions of a building.

2.1. Cross-Laminated Timber

CLT panels are a relatively new type of prefabricated panel. They consist of multiple plies of boards of wood, with the orientation of each adjacent layer perpendicular to the others, adhered together. Each ply is adhered cross-wise to the adjacent ones to form a monolithic slab which may be used for a multitude of structural roles- from shear walls and diaphragms to floors.

Figure 2.1: 3-Ply CLT Panel Sample

The initial development of CLT took place in Lausanne and Zurich, Switzerland, in the early 1990s (Crespell & Gagnon, 2010). However, it was not until 1996 that a joint industrial-academic research project resulted in the development of modern CLT (Crespell & Gagnon, 2010).The Stadhaus building, in Murray Grove (Architects: Waugh Thistleton), England, is one of the hallmark buildings of CLT construction since it is one of the earliest large scale buildings made out of CLT panels, Figure 2.2.

Figure 2.2: Murray Grove by Waugh Thistleton (Waugh Thistleton, 2011)

The superstructure of this 8+1 storey building was built from CLT panels in 27 days with a crew of 4 people. The building consists of 29 apartments as a mix of private and affordable housing.

2.1.1. Benefits of Cross Laminated Timber

Recent interest in cross laminated timber arises from the relatively minor environmental impact of the production and construction of CLT in buildings, as the products (other than the adhesives) are made from renewable resources. The product is also reusable and recyclable and may also be used as a carbon sequestration technique by storing carbon stored in the wood into structures.

The literature also suggests that panelized CLT systems also reduces waste and increases profitability by decreasing construction times. Buildings, such as Stadhaus, were built without the use of a tower crane by a crew of only 4 carpenters. FP Innovations (Crespell & Gagnon, 2010) states that the shell was constructed at a rate of 3 days per floor.

CLT panels also have very good seismic response (FP Innovations, 2011). The ductility and toughness enables the building to sway and absorb lateral and vertical earthquake loads. Any damage incurred results in localized deformation of the nails and screws instead of large scale failures (FP Innovations, 2011).

Finally, despite being made of flammable material, CLT panels have excellent fire performance ratings. As wood burns, an insulating char layer forms, protecting wood deeper within the structure, provided the structure is of sufficient dimension. Furthermore, the high temperature gradient results in an inward motion of any remaining liquid water, further enhancing the fire performance of the wood.

2.1.2. Materials

CLT panels are built by using wood boards or composite material (such as laminated veneer lumber). Dimensional lumber is the main input material; lower quality wood composites may be used in the interior plies. The most common type of wood used is softwoods, although hardwoods may also be used. Hybrid panels, made from composite wood, may use oriented strandboard (OSB), laminated strand lumber (LSL), and laminated veneer lumber (LVL).

Figure 2.3: Oriented Strandboard (OSB) (Nordbord, 2011)

Figure 2.4: Laminated Strand Lumber (LSL) (LP Corp, 2011)

Figure 2.5: Laminated Veneer Lumber (LVL) (Boise Cascade, 2011)

The adhesives are sprayed at approximately 0.2 kg/m^2 on the CLT panels (KLH, 2011). Polyurethanes are the most commonly used adhesives, but polyisocyanurates, melamine-urea-formaldehyde (MUF), and phenol-resorcinol-formaldehyde (PRF) are also used (FP Innovations, 2011). The boards may be either face - or edge – glue. The former consisting of only the face of the boards having adhesives applied to them, whereas edge glued panels also have the sides of boards coated with adhesive as well. While most CLT panels are attached with adhesives, some use nails or wooden dowels.

2.1.3. Production

The boards are laid flat and aligned in such a way that the long side edges are touching. An adhesive coating is then applied. Then, the next layer of boards is laid with the grain perpendicular to the preceding layer. This process continues until the desired thickness is achieved. The composite is then put through a press or a heavy roller to firmly bond the plies together. Once the panels are made, they are planed and sanded and then placed in a CNC router, to cut the required holes and openings for windows, doors, and service channels. Some manufacturers will make a cut along the edge of the laminated boards to induce a stress relief joint (Wang J. , 2011).

Polyurethanes are a common adhesive used in CLT production (FP Innovations, 2011). The adhesives can cure under ambient indoor environments, although more rapid curing occurs at higher temperatures. Typical curing times range from 1-4 hours, depending on temperature. FP Innovations uses an Emulsion Polymer Isocyanate for the construction of their CLT panels. This adhesive is used because it is considered to have increased water and fire resistance compared to other adhesives (Wang J. , 2011)

Typically, the panels are symmetrical about the sectional axis. That is, the panels usually have 3, 5, or 7 or more layers. When installed, the panels are oriented such that the long axis of the wood is parallel to the longer span.

2.1.4. Manufacturers

Europe has several manufacturers which are producing CLT panels. As the industry is still very new in Canada, there are only a few manufacturers.

Table 2.1: CLT Manufacturers and Production Quantities (Crespell & Gagnon, 2010)

Manufacturer Name	Production Quantity (m^3)	Country of Origin
KLH	71,000	Austria
Binderholz	25,000	Austria
Martinsons	5,000	Sweden
Stora Enso	60,000	Austria
Moelven	4,000	Norway
Nordic Engineered Wood	-	Canada

As demand grows, it is anticipated that new manufacturing companies will emerge in Canada, particularly in provinces which have a strong lumber industry.

2.2. The Building Enclosure

Buildings are designed and built to provide a space with a suitable interior environment for the needs of the user. In many instances, it must also satisfy human needs as well- both physiological and psychological (Straube & Burnett, 2005). The part of the building that helps separates the interior environment from the exterior is known as the building enclosure. The enclosure fulfills its functions by controlling mass and energy flows from the interior and exterior environment. The many functions of the building enclosure can be grouped into four broad categories (Straube & Burnett, 2005):

1. Support
2. Control
3. Finish
4. Service Distribution (a building function imposed on the enclosure)

The support function is to provide the necessary structural support for the enclosure. Sometimes, especially in smaller or low-rise buildings, the support function of the building is also part of the enclosure support. The control function is used to control or regulate the flow of any of the environmental effects from both the interior and exterior. The finish function meets aesthetic needs. Lastly, the distribution function, which is sometimes included in the requirements of the enclosure, provides the means to distribute various services, and utilities that are used by the building and the occupants (e.g., electric power, water, security systems, etc.).

 Some of the elements of a building may satisfy the needs of several of the functional categories at the same time. Cross Laminated Timber is one such building material. CLT panels may provide support for the building and the enclosure while also providing some control functionality (of fire, sound, heat, air, vapour, light, etc.) and, depending on the design intent, a finish function as well.

The following sections discuss the details surrounding the functionality of CLT panels with respect to its salient mechanism and properties.

2.2.1. Support

For the building enclosure to be functional, it must possess the capacity to support itself against various structural loads and transfer them to the primary structure or foundation. The support role of the enclosure is often separate from the main structural support of the building, as it is only responsible for ensuring structural viability of the enclosure, but the two may be intertwined and hence indistinguishable, depending on the design and structure of the building. The enclosure must be able to withstand the various forces, pressures, and loads such that its structural capacities and deflections meet the relevant building codes. The enclosure must be able to collect and transfer all dead loads and live loads, which include forces generated by wind, snow, earthquake, and occupants.

By virtue of its design and constituent materials, CLT panels are relatively strong and of moderate weight. While heavier than stick framed construction, they do provide better structural performance. Contrariwise, they do not possess the same structural performance as more massive construction material, like concrete, but benefit from a much lighter weight.

The panels possess strong shear and moment capacities, enabling them to be used in shear walls, floors, diaphragms, and vertical supports. The boards in each layer are arranged such that the strong axis of the wood, that is parallel to the grain, is oriented in the same direction as structural load (FPL, 2010).

A discussion of the structural merits of CLT panels is beyond the scope of this work, but further information may be found in the CLT handbook (FP Innovations, 2011).

2.2.2. Control

CLT panels, if used as part of the building enclosure, also perform control functions, either as a single component or as part of an assembly. The following lists the most common phenomena that are typically controlled by a building's enclosure;

- Heat
- Air
- Moisture (precipitation, built-in, vapour)
- Fire/Smoke
- Access (e.g., People)
- Sound

Heat, air, moisture, and fire are of great significant to CLT performance and will thus be treated in greater detail in the following sections. However, the level of performance of CLT panels with respect to heat, air, and moisture do not conform to performance requirements expected of modern wall assemblies. Consequently, additional dedicated control layers are required for many building applications. Nevertheless, when used in conjunction with dedicated control layers, CLT panels may help increase the overall performance of the enclosure.

2.2.2.1. Heat

The control of heat flow through the building enclosure is vital if thermal comfort is to be achieved while simultaneously reducing the environmental impact of the building by reducing the energy input requirements to maintain the indoor thermal environment. The insulating properties of the building, in combination with moisture, are also important in determining areas where condensation may occur and consequently, potential areas for durability issues. It is therefore of utmost concern that the thermal controls of the building be considered as part of the building enclosure system, and not separate from the air and moisture control layers.

Current Canadian code requirements for minimum insulation levels vary by jurisdiction. However, an installed insulation with thermal resistance of 3.5RSI (R-20) is common for many residential walls in most climates across Canada (OBC, 2006). CLTs typically possess a conductivity similar to wood, approximately 0.1 to 0.14 $W \cdot m^{-1} \cdot K^{-1}$ (R-1.0 to R-1.4 per inch) (Straube & Burnett, 2005). However, at thicknesses of up to 130mm (5 inches), this can result in thermal resistances of 0.92 to 1.3RSI (R-5.2 to R-7.4). On its own, the thermal resistance of CLT panels is insufficient to meet code requirements and thus alternative insulating strategies must be considered.

2.2.2.2. Air

The control of air is one of the more important functions that can be expected of a building enclosure. Air leakage can pose a durability problem to the structure and enclosure as a result of moisture condensation leading to various decay mechanisms. Simultaneously, the air leakage also results in significant heat loss. CLT panels, by virtue of their manufacturing processes, do not typically possess any intrinsic air leakage resistance (FP Innovations, 2011). Although a significant resistance to airflow is inherent in wood, checks, cracks, and above all, panel joints will allow unacceptable levels of air flow. Consequently, an air barrier of some type will need to be used in conjunction with CLT panels. The exception to this is edge-glued CLT panels. Testing by other researchers in the NEWBuildS research organisation is currently under way in to assessing the air leakage resistance of edge-glued CLT panels and manufacturers recommend using tape to seal the joints between all panels.

2.2.2.3. Moisture

As CLT panels are made of organic materials, exposure to moisture may result in a multitude of problems. Should moisture controls not be in place, decay mechanisms may start to degrade the structure of the wood or break chemical bonds in the adhesive. In a worst case scenario, the degradation of the structure of CLT panels from such decay mechanisms may pose life-safety issues to people, as well as threaten the functionality and viability of the structure itself.

It is therefore of utmost importance that a layer that resists liquid moisture be included in the wall assembly to control external sources of moisture, such as precipitation, ground water, and use-derived sources of water (such as sprinklers).

Consideration must also be made for interior sources of moisture, either from bulk convection from air leakage or from water vapour diffusion through the wall assembly. Of similar importance is the presence of in-built moisture during construction. It is the purpose of this thesis to quantify the impacts related to the various moisture loads and to provide suggestions in managing any moisture related concerns.

2.2.2.4. Fire

Fire poses one of the greatest threats to the built environment. Tremendous efforts are undertaken to minimize the threat of fire and to mitigate any associated damages. CLT panels are a flammable product and could contribute to the fire load in a building under certain circumstances. However, under most circumstances, solid wood members are intrinsically resistant to the effects of fire. As a fire burns, the outer layer of wood experiences pyrolysis leaving behind a char layer. This char layer helps insulate the interior portions of the wood member from the heat of the fire.

A precedent has been set with regards to the use of solid wood members in structural applications. The National Building Code and the relevant fire codes acknowledge that solid timber construction possesses an intrinsic resistance to fire (NBC, 2010). For high levels of fire resistance, additional fire control layers, likely in the form of gypsum board panels or intumescent paints, can be added.

FP Innovations has some slight concerns with respect to the failure of the adhesive holding the lamina together. An adhesive failure could result in the layers being shed from the structure, exposing

undamaged layers underneath. Testing for the fire resistance of CLT panels is currently underway, as of the writing of this thesis. Preliminary results suggest that CLT panels behave similarly to solid timber construction.

2.2.2.5. Sound

It is possible for CLT panels to exceed the sound transmission code requirements in floors and walls (Crespell & Gagnon, 2010). The additional mass of a CLT panel relative to steel and wood stud walls will deliver superior performance. Standard sound dampening techniques, similar to those used for solid structural systems, should be employed.

2.2.3. Distribution

The distribution functionality must be carefully considered when it comes to CLT panels since no interstitial space exists inside the panels to run ductwork, power cables, plumbing, or other wires through the building.

The standard construction practice to overcome this limitation is to build false drywall interior of the CLT panels using nominal dimensional lumber (i.e. 2"x2" studs). This provides some fire protection to the CLT panels while also creating a space to run wires and cables for power outlets, phone and Ethernet jacks inside the drywall. However, alternative strategies must be considered if the architect desires the CLT panel to be exposed to the interior. Some such alternatives include eliminating a layer in the CLT panel to use as a conduit for the required utilities, or underfloor distribution strategies. Sawn wiring chases while practical, will impact the structural performance and require tight coordination early in the design process.

2.2.4. Finish

The finish function is a natural part of all enclosures, whether intentionally designed and designated or not. The finish of the enclosure must endure environmental stresses, from both the exterior (solar radiation, precipitation, temperature fluctuations, etc.) and the interior (humidity, damage from scuffs and scratches, spills, etc.). CLT panels are frequently covered on the exterior by a cladding system, as exposure to the elements could pose durability issues to the panels.

2.3. The Perfect Wall

The logical conclusion that is drawn from the requirements mentioned above has been dubbed the "perfect wall" (Lstiburek, 2008). This enclosure design concept was pioneered by Canadian researchers e.g., Hutcheon, 1963. A sectional view of the perfect wall may be found in Figure 2.6.
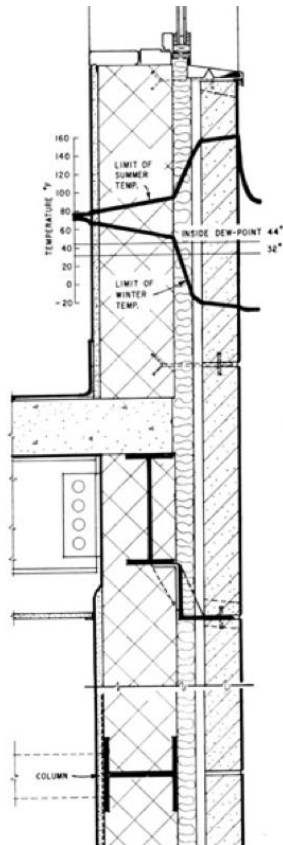
Figure 2.6: Sectional View of the Perfect Wall (Hutcheon, 1964)
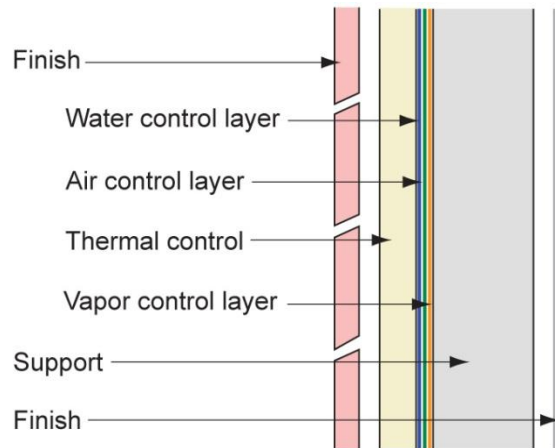
Figure 2.7: The Perfect Wall (Lstiburek, 2008)

The benefits of such a wall arrangement are that all the potentially UV-sensitive components are protected by a cladding and all potentially temperature sensitive layers are located within the thermal layer (and hence kept at stable room temperature). Further, all the potentially moisture sensitive components are located inside a water control layer. By virtue of the position of the thermal layer, the structure is maintained near indoor temperatures year round- any moisture accumulation will thus have the ability to dry to the interior under near constant drying conditions. Further, because the vapour and air control layers are also maintained near interior temperature conditions and are situated outside of

the structure, the proclivity for moisture condensation to occur within the structure is minimized, due to the dew point occurring in areas which are tolerant or resistance to moisture.

The support properties of CLT panels predispose it as an ideal building material to be used as the support function in a perfect wall system.

2.4. Wood Anatomy

Wood is a complex biological structure, a composite of many chemistries and cell types acting together to serve the needs of a living plant (FPL, 2010). Wood has evolved over the course of millions of years to serve three main functions in plants: conduction of water from the roots to the leaves, mechanical support of the plant body, and storage of biochemical (FPL, 2010). There is no property of wood- physical, mechanical, chemical, biological, or technological- that is not fundamentally derived from the fact that wood is formed to meet the needs of the living tree (FPL, 2010).Understanding the basic requirements dictated by these three functions and identifying the structures in wood that perform them allow insight to the realm of wood as an engineering material (Hoadley, 2000).

Wood is a natural, orthotropic, and inhomogeneous material- that is, its properties change depending on orientation, location within the tree, and history (i.e. previous micro-climatic environmental stimuli) (FPL, 2010). The three defined orientations that are used to describe wood properties are: longitudinal/sectional (X), radial (R), and transverse orientations (T).
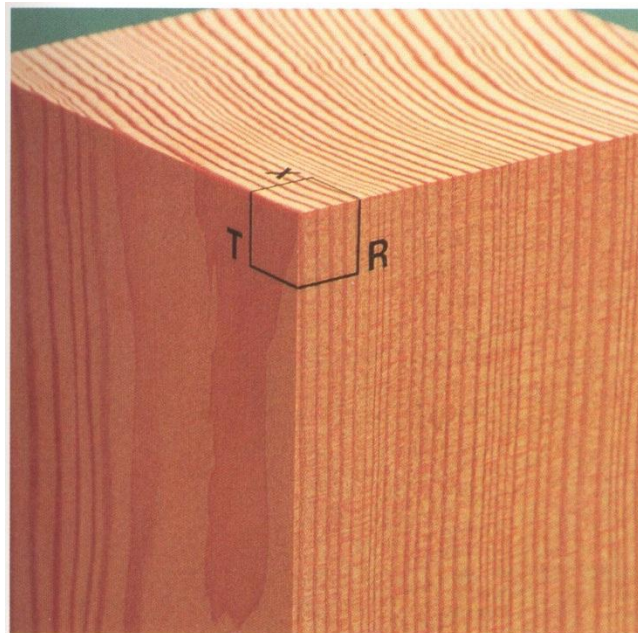
Figure 2.8: Transverse (X), Radial (R), and Tangential (T) Directions in a Wood Prism (Hoadley, 2000)

A scanning electron microscope image of Eastern White Pine shows the differences between the three orientations (see Figure 2.9).
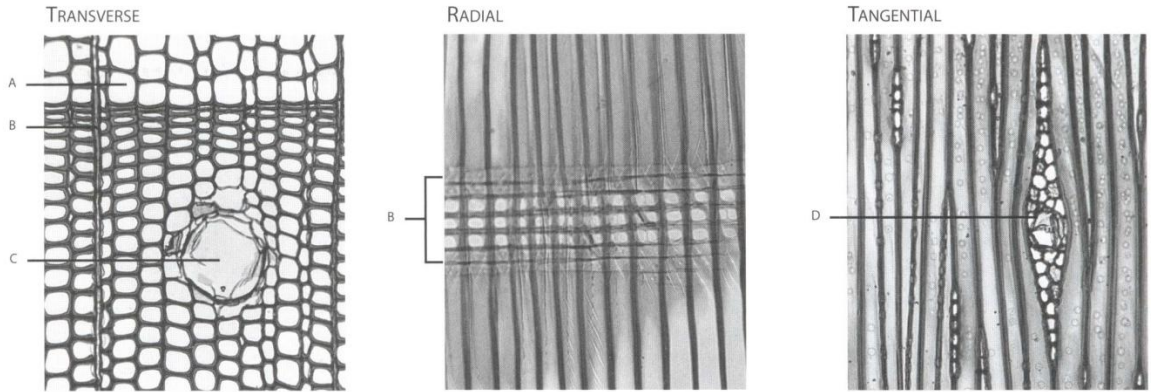
Figure 2.9: Transverse, Radial, and Tangential Sections of Eastern White Pine (Hoadley, 2000)

In the above figure (Figure 2.9: Transverse, Radial, and Tangential Sections of Eastern White Pine , (A) represents tracheids, (B) is a narrow ray, (C) is a resin canal, and D is a fusiform ray. The following sections will further elaborate on aspects and properties of the various wood cells.

2.4.1. Anatomy of Wood

The tree is composed into two main sections- the shoot and the roots. The shoots consist of the trunk, branches, and leaves, whereas the roots are responsible for water and mineral nutrient uptake as well as mechanical anchoring for the shoots (FPL, 2010). The components of the tree are nicely summarized in Figure 2.10.
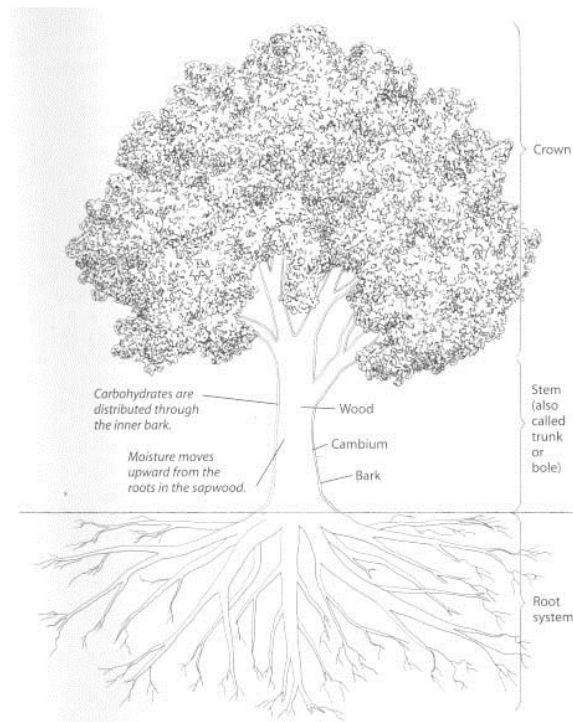
Figure 2.10: Parts of the Tree (Hoadley, 2000)

14

The trunk consists of the following layers, from the exterior to the interior: outer bark, inner bark, vascular cambium, sapwood, heartwood, and the pith. These layers may be found in Figure 2.11.
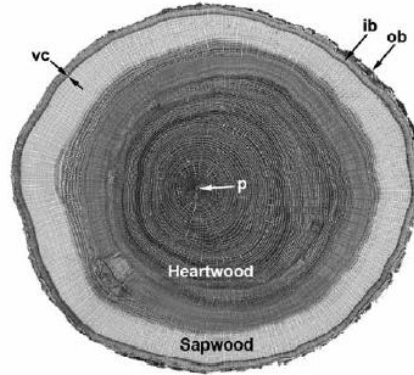
Figure 2.11: Macroscopic View of a Transverse Section of *Quercus alba* Trunk (White Oak) (FPL, 2010)

The **outer bark (ob)** serves to protect the interior portions of the trunk as well as reduce evaporative losses. The **inner bark (ib)** is the portion of the tree where the sugars produced by photosynthesis are transported through the tree to the areas of growth, known as secondary phloem cells. Immediately interior of the inner bark is the **vascular cambium (vc)**. The vascular cambium serves to produce both the inner bark (phloem), to the exterior, and wood (secondary xylem), to the interior. The next interior adjacent of the vascular cambium is the **sapwood**, or secondary xylem- complex vascular tissue responsible for the transport of water and minerals of a plant from the roots to the leaves. The **heartwood** is non-conductive and accumulates various substances (such as oils, gums, resins, and tannins), often giving it a different colour, decay resistance, and aromatics than sapwood (Raven, Evert, & Eichhorn, 2003). The **pith (P)** is the remnant of the early growth of the trunk.

Growth rings are a result of seasonal activity of the vascular cambium. Growth rings are categorized as early wood and late wood, depending on the time of growth during the year. The width of growth rings varies with environmental factors such as light, temperature, rainfall, available soil water, and the length of the growing season (Raven, Evert, & Eichhorn, 2003). Early wood can be distinguished from late wood as it is usually lighter in colour and wider- due to some of the more favourable growing conditions. The width of growth rings is roughly proportional to the amount of rainfall experienced in a given year (FPL, 2010).

2.4.2. Sapwood

Sapwood is an area in the trunk whereby the parenchyma cells- living, generally thin walled cells of variable size and form- are still alive and metabolically active. Sapwood is not only responsible for the conduction of sap, but also for the storage and synthesis of biochemicals, such as the storage of photosynthate- typically starches and lipids. The nutrients and chemicals used to create a new flush of leaves or needles are stored in the parenchyma cells of the sapwood (FPL, 2010).

2.4.3. Heartwood

Heartwood is formed by the parenchyma cells along the sapwood/heartwood boundary. These cells deposit chemicals, known as extractives, a by-product of cellular metabolism, by pushing them into the dead parenchyma cells in the heartwood. These extractives, or secondary metabolites, such as oils, waxes, resins, and tannins, are believed to be inhibitory or even toxic to living cells (Raven, Evert, & Eichhorn, 2003). The accumulation of these substance results in the death of the wood cell. A natural resistance to decay mechanisms results in the accumulation of these extractives- consequently, heartwood is more resistance to rot than sapwood.

2.4.4. The Wood Cell

A living plant cell consists of the protoplast and the cell wall, where the former is the sum of all living contents that are bounded by the cell membrane- a largely carbohydrate matrix extruded by the protoplast to the exterior of the cell membrane. The cell membrane protects the cell from osmotic lysis and provides mechanical support to the plant (Raven, Evert, & Eichhorn, 2003). However, the cell membrane provides a much more important role in the overall function of the tree. In mature cells, to achieve full functionality, often times the protoplast must be removed. Cells without their protoplast are known as lumen. The lumen is a critical component of many cells, whether in the context of the amount of space available for water conduction or in the context of a ratio between the width of the lumen and the thickness of the cell wall (FPL, 2010).

Wood cells are predominantly oriented either axially, known as fusiform initials, or radially, known as ray initials. The orientation of the cells helps in the distribution and storage of nutrients and minerals throughout the depth and height of the tree. Consequently, there is a direct and continuous link between the most recently formed wood, the vascular cambium, and the inner bark. Cells in the axial system are several times longer than wide; it provides the long-distance water transport and majority of the mechanical strength of the tree. The cells in the radial system are longer perpendicular to the longitudinal axis and provide lateral support to the tree as well as lateral transport of biochemical.

The cell walls in wood give rise to the majority of the structural properties of wood. The cell is comprised of three main regions: the **middle lamella (ML)**, the **primary wall (P)**, and the **secondary wall (S)** (FPL, 2010). In each region, the cell wall has three major components: cellulose microfibrils (with characteristic distributions and organizations), hemicelluloses, and a matrix or encrusting material, typically pectin in primary walls, and lignin in secondary walls (Panshin & deZeeuw, 1980). The following figure depicts the various sectional components of a wood cell.
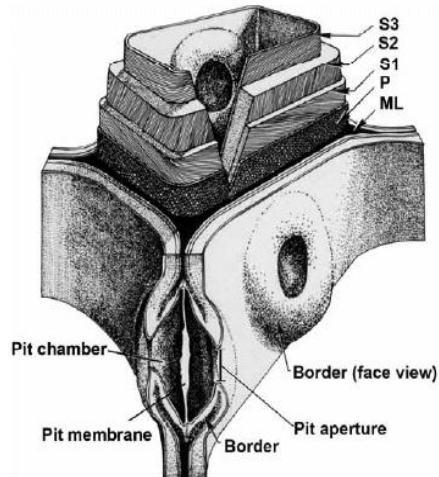
Figure 2.12: Wood Cell Wall Sectional View (FPL, 2010)

Cellulose can be understood as a long string-like molecule with high tensile strength; microfibrils are a collection of cellulose molecules into even longer, stronger thread-like macromolecules. Lignin is a brittle matrix material. The hemicelluloses are small, branched molecules thought to help link the lignin and cellulose into a unified whole in each layer of the cell wall.

The **middle lamella** functions to bond the adjacent cells to each other- it is lignified.

The **primary wall** is characterized by a largely random orientation of cellulose microfibrils. Microfibril angles range from 0° to 90°. The primary wall is thin and usually indistinguishable from the middle lamella.

The **secondary cell** wall is composed of three layers. As the protoplast forms the cell wall layers, it progressively reduces the lumen volume. The first secondary cell wall layer that is adjacent to the primary wall, is generally thin, and has a large microfibril angle compared to the grain of the wood (roughly 50° to 70°). The next inner wall layer is arguably one of the most important with regards to providing the wood properties at a macroscopic level (Panshin & deZeeuw, 1980) (Kretschmann, Alden, & Verill, 1998). The secondary layer of the secondary cell wall has a lower lignin percentage and a low microfibril angle (5° to 30°) and it has a strong, but not entirely understood, relationship with macroscopic wood properties (Kretschmann, Alden, & Verill, 1998). The third layer of the secondary wall is thin and has a high microfibril angle (>70°), and is similar to the first layer- it has the lowest percentage of lignin of all the three layers.

Pits are the means by which communication and transport of biochemicals occurs from adjacent cells in a living plant. Pits are thin areas in the cell wall which allow mass transfer from one cell to another. Pits are usually paired with adjacent cells, but if a pit fails to connect with the one of an adjacent cell, it is termed "blind". There are three varieties of pits: bordered, simple, and half-bordered (Esau, 1977) (Raven, Evert, & Eichhorn, 2003).

Bordered pits are so named because the secondary wall overarches the pit chamber and the aperture is generally smaller or differently shaped than the pit chamber, or both. The status of the bordered pits has great importance in the field of wood preservation and can affect wood finishing and adhesive bonding.

17

2.4.5. Differences between Hardwoods and Softwoods

Hardwood, classified as angiosperm wood, and softwoods, as conifer wood, are differentiated predominantly by the lack of vessels in softwoods. Hardwood and softwood do not refer to the relative strength of each species- some hardwoods are weaker than many softwoods, whereas some softwoods are harder than some hardwoods.

2.4.5.1. Microscopic Structure of Softwoods

The structure of softwoods is relatively simpler than those of hardwoods. Softwoods are predominantly characterised by a high number of tracheids and few axial or radial parenchyma. Tracheids are long cells that have an aspect ratio more than 100- they are tapered and overlap adjacent cells across both the top and bottom 20% to 30% of their length.
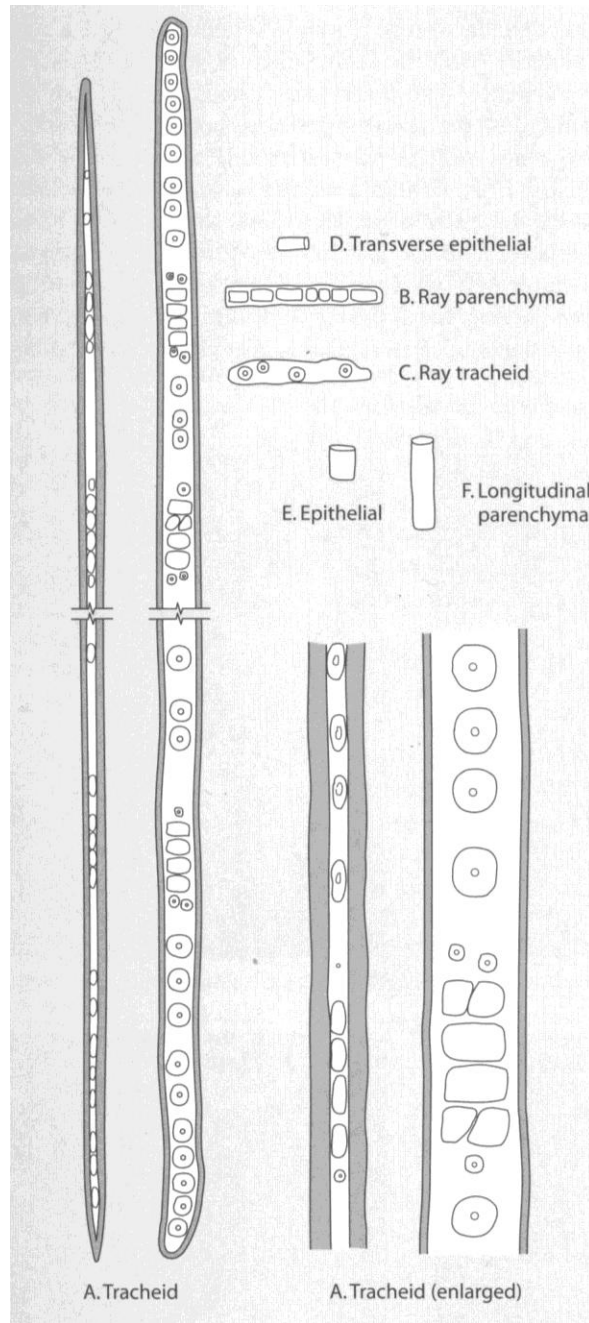
Figure 2.13: The Tracheid Cell (Hoadley, 2000)

From a transverse section, tracheids appear square. They are a major constituent of softwoods and compose in excess of 90% by volume. They serve to aid in the transport of fluid and provide mechanical strength to the tree- this is achieved by circular bordered pits that are concentrated at the long tapered ends of the cells. Consequently, water must flow through a zigzag path as it goes from one cell to the next via the pits. As the pits have a membrane, flow resistance is significant. Due to the resistance and narrow diameter of the lumina, tracheids are relatively inefficient compared to the conducting cells of hardwoods.

Axial parenchyma structures are also sometimes present in softwoods. These are similar to radial parenchyma cells, except oriented longitudinally. Resin canals are also found in some species of pine, spruce, Douglas-fir, and larch. These are present axially and radially. These structures are intercellular voids in the wood and are lined with specialized parenchyma cells that function in resin production. Resins canals are typically produced from wounding, pressure and injuries by frost and wind. Apparently, resin production helps protect the plant from attack by fungi and bark beetles (Raven, Evert, & Eichhorn, 2003). The following scanning electron micrograph shows the boundary between early wood and late wood in a softwood tree, as identified by the square shape of the tracheid wood cells.

2.4.5.2. Microscopic Structure of Hardwoods

The primary difference between conifers and angiosperms is the existence of vessels in the latter. Vessels are specialized water conducting cells in hardwoods. A second type of hardwood cells are fibers. Fibers function almost exclusively as structural elements supporting the cells. They are shorter than tracheids. The thickness of the fibers plays an important role in the macroscopic structural capacities of the wood. Further, hardwoods have a greater number of rays, and those rays usually consist of a greater number of cells than do those in softwoods. The following is a scanning electron micrograph of hardwood, identified primarily by the presence of the large vessels running vertically along the specimen.
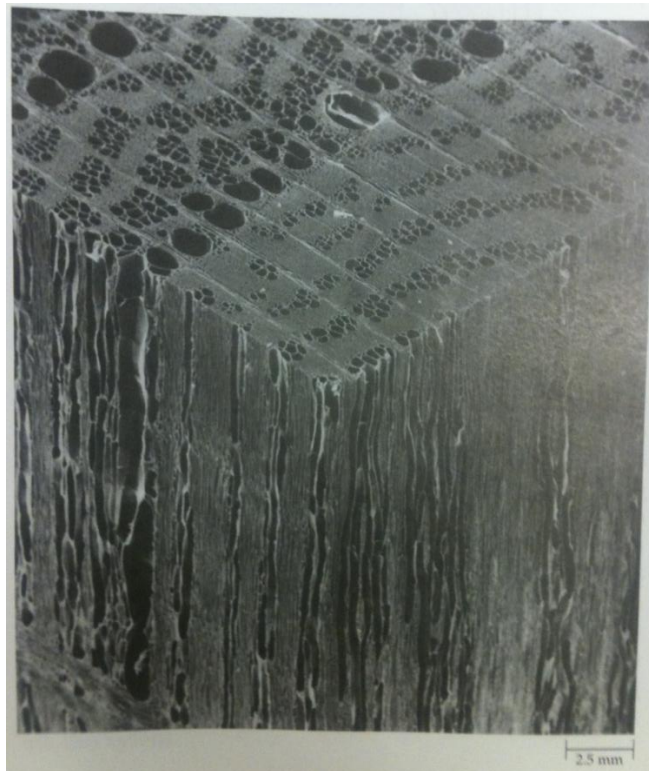
Figure 2.14: Scanning Electron Micrograph of American Elm (Raven, Evert, & Eichhorn, 2003)

2.4.5.3. Reaction Wood

Reaction wood is the type of wood that is grown in branches to counter the effects of gravity. Hardwoods and softwoods differ in their approach to reaction wood. In hardwoods, the reaction wood is known as tension wood. This wood is produced by increased activity in the vascular cambium on the top side of the stem. It is recognized by eccentric growth rings in that stem. To ensure the stem is straightened, a tension force must be generated. The top portion of the cells in tension reaction wood are distinguished by the presence of gelatinous fibers with very little or no lignification. The shrinkage of tension wood rarely exceeds 1%. Compression wood, or the reaction wood generated by softwoods, is a result of increased production in the vascular cambium on the underside of the stem. Compression wood has more lignin and less cellulose than normal wood. Consequently, the shrinkage rates are often ten or more times as great of that of normal wood (Raven, Evert, & Eichhorn, 2003).

2.4.6. Wood Properties

Macroscopic properties of wood such as density, hardness, bending strength, and others are properties derived from the interrelationship of the cells that constitute the wood make-up. Such larger-scale properties are based on chemical and anatomical details of wood (Panshin & deZeeuw, 1980). With respect to moisture, the hydroxyl groups in the cell walls are highly hygroscopic (i.e., attractive to water). However, the presence of lignin minimizes the capacity of the cell walls to adsorb moisture. Consequently, wood cells have a great affinity to water, but are limited in its capacity to store it within the cell wall.

The wood structure determines the wood density. The density increases as the proportion of cells with thick cell walls increases. Hardwood density is dependant not only on the fibre wall thickness, but also the number of voids created by vessels and parenchyma. It should be noted that the microfibril arrangement in the juvenile wood is usually at a high angle compared to the grain of the wood, particularly in softwoods. This results in relatively larger shrinkage and swelling characteristics compared to the surrounding mature wood.

2.5. Moisture Relation and Physical Properties of Wood

Wood is a hygroscopic material. That is, its moisture content varies can vary depending on the temperature and relative humidity of its surrounding environment. Furthermore, as an organic material, wood's properties and performance are impacted by its moisture content. The most common method of reporting the moisture content of the wood, based on dry mass, is expressed by equation (1).

$$MC = \frac{m_{wet} - m_{dry}}{m_{dry}}\%$$

(**1**)

where,

  MC= Moisture Content (%)
  m_{wet}= Wet mass of wood sample (kg)
  m_{dry}= Dry mass of wood sample (kg)

Water exists in three states in wood: free water (inside vessels, lumen, and cavities), as bound water (adsorbed to cell walls), and as vapour (inside vessels, lumen, cavities). The point at which free, or bulk, water starts to accumulate is known as the fibre saturation point. The fibre saturation point is operationally known as a state whereby the physical properties and characteristics of wood no longer change as a function of moisture content. The fibre saturation point is roughly 30%MC, but different species, and even different areas of wood in the same tree, may fluctuate by a few percentage points (FPL, 2010). There is a large gradation between the point at which bound water and free water occur- below the fibre saturation point, some lumen may be partially, or completely, filled with water. Equally, above the fibre saturation point, some cell walls may still be relatively dry and some lumen not yet filled with water.

Wood experiences sorption hysteresis- the moisture content history of the wood impacts the rate and capacity to absorb/desorb moisture in the future. Generally, the adsorbed/desorbed moisture content does not vary more than by 0.8% MC (FPL, 2010).

2.5.1. Equivalent Moisture Content

When wood is protected from liquid water and solar radiation, the equivalent moisture content is dependent on the temperature and relative humidity of the air surrounding the wood in question. Wood, under such conditions, may experience both long-term and short-term change in its local environment; seasonal fluctuations for long term effects, and diurnal fluctuations for short term effects. Short-term changes in relative humidity and temperature can only affect the outermost surface of the wood, as neither liquid or vapour phase water can move through solid wood very quickly. The equilibrium moisture content is a state of wood whereby there is no net gain or loss of moisture in the wood sample from interactions with the ambient environment.

2.6. Decay

Decay is the process whereby biological agents cause degradation of organic materials. The agents usually responsible are fungi. Reasons to control fungi propagation are diverse- from minimizing structural damage, to protecting indoor air quality from toxigenic and allergenic mould spores, and even for aesthetic reasons. The difference between mould and fungi is that mould is a subset of the fungi domain.

Typically, moulds only feed on the starch and other sugars that are stored within the wood cells (Raven, Evert, & Eichhorn, 2003). Rots, however, possess the capacity to break down the cellulose and lignin of the actual cell walls. Consequently, as CLT panels are structural members, maintaining adequate structural capacity is of utmost consideration, and rot is the primary concern.

Rots are generally divided into three classes: brown rot, white rot, and soft rot (FPL, 2010). Brown rots are fungi that break down hemicellulose and cellulose- leaving the brown lignin behind, which is how it was given the name. Soft rots secrete an enzyme that breaks down the cellulose in the wood, thus leading to microscopic cavities inside the wood. Lastly, white rot is a fungus that breaks down the lignin in the wood, leaving the light coloured cellulose behind. However, some white rots also consume the cellulose.

2.6.1. Conditions for Growth

Fungal growth only occurs if five requirements are satisfied: temperature, oxygen, moisture, nutrients, and presence of spores (Wang, Clark, Symons, & Morris, 2010). Typically, temperatures must be above 10°C but below 40°C; temperatures below 10°C result in much slower biological activity, whereas temperature above 40°C results in dehydration of the cells and hyphae. Optimal wood decay fungi growth was found to be in the range of 21 to 32°C by some researchers (Wang, Clark, Symons, & Morris, 2010). Appropriate access to moisture is also required- usually in excess of 80%RH for the start of fungal growth (Sedblauer, 2004). However, most rots require moisture contents in equilibrium with over 95%RH for successful proliferation (Viitanen & Paajanen, 1988). As an example of the strong influence of the environment on fungi, Figure 2.15 plots the germination time and propagation rates for a particular mould species as a function of RH and temperature.
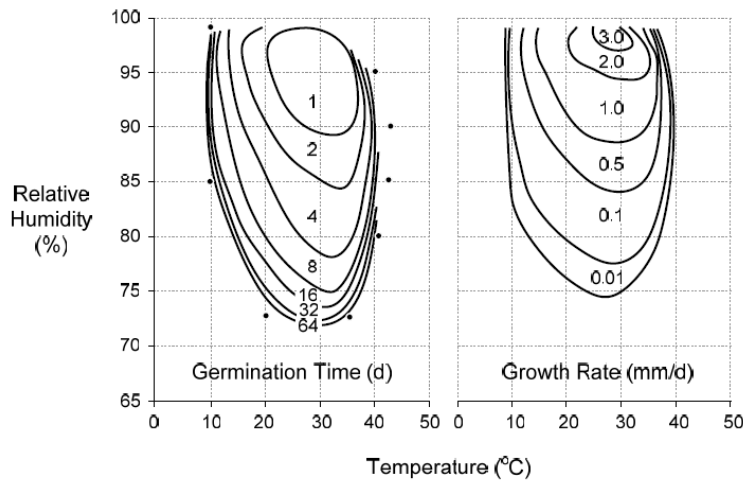
Figure 2.15: Relationship between Relative Humidity, Temperature, Germination time, and Growth Rate for Aspergillus Mould Spores (Sedblauer, 2004)

In general terms, if the relative humidity remains below 80% and the temperature below 10°C, moulds and rots should not present a risk to wood structures.

Chapter 3- Moisture Physics Background

This chapter reviews the moisture physics, relations, and equations which govern the various physical phenomena of moisture storage and transport that occur within the built environment, as it pertains to CLT panels.

3.1. The Water Molecule

The size and properties of the water molecule are important in its interrelated properties with the wood cell- and consequently, the macroscopic moisture behaviour of wood. The water molecule is composed of one oxygen atom (O) and two hydrogen (H) atoms bonded covalently, thus giving its stoichiometric identity of H_2O. Oxygen possesses 6 valence electrons and Figure 3.1 demonstrates this arrangement.
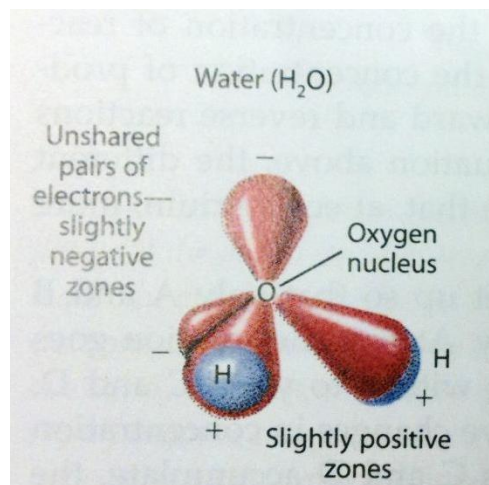
Figure 3.1: The Water Molecule (Raven, Evert, & Eichhorn, 2003)

Oxygen's high electronegativity results in disparate sharing of the electrons in the covalent bond, known as a polar covalent bond. This results in a slight positive charge on the end with the hydrogen atoms. The remaining four electrons are paired into two orbitals, resulting in a slight negative charge. The angle which best minimizes electromagnetic forces between the charged ends results in the molecule taking the form of a tetrahedron, with an angle of 104.5° between each point. The polarity of the water molecule plays an important role in its capacity to bond with surfaces, further enhanced by some van de Waal's forces and hydrogen bonding.

The average separation distance of the OH bond is approximately 0.096nm, whereas the equivalent ionic diameter of the molecule is 0.282nm (Franks, 1984). These dimensions are important in the movement and storage of water in various media.

3.1.1. Four State of Moisture

Water exists in four common states: gas, liquid, solid, and adsorbed. Each state carries its own characteristics, properties, and associated problems when interacting with the built environment. With respect to CLT panels, the primary water states concerned are gaseous, liquid, and adsorbed. The formation, storage, and movement of ice within wood is not a concern with respect to decay as

biological activity comes almost to a standstill below the freezing point of water. The relationship between the four states may be seen in the following figure.
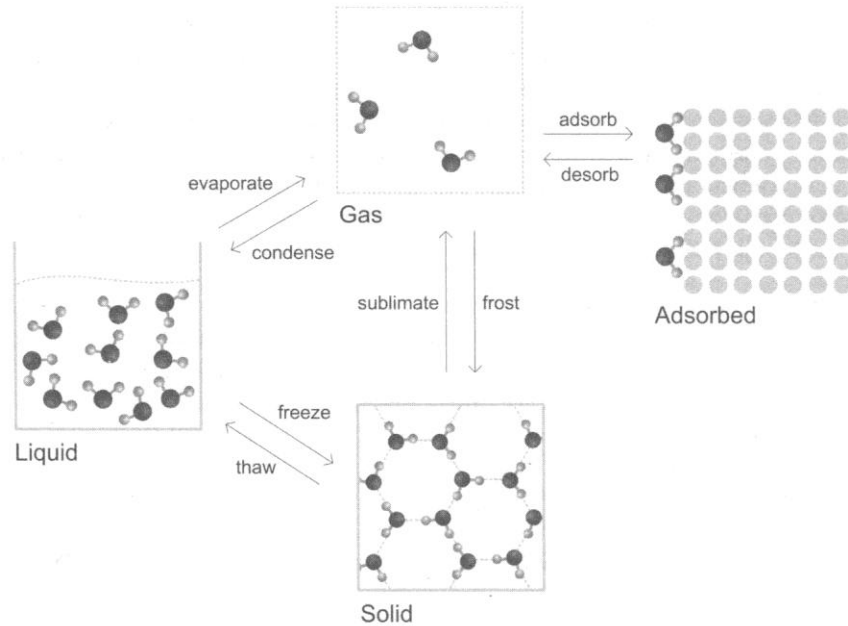
Figure 3.2: Moisture States and Phase Changes (Straube & Burnett, 2005)

Under most circumstances, sorbed water will only change phases with gaseous water vapour. However, in very small pore sizes, adsorbed water may reach thicknesses to the point where it condenses inside the pores.

3.1.2. Psychrometrics (Storage of Water in Air)

Psychrometrics is the study of gas mixtures- most commonly, water vapour in air. An understanding in psychrometrics is required to understand the relationship between vapour pressure, or moisture content, temperature, and relative humidity and the effects these variables have on the moisture characteristics of hygroscopic materials. The psychrometric chart, as presented in Figure 3.3, is frequently used to graphically depict the relationship between these variables.
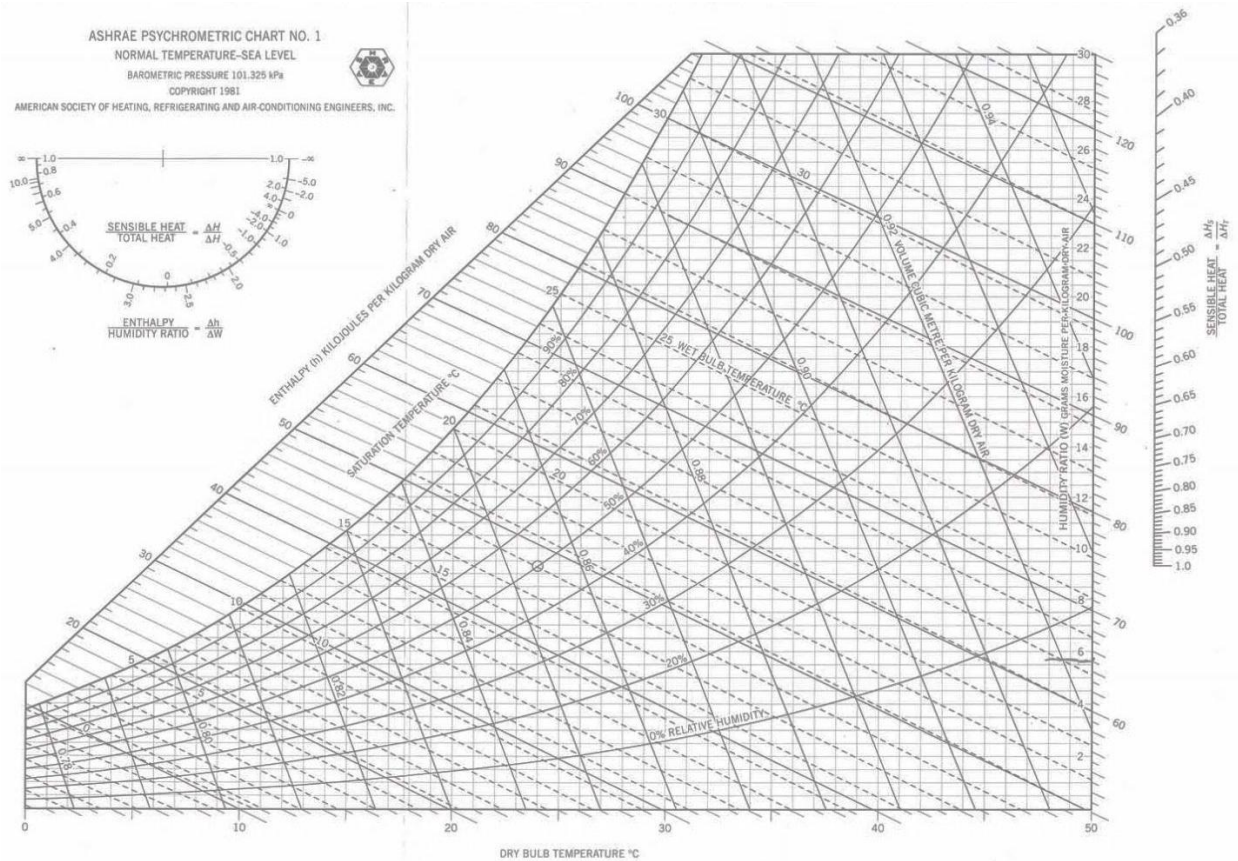
Figure 3.3: The Psychrometric Chart (ASHRAE, 2009)

The amount of water vapour which can be stored in a unit volume of air is highly sensitive to the dry bulb temperature. An appropriate analogy is to view air as a sponge which can soak up water vapour as well as other gases. With increased temperature, the sponge gets bigger and can thus store more water. However, at isothermal conditions, the sponge can only absorb a given amount of water before it is saturated- this is known as the saturated vapour pressure. The total moisture storage capacity of a volume of air at a specific temperature follows the Hyland-Wexler equation for saturated vapour pressure over liquid water from 0-200°C (ASHRAE, 2009):

$$ln(p_{ws}) = C_1/T + C_2 + C_3 T + C_4 T^2 + C_5 T^3 + C_6 lnT \qquad (2)$$

where,

        C_1= -5.800 220 6E+03
        C_2= 1.391 499 3E+00
        C_3= -4.864 023 9E-02
        C_4= 4.176 476 8E-05
        C_5= -1.445 029 3E-08
        C_6= 6.545 967 3E+00
        C_7= -5.800 220 6E+3
        p_{ws}= saturation pressure [Pa]
        T= absolute temperature [K]

The psychrometric chart is simply the results of plotting vapour pressure, along the vertical axis, and temperature, along the horizontal axis, with the saturated vapour pressure line bounding the upper limit of saturated water vapour in air. The relative humidity is the ratio of the quantity of vapour to the saturated vapour pressure at a given temperature, as described by equation 3:

$$RH = \varphi = \frac{p_w}{p_{ws}}$$ (3)

where,

RH= relative humidity [-]
p_w= vapour pressure [Pa]
p_{ws}= saturated vapour pressure [Pa]

It is often useful to express the moisture content of the air in mass terms, e.g., grams of vapour to kilograms of dry air. The moisture content is a result of rearranging of the ideal gas law, as seen in Equation 4,

$$PV = nRT$$ (4)

where,

P= pressure [Pa]
V= volume [m^3]
n=quantity of substance [mol]
R= gas constant [J·K^{-1}·mol^{-1}]
T= absolute temperature [K]

The ideal gas law equation, Equation 4, is an amalgamation of Boyle's Law, Charles' law, Gay-Lussac's law, and Avogadro's law, and demonstrates the relationship between pressure, volume, and temperature. Using the knowledge of Dalton's law, which states that the pressure of a gas mixture is equal to the sum of the pressures of the individual gases, we can rearrange Equation 4 as a ratio of water vapour to dry air, as shown in the following equation:

$$W_c = \frac{0.621\,945 \cdot p_w}{p_t - p_w}$$ (5)

where,

W_c= water content [kg$_v$·kg$_{air}^{-1}$]
p_w= vapour pressure [Pa]
p_t= total pressure [Pa]

The 0.621945 coefficient is a result of dividing the gas constant of water vapour with that of dry air multiplied by the ratio of molecular mass for the respective gases.

The temperature of a sample of air containing water vapour at which condensation forms on non-porous surfaces is known as the dew point temperature. For temperatures between 0°C and 93°C, the dew point temperature is given by Equation 6,

27

$$t_d = C_8 + C_9\alpha + C_{10}\alpha^2 + C_{11}\alpha^3 + C_{12}(p_w)^{0.1984} \qquad (6)$$

where,

t_d= dew point temperature [°C]
α= ln p_w
p_w= water vapour partial pressure [kPa]
C_8= 6.84
C_9= 14.526
C_{10}= 0.7389
C_{11}= 0.09486
C_{12}= 0.4569

This equation becomes important when determining the layers in a wall assembly which experience water vapour condensation, particularly with respect to air leakage.

3.1.3. Moisture Storage in Materials

A material's ability to store water is dependent primarily on its porosity, specific surface area, and its hygroscopicity. Apparently solid materials may have significant porosity, given as a percentage of voids within a unit volume of material, and high specific internal areas, given as an area per unit volume of material. The voids in a material form an interconnected network of pathways and dead ends. Figure 3.4 demonstrates a representative porous material.
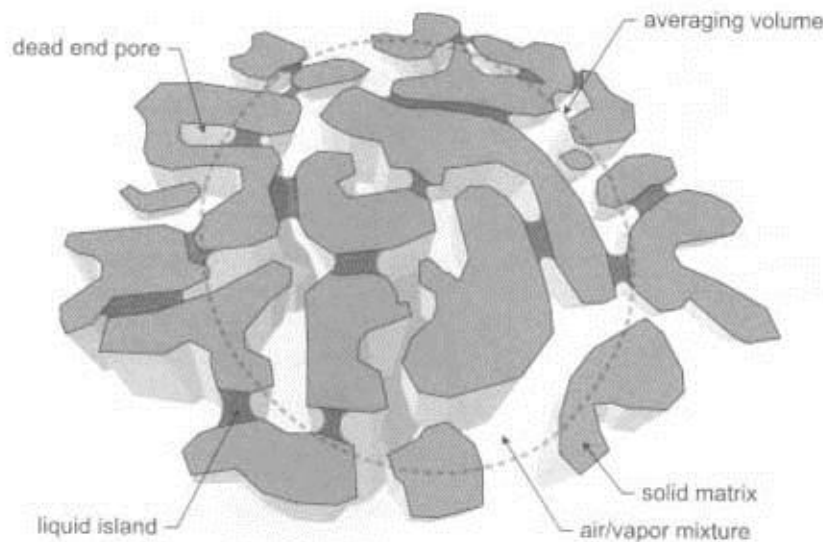
Figure 3.4: Representative Porous Material (Straube & Burnett, 2005)

Water can be stored in five different ways in a material, as summarized in Table 3.1, in increasing magnitude of storage capacity:

Table 3.1: Moisture storage mechanisms (Straube & Burnett, 2005)	
Moisture Form	Storage Location
Free water vapour	In pore volume (porosity)
Adsorbed water vapour	On pore walls (specific area)
Capillary condensed water	Held in very small pores
Capillary bound liquid water	Held by surface tension in pores
Unbound liquid water	Held by containment

For free water vapour, the moisture exists in a gaseous mixture with air inside the pore volumes of the material. Adsorbed water vapour results in water molecules bonding with the surface of the material- it collects on the pore walls. Capillary condensed water occurs when the thickness of the water molecules adsorbed to the surface reaches such a point that contact is made with adsorbed water on opposite pore walls. Capillary bound liquid water is held by surface tension in the pores. Lastly, unbound liquid water is stored within the pores of the material. The various storage states are labelled on the sorption isotherm below (see Figure 3.5).
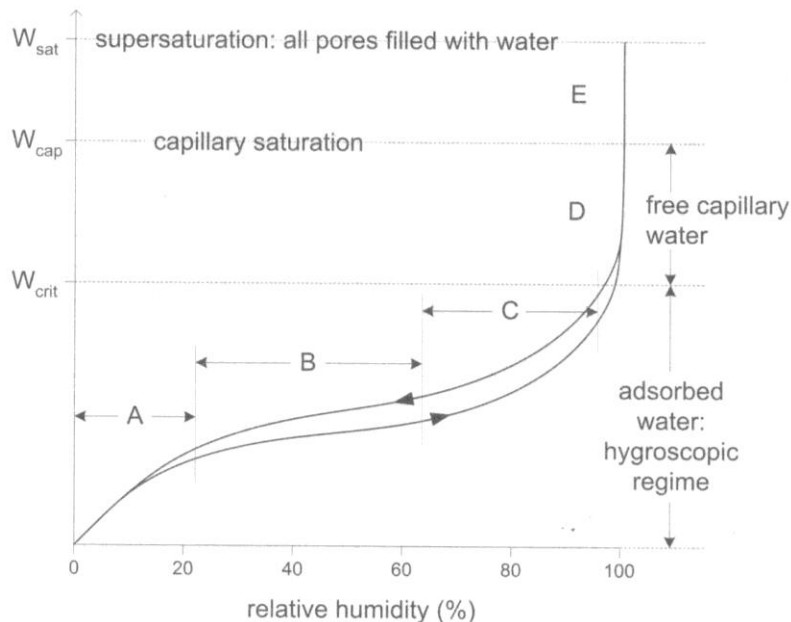
Figure 3.5: Sorption Isotherm (Straube & Burnett, 2005)

The area marked A consists of a single layer of water molecules adsorbed to the surface; B is a continuation of A, in that multiple layer of water molecules form on the surface walls. This is known as the hygroscopic range. At the range indicated by C, capillary condensation occurs, and at D, capillary suction is the dominant acting storage mechanism, in the free water range (Straube & Burnett, 2005). Above the capillary saturated point, indicated by E, bulk water exists within the pores of the material. Directional arrows are required due to the hysteresis of moisture storage- uptake and drying to not follow the same curve. It is hypothesised that an "ink bottle" effect, capillary actions resulting in a localized high pressure area, could reduce the amount of moisture loss when the material dries.

As the material and mechanical properties of wood change at different temperatures, it follows that the sorption isotherm of wood would similarly change. At lower temperatures, water has a higher propensity towards condensation, following the concepts of psychrometrics and water vapour condensation in porous networks; the corollary also holds true. However, in the temperature range that most building materials may experience, the variations are not significant, as can be seen below in Figure 3.6.
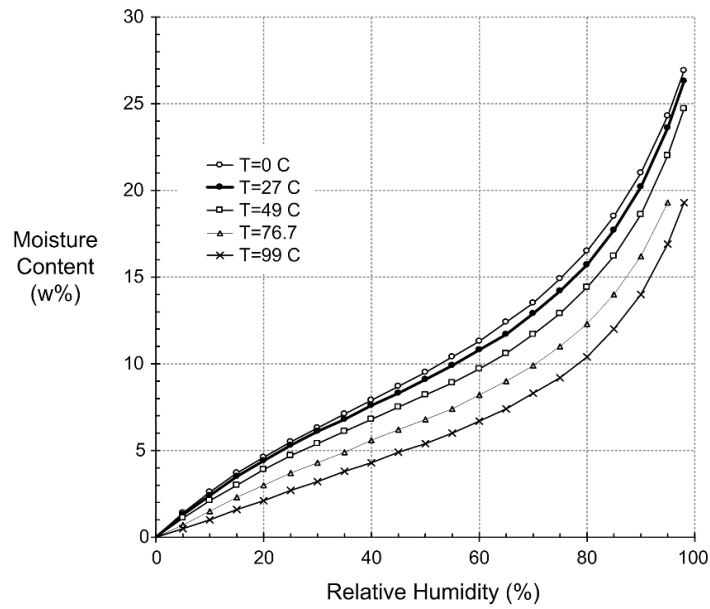
Figure 3.6: Temperature Dependant Sorption Isotherm (Straube & Burnett, 2005)

The data contained in the above plot derives from equilibrium moisture content values from a wood specie in the US FPL Wood Handbook (FPL, 2010). Even at very high relative humidities (i.e. 95%) and with a 60°C temperature difference (from 4.4° to 65.6°C), the total moisture content changes by only 3.9% M.C. Consequently, for simplification purposes, it is common to assume a singular sorption curve for many building materials.

3.1.4. Moisture Movement in Porous Media

Moisture movement in porous media is usually described by Fickian equations. Some of the driving potentials for moisture flow include temperature, relative humidity, water vapour pressure, water vapour density, liquid capillary pressure, suction pressure, moisture content, and chemical potential (Claesson, 1993; Hens, 1996). There are generally three independent state variables, but when air pressure is considered to be constant, only two commonly used driving potentials remain: temperature and water vapour pressure (Galbraith, McLean, & Guo, 1997), or temperature and relative humidity (Künzel, 1995). The relative contributions to moisture flow from these driving potentials are not equal, nor do they vary linearly. To further compound the complexity is any anisotropy in the material's porous system. Consequently, each driving potential's impact on moisture flow must be considered separately from a theoretical perspective, or lumped into appropriately designed empirical coefficients which account for the multiple flow mechanisms.

It is generally accepted that there are five mechanisms at work that contribute to moisture flow in porous media. A summary of the transport phenomenon, their driving potential, and the affected water phase may be found below (Table 3.2).

Table 3.2: Summary of moisture transport mechanisms (Straube & Burnett, 2005)

Mechanism	Water Phase	Driving Potential
Diffusion	Gaseous	Water Vapour Concentration
Effusion	Gaseous	Water Vapour Concentration
Surface Diffusion	Adsorbed	Relative Humidity
Capillary Transport	Liquid	Capillary Suction Pressure
Osmosis	Liquid	Solute concentration

However, in building applications, two mechanisms tend to dominate the contribution to moisture movement- diffusion and capillary transport. Surface diffusion also participates in moisture flow, but from a macroscopic perspective, it is difficult to distinguish separately from diffusion or capillary transport. The following figure demonstrates the relative contributions to diffusivity for these three main transport mechanisms.
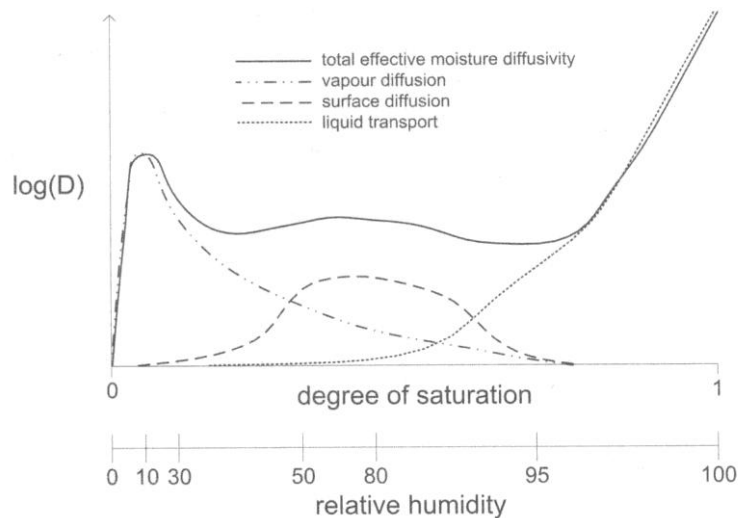
Figure 3.7: Effective Hypothetical Moisture Diffusivity based on Vapour, Surface Diffusion, and Capillarity (Straube & Burnett, 2005)

The general equation which describes the flow of moisture in porous material is as follows (Straube & Burnett, 2005):

$$\dot{m}''(w, T) = -D_v(\varphi, T) \cdot \nabla \rho_v + D_{T,v}(w, t) \cdot \nabla T - \{D_a(w, T) + D_l(w, T)\} \cdot \nabla w \qquad (7)$$

where,

        w= moisture content [kg·m^{-3}]
        φ= relative humidity [-]
        T= absolute temperature [K]
        $\dot{m}''$= mass flux density as a function of w, T [kg·m^{-2}·s^{-1}]
        D_v =vapour diffusion coefficient, function of ф,T [m^2· s^{-1}]
        $\nabla \rho_v$= vapour density concentration gradient [kg$_{vapour}$·m^{-4}]
        $D_{T,v}$ = thermal vapour diffusivity (Soret effect) [m^2·K^{-1}·s^{-1}]
        D_a = adsorbed diffusivity as a function of w, T [m^2· s^{-1}]
        D_l = liquid diffusivity as a function of w, T [m^2· s^{-1}]
        ∇w= moisture content gradient [kg$_{liquid}$·m^{-4}]

However, as the experimental tests for the CLT samples were maintained at isothermal conditions, the temperature effects are neglected. Further, the component of surface diffusion is lumped in with the capillary transport. Thus, the equation collapses to the following form:

$$\dot{m}''(w) = -D_v(\varphi) \cdot \nabla \rho_v - D_l(w) \cdot \nabla w \qquad (8)$$

The following subsections discuss vapour diffusion and capillarity transport in greater detail.

3.1.4.1. Vapour Diffusion

There are two processes by which gaseous water molecules will move through a gas. Fickian diffusion is the process whereby molecules, via Brownian motion, will collide with one another until entropy is maximised. The other is Knudsen diffusion, known as effusion, whereby the water molecule will collide with the pore wall more so than other water molecules. However, effusion is less significant than diffusion; consequently the remaining discussion will focus solely on diffusion.

Vapour diffusion functions under the same general set of equations that govern diffusive flows. Fick's Law states that the rate of flux is proportional to the concentration gradient of the substance. That is, a higher concentration gradient generates a higher rate of flux. The constant of proportionality, D, is negative, as entropy increases. Equation 7 is a modified version of Fick's Law to describe the motion of water vapour diffusion in one dimension:

$$\frac{dm}{d\theta} = -\mu \cdot \nabla p \qquad (9)$$

where,

        dm/dθ= mass flow [kg·s^{-1}]
        μ= proportionality constant, or diffusivity/permeability [kg·Pa^{-1}·m^{-1}·s^{-1}]
        ∇p= vapour pressure concentration gradient [Pa·m^{-1}]

Whole libraries of permeability values exist for various building materials. However, these values are aggregate diffusivities which also include the impact of surface diffusion, governed by RH, as well as intrinsic capillarity, from free water inside the tested material.

A more detailed equation exists that considers only the vapour diffusive components of moisture flow. Equation 10, developed by Krus (Krus, 1995), demonstrates the relationship between the mass flow density and the relative humidity:

$$\Delta g = g_w = -\left(\frac{1}{\mu} - \frac{1}{\mu^*}\right) \cdot \frac{D_D}{RT} \cdot \frac{dp}{dx} = -\left(\frac{1}{\mu} - \frac{1}{\mu^*}\right) \cdot \frac{D_D \cdot p_s}{RT} \cdot \frac{d\varphi}{dx} \qquad (10)$$

where,

      Δg = mass flow density [$kg \cdot m^{-2} \cdot s^{-1}$]
      g_w = mass flow density [$kg \cdot m^{-2} \cdot s^{-1}$]
      D_D = vapour diffusion coefficient of air [$m^2 \cdot s^{-1}$]
      μ = water vapour diffusion resistance [-]
      μ^* = water vapour diffusion resistance (fictional) including liquid transport [-]
      R = gas constant for water vapour [$J \cdot kg^{-1} \cdot K^{-1}$]
      T = absolute temperature [K]
      p_s = saturated water pressure [Pa]
      φ = relative humidity,

which becomes

$$g_w = -D_v \frac{dw}{dx} \qquad (11)$$

such that

$$D_v = \frac{D_D p_s}{RT}\left(\frac{1}{\mu} - \frac{1}{\mu^*}\right) / \frac{dw}{d\phi} \qquad (12)$$

Equation 12(12), now defines the mass flow density in terms of the moisture content concentration gradient and a diffusion constant, D_v. The derivative of the moisture content with respect to relative humidity is the slope on the sorption isotherm at the specified relative humidity. Many of the coefficients included in equation (12) are difficult to isolate and test in laboratory settings. Instead, the experimental approach utilized to determine the vapour diffusivity is to obtain overall vapour permeance values at specific relative humidity levels. Unfortunately, vapour permeance testing for CLT panels lies outside the scope of this thesis. Instead, as the primary constituent of CLT panels is wood, vapour diffusivities for the appropriate wood species were utilized.

3.1.4.2. Capillary Transport

Capillary suction is a result of molecular attraction between the surface and water molecules, such as the van de Waals forces discussed in 2.2.1, within pores of equivalent diameter less than 0.1mm (ASHRAE, 2009). Capillary suction is defined as,

$$s = \frac{2 \cdot \sigma cos\theta}{r} \qquad (13)$$

where,

      s = capillary suction [Pa]
      σ= surface tension of water [N·m^{-1}]
      r = equivalent radius of capillary [m]
      θ = contact wetting angle [degrees]

Capillary suction can also be linked back to the relative humidity of the air inside the pores, as per Kelvin's equation (Hiemenz & Rajagopalan, 1997):

$$\varphi = exp\left(-\frac{s}{\rho_w R_{wv} T}\right) \qquad (14)$$

where,

      φ=relative humidity
      s=suction pressure [Pa]
      ρ_w= water density [kg·m^{-3}]
      R_{wv}= gas constant for water vapour [J·kg^{-1}·K^{-1}]
      T= absolute temperature [T]

The relationship is a result of the complex interactions of water vapour molecules and the forces bonding the water molecules of the meniscus to the pore walls.

Suction is not the only force that acts on water flowing through pores. Friction forces are also generated with the flow of water. A parallel-tube approach is sometimes used (Krischer, 1963) to model liquid water flow through an unsaturated material because it allows for the use of the Hagen-Poiseuille equation:

$$Q = \frac{\pi \cdot r^4 \Delta p}{8 \mu L} \qquad (15)$$

where,

      Q= fluid flow [m^3·s^{-1}]
      r= effective pore radius [m]
      Δp= pore vapour pressure [Pa]
      μ= fluid dynamic viscosity [Pa·s]
      L= effective pore length [m]

Equation 4 can be rewritten to identify the pressure drop from fluid flow through the pore pathways:

$$P = \frac{8\mu L}{\pi \cdot r^4 Q}$$

(16)

In a transient setting, large pores will fill up more quickly than smaller pores due to the lower fluid flow resistance. However, as time elapses, capillary suction of the smaller pores will draw water from the larger pores. If the large pores are still in contact with a source, these will rapidly replenish, resulting in complex absorption behaviour for the porous material. In the case of drying, the large pores rapidly lose their water, whereas the smaller pores may sometimes retain the water, due to the strong capillary forces.

3.1.4.3. Effective Diffusivity

The complexities of modelling a flow network, as well as appropriately characterising the interconnectedness and dimensions of the pore network, generates the desire to take a lumped, simplified, phenomenological approach towards determining moisture flow. With the advent of nuclear magnetic resonance imaging and gamma ray imaging, transient water content profiles are now capable of being observed in porous media. It has been found that a modified version of Darcy's equation enables the calculation of water uptake in the liquid regime with generally good agreement with observable phenomena (Krus & Künzel, 1995). The equation hinges on the determination of the water absorption coefficient, or A-value, and relating that to the amount of water absorbed per unit area. By observing the moisture front profile, the A-value has been correlated to the effective moisture diffusivity of the material.

The A-value is determined from the slope of mass versus the square root of time during a water absorption test. The equation takes the form as follows (Krus & Künzel, 1993):

$$m_w = A \cdot \sqrt{t}$$

(17)

where,

    m_w= mass of water absorbed per unit area [$kg \cdot m^{-2}$]
    A= absorption coefficient [$kg \cdot m^{-2} \cdot s^{-0.5}$]
    t= time [s]

The absorption coefficient can be determined by a simple test involving the placing of a porous material in water. Hydrostatic forces should be minimized to ensure that only capillarity and diffusion transport occur. This is achieved by keeping the water level not more than a few millimeters above the material Surface. By plotting the mass gain against root time, the following plot is generated:
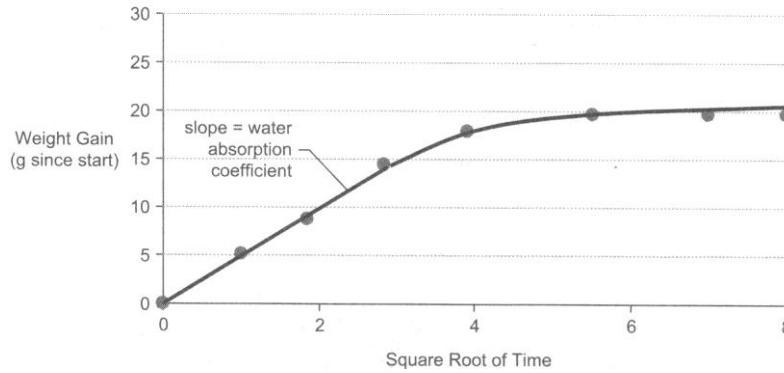
Figure 3.8: Water Uptake Test (Straube & Burnett, 2005)

Kunzel and Krus (Krus & Künzel, 1993) have correlated the absorption coefficient with an approximate diffusivity for inorganic and wood-based materials by observing the shape of the advancing moisture front. The average liquid diffusivity can be determined by using Equation 18:

$$D = \frac{\pi}{4}\left(\frac{A}{w_c}\right)^2 \tag{18}$$

where,

D= diffusivity ($m^2 \cdot s^{-1}$)
A= absorption coefficient ($kg \cdot m^{-2} \cdot s^{-0.5}$)
w_c= capillary saturated moisture content ($kg \cdot m^{-3}$)

However, for the diffusivity at a specific water content, Equation (19) can be used (Krus & Künzel, 1995):

$$D = 3.8 \cdot \left(\frac{A}{w_c}\right)^2 \cdot 1000^{[w/w_c - 1]} \tag{19}$$

Once the A-value is obtained and the capillary saturated water content is determined, the effective liquid diffusivity of the material is also determined.

Chapter 4- Experimental Program

To assess the effects of the moisture durability of the CLT panels, two experiments were devised to determine the moisture area densities of the wetted and drying samples. If the moisture characteristic of the wood samples can be categorized, in terms of the rate of uptake and drying, then this information can be input into a hygrothermal modelling program to run simulations in a multitude of climates and wall assemblies. The results of these models can help determine the propensity of the wood samples to experience environmental conditions conducive to decay. The first experiment was devised to calibrate WUFI to a simple water uptake test for clear sections of wood. The experiment also assesses the impacts of moisture uptake test repeatability and the effects that cracks impose on the absorption coefficient. The second experiment involves subjecting a 24"x24" CLT panel to water absorption and drying tests.

4.1. Clear Section Test

The intent behind these tests is to assess the capacity to model moisture uptake in WUFI for a simplified experiment, to determine the repeatability of moisture uptake tests, and to evaluate the impact of crack width on the moisture absorption coefficient. The testing comprised of multiple rounds of wetting and drying, with some of the samples being cut to mimic a natural crack between two boards in CLT panels.

The tests were not exhaustive and intended only to provide an initial estimate of the order of magnitude of the effects listed above.

4.1.1. Samples

A total of 10 samples were created. The samples consist of 2x6 SPF lumber that was stored in a humidity and temperature controlled lab for an extended duration. The samples were cut into 5.5"x5.5"x1.5" prisms. One of the samples had a prominent knot passing through the entire depth; this was selected for comparison purposes.

Figure 4.1: Three Samples, Clear, 1/16", 1/8" Cut

During drying, some of the samples started to leak sap and resin. The samples which exhibited such behaviour were samples 3 & 7.

To reduce the experimental behaviour to one dimensional flow, vapour and water impermeable membranes were used to wrap the samples. A polyethylene-faced bitumen membrane was first used to seal the samples. Aluminum tape was then used to seal any joints in the first membrane.

4.1.2. Procedure

The procedure used to undertake this testing was divided into two phases, a wetting and drying phase, each conducted in four separate rounds. The drying phase was used to dry the samples down to comparable moisture contents. The wetting phase consisted of placing the samples in an imbibition pool, placed in such a manner to minimize hydrostatic forces. The samples were wrapped in a vapour impermeable and waterproof self-adhering membrane, with aluminum tape used to seal the joints and corners. Table 4.1 provides the schedule that was followed for the testing.

Table 4.1: Testing Schedule

Round	Drying	Wetting	Notes	Purpose
1	60°C 0% MC	30% MC	Samples dried without waterproof membrane.	To obtain dry mass and initial absorption coefficient.
2	30°C 10% MC	30% MC	Samples dried with waterproof membrane. Six samples cut according to test parameters.	To determine effects of cracks and gauge influence of A-value fluctuation on repeated wetting.
3	30°C 10% MC	30% MC	Samples dried with waterproof membrane.	To determine repeatability of absorption coefficient testing.
4	60°C 0% MC	30% MC	Membrane removed and samples dried to 0% MC. New membrane installed.	To determine repeatability of absorption coefficient from 0% MC.

4.1.2.1. Drying

To ensure comparability between the samples, and since the properties of wood vary with moisture content, all the samples were dried to the same level. The drying phase was further divided into low temperature (30°C) and high temperature (58°C) series; depending on whether the samples were covered in a vapour tight membrane or not. The low temperature was also selected to minimize rapid shrinking from the saturated samples; which may cause undue stress to the samples, possibly resulting in damage. A small fan was placed inside the oven to minimize temperature stratification and to aid in the removal of moisture from the samples.

The **first round** of testing exposed the samples to a high temperature drying regimen. This was utilized to determine the dry mass of the samples- essential for gravimetric measurements. The samples were dried until two consecutive weighings did not differ more than 0.1% of the original mass. The following **second** and **third round** of testing saw the samples exposed to the low temperature drying regimen- to minimize damage to the waterproof membrane. The target moisture content was set to 10% MC. The **fourth round** was again at high temperature drying, but the waterproof membrane was removed. The samples were brought back down to 0% MC- attempting to replicate the conditions to the first round of testing.

The samples were weighed periodically throughout the drying phases to determine if they hit the target mass.

4.1.2.2. Wetting

The samples were placed faced down into an imbibition pool on a support structure to ensure that the water level was not more than 2-3mm above the face of the sample. This was done to minimize hydrostatic forces. The samples were weighed periodically and the values and time were logged.

4.1.3. Creating a Cut

After the first round of testing, a series of modifications were made to the samples to attempt to mimic cracks between the boards in CLT panels. The samples were divided into three categories- uncut, 1/16" cut, and 1/8" cut. The uncut samples were selected based on their calculated A-value- the samples with the highest, lowest, and median A values were selected to determine repeatability in the test method to obtain the moisture absorption coefficient. The remaining samples were divided into the 1/8" and 1/16" cut groups. The cut was made parallel to the grain to half the thickness of the sample, roughly in the center of each sample. The peel and stick membranes were removed in the locations where the cut was to be made. Repairs were made to the self-adhering membrane where required.

The 1/8" were cut down the center using a table saw, whereas the 1/16" group were cut using a bandsaw. It should be noted that the samples cut with a bandsaw did not result in a uniform depth due to flexing of the blade.

4.1.4. Results

The data collected from the test were the A-value from the samples for each testing phase. The following table demonstrates the original A-value from round 1 testing compared to the results from rounds 2 through 4. The cells shaded in pink represent uncut samples, the cells in blue represent the small cut samples, and the cells in green represent the large cut samples.

Table 4.2: A-Values from 4 Test Rounds in the Clear Sample Test, in $kg \cdot m^{-2} \cdot s^{-1/2}$

Sample	Round 1	Round 2	Round 3	Round 4
3	6.34E-03	4.94E-03	5.92E-03	6.01E-03
7	4.10E-03	3.31E-03	3.13E-03	4.64E-03
8	4.63E-03	4.04E-03	4.68E-03	4.89E-03
K	6.17E-03	4.42E-03	4.45E-03	6.22E-03
1	4.82E-03	3.95E-03	4.17E-03	5.38E-03
2	5.15E-03	4.24E-03	4.27E-03	5.72E-03
9	4.42E-03	4.03E-03	3.37E-03	5.11E-03
4	4.16E-03	3.21E-03	2.83E-03	4.42E-03
5	4.14E-03	3.41E-03	3.43E-03	4.81E-03
6	5.53E-03	5.10E-03	4.80E-03	5.20E-03
Average	4.95E-03	4.07E-03	4.11E-03	5.24E-03

Table 4.2 shows there is a decrease in the A-values in rounds 2 and 3. Since the samples were only dried to roughly 10% MC for rounds 2 and 3, it is possible that residual water remained stored in parts of the pore network and created dead ends in the pore network. A visual depiction of the above data is provided in Figure 4.2. The A-value from round 1 was plotted on the x-axis, whereas the A-value from round 2 (triangle marker), and round 3 (square marker), were plotted on the y-axis. The line running at a 45° angle represents an unchanged A-value from subsequent testing rounds. It does not represent the line of agreement, as some variations occur between rounds 1, 2, and 3 (such as some samples having been cut). It is only used to visually demonstrate deviations between rounds.
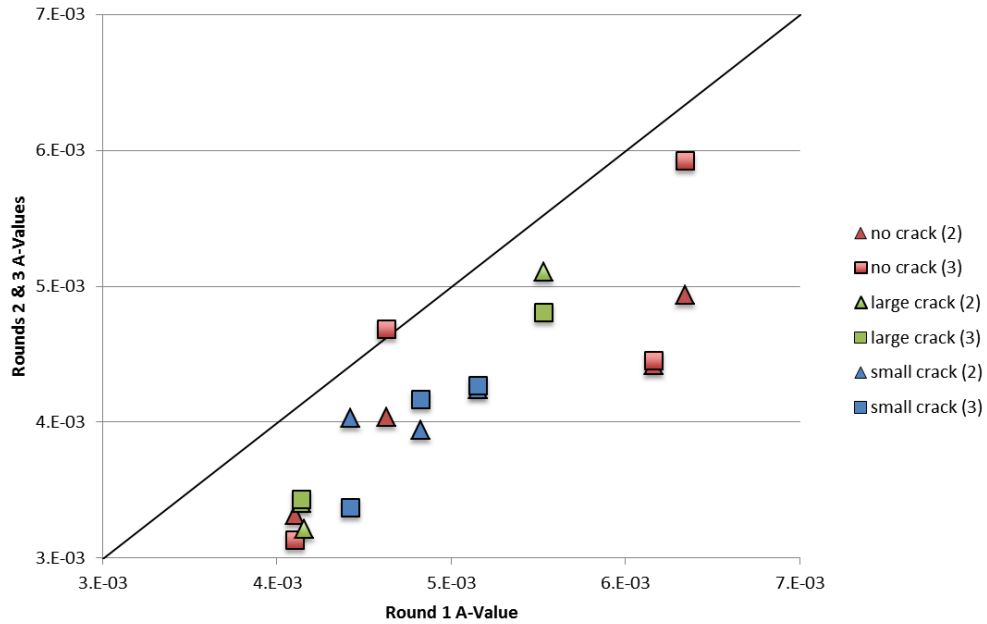
Figure 4.2: A-Value Comparisons from Round 1 vs. Rounds 2/3

Figure 4.2 shows all data points lie below the 45° line, e.g. the A-value from rounds 2 and 3 are less than the first round of drying. There seems to be no distinct pattern between rounds 2 and 3. Further testing with a larger sample size would be required to determine rates of A-value degradation between subsequent wetting and drying routines.

More importantly, the difference between round 1 and round 4, of which both samples were brought to near zero moisture content, should more appropriately reflect the difference between the pristine sample and the samples cut with the small and large crack. The results are plotted in Figure 4.3.
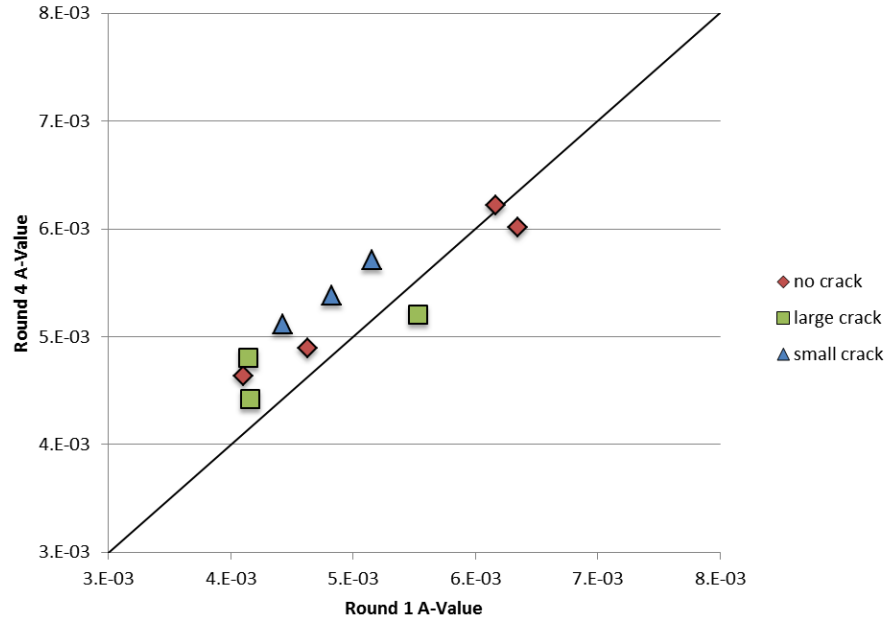
Figure 4.3: Results from Phase 1 vs. Phase 4

While the sample size is relatively small, it can be seen that all of the A-values from the small crack all exceed the 45° line of equality. The data also seems to suggest that the large crack samples are also slightly higher than the pristine samples, but further testing is required to identify if there is a statistical difference.

To mathematically verify the impact of the capillary action of the small crack, the following equation was utilized (ASHRAE, 2009):

$$h = \frac{T2l_c}{\rho g A_c}$$
(20)

where,

  h = capillary suction height [m]
  T = surface tension of water [N·m^{-1}]
  l_c= length of cut [m]
  ρ= density of water [kg·m^{-3}]
  g= acceleration due to gravity [m·s^{-2}]
  A_c=cross-sectional area of the cut [m^2]

With an assumed cut length of 141mm, the cut width of 1.6mm and including an extra 2mm from the level of the water, the effective capillary suction height is approximately 11mm. The depth of each cut is approximately 19mm. Consequently, the net increased surface area exposed to water (excluding 2-dimensional effects) is roughly 15% higher than the pristine samples. When this new calculated area is used to determine the A-value, the difference between the average A-values from rounds 1 to 4 for the small cut decreases from 12% to 2.8%. Insufficient capillary suction was found to occur with the 3.6mm sample- possible explanation for the marginally higher A-values is due to increased surface area for vapour diffusion.

4.2. CLT Panel Testing

To understand the moisture characteristics of full CLT panels, a second set of tests were devised to ascertain these properties. Unlike the clear section tests previously conducted, the CLT panels were selected to be sufficiently large such that the salient properties would not be compromised during testing- the samples include checks, cracks, pitch pockets, and other deviations from ideal conditions.

The moisture content of the samples was determined using both electrical resistance and gravimetric methods. The gravimetric values are used to assess the net moisture absorbed into the samples whereas the electric resistance pins, installed at various depths, were utilized to define the moisture profile through the samples.

Due to the intrinsic properties of the samples, the dry mass could not be determined- permanent deformation and damage to the sample would occur if dried down to near 0%MC. Consequently, a focus is placed instead on the rate of moisture movement instead of absolute values.

4.2.1. Samples

A total of 12 samples were received from Forintek. There were four types of CLTs that were received and three samples of each type: Eastern SPF (E), Western SPF (W), Western Hemlock (H), and European (Er). Each sample was 24"x24" in plan dimension; the thickness varied on the number of plies. The E, W, and H samples were built with 5 plies, whereas the Er samples had only 3 plies. The samples were face glued with a polyisocyanurate adhesive in a small scale manufacturing press. Figure 4.4 and 4.5 show a cut-away view of the panels.
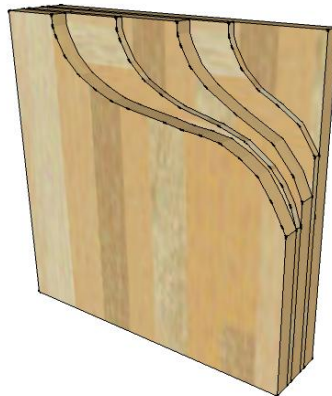
Figure 4.4: Five Ply CLt Panel Cut-Away
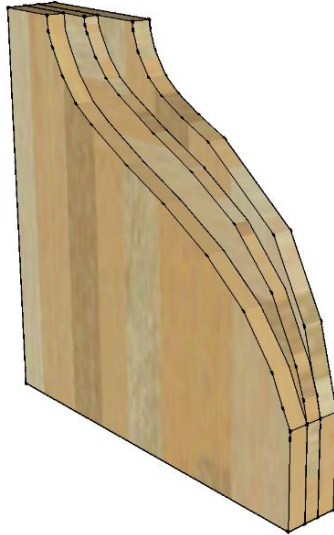
Figure 4.5: Three Ply CLT Cut-Away

The five-ply samples have two thicknesses- the first (1), third (3), and fifth (5) plies were 34mm thick, whereas the second (2) and fourth (4) were 18mm. In the three-ply samples, the outer layers were 30mm thick, whereas the central ply is 34mm. The samples were photographed and documented- the following tables summarize the findings.

Table 4.3: Summary of Sample Observations

Sample	Observation
Eastern SPF	Portions of the eastern SPF samples have pitch pockets (sample E1-back) The lumber was very knotted. Cracks between the lumber extend the full depth to the underlying ply in some samples. Crack widths vary from 1 to 3mm. Wood checks were observed and all samples- severity varies.
Western SPF	Western SPF samples are similar to the Eastern SPF- no pitch pockets were found and lumber was not as knotted.
Hemlock Fir	Much heavier than the other samples Exhibits same checking, splits, and cracking as E-SPF and W-SPF Some cracks run tangentially (splitting along earlywood and latewood)
European	Much lighter than other samples- 3 plies Unknown wood- some type of softwood Deep groves were observed between the boards. Forintek stated grooves are sometimes cut to control dimensional changes Pitch pockets were found, as well as areas wet to the touch (after being held at 21°C and 40% for several weeks). Less cracking and checking than the other three wood types.

Table 4.4 lists all the samples and their measured characteristics.

Table 4.4: Sample Dimensions, Mass, and Moisture Content

C.L.T. Type	Sample Number	Dimensions (mm) (LxHxW)	Mass (g)	Density (kg/m^3)	Surface M.C. (%)
Eastern S.P.F.	E-1		24081.8	491.7	7.0
	E-2	609.6x609.6x131.8	23940.1	488.8	6.9
	E-3		23348.5	476.7	7.0
Western S.P.F.	W-1		24479.3	499.8	6.9
	W-2	609.6x609.6x131.8	24457.2	499.4	7.0
	W-3		24521.7	500.7	6.8
Hemlock	H-1		26057.6	532.0	7.0
	H-2	609.6x609.6x131.8	25354.5	517.7	7.0
	H-3		25303.8	516.6	7.0
European	Er-1		16449.7	335.9	6.5
	Er-2	609.6x609.6x115.9	16509.1	337.1	6.4
	Er-3		16982.0	346.7	6.8

L=length, H=height, W= width

It can be observed from the samples that the density fluctuates with the wood species type- denser woods have a higher CLT panel density than the corresponding less dense CLT wood panel. However, due to the intrinsic properties of the construction process of the CLT panels, the voids, cracks and gaps between the boards and plies results in a slightly lower than average density for equivalent wood species. This will result in different porosities as well- no published data is currently available.

4.2.2. Apparatus

Two measuring strategies were utilized to ascertain the moisture behaviour within the wood samples; a gravimetric method, and an electric resistance method, as discussed below.

4.2.2.1. Gravimetric Method

The apparatus consists of a large set of scales with a 5 pound (2.27kg) beam load cell on one end and a counterweight on the other hand. This enables precise measurements to be taken with large sub-assembly scale samples. The resolution of the load cell is 0.25% of total weight- yielding a maximum weight error of 5.7g. When taken in combination of the mass of the CLT panels (in the order of magnitude of 18000g when wetted), this yields a %-wt error of roughly 0.03%. However, some losses are likely to accrue by having to overcome slight amounts of static friction in the bearings of the lever arm in the scales. Further errors may arise from signal noise in the data logging system and any swaying of the counterweight upon loading. To partially overcome some of these errors, 5g and 100 g calibration weights are applied before each test, and the 100g weight yields a voltage that, when converted, is approximately equal to 100g.

Figure 4.6: Five-Pound Capacity Beam-Type Load Cell

Load cells return a voltage in response to the applied force. As the voltage is linearly proportional to the load, it is sufficient to collect a few data points and calculated the slope and intercept for each load cell. Each load cell was calibrated in this way. Table 4.5 summarizes the slope and intercept for the linear equation for converting voltage to mass.

Table 4.5: Slope and Intercept from Load Cell Calibration (12V)

Scale	Slope	Intercept	R^2
1	-0.0021	-0.4576	1
2	-0.0025	0.041	0.999
3	-0.0024	-0.1776	1
4	-0.0025	0.0212	1
5	-0.0025	0.0101	1
6	-0.0024	0.1652	1

The scale set-up is best depicted in Figure 4.7.

Figure 4.7: Gravimetric Scale Set-up

Each load cell is connected to a Campbell Scientific CR1000 data logger. Data scans are taken every 5 minutes and an average of these readings is made every 30 minutes. Consequently, the data file collected by the data logger is input into a spreadsheet and the required conversions are made to return the mass loss of each sample. Changes in the counterweight mass required some modifications to the spreadsheet to allow for continuity of the mass loss.

4.2.2.2. Electric Resistance Method

The electric resistance method of moisture measurement functions on the basis that the electrical resistance of the wood changes with respect to the water content. Increase water content enables easier flow of an electrical current; thus, the higher the water content, the lower the electrical resistance. The electric field is measured using pins inserted into the wood. Due to the intrinsic properties of wood and moisture content pins, the readings only reflect the moisture content of a small section of the wood. Further, the existence of any cracks, checks, vessels, pitch pockets, or resin canals may cause disruptions in the electric field. Typically, electric resistance readings are not as accurate as gravimetric methods. Consequently, in this study, the electric resistance readings are used to generate a relative profile of the of the moisture profile throughout the specimen.

The value returned from the MC pins is an electrical resistance, given in Ohms. Higher moisture contents have lower electrical resistance due to increase electron flow through the material, further enabled by the water within the pore network. Very dry wood has a very high resistance, in the range of GigaOhms.

The electrical resistance is calculated by measuring the voltage drop across a known resistor, compared to the total voltage applied through the circuit. Figure 4.8 demonstrates the basic set-up to determine the electrical resistance of wood.
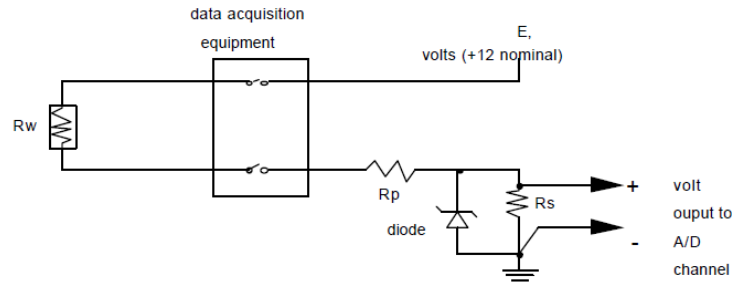
Figure 4.8: Circuit Schematic for Electric Resistance Measurements (Straube, Onysko, & Schumacher, 2002)

In the above schematic, R_w is the wood resistance, R_p is a resistor to protect short circuiting, and R_s is the sensing resistor. The applied voltage across the assembly is E, and V is the voltage measured across the sensing resistor. The diode is used to restrict excess voltages in the case that a short circuit occurs through the pins. Using Ohm's Law, that the current is proportional to the voltage potential times the inverse of the resistance, the resistance of the wood can be easily determined:

$$R_W = R_S\left(\frac{E}{V}\right) - R_p - R_S \qquad (21)$$

The following mathematical relationship was found by the US Forest Product Labs to related the electric resistance to the moisture content (in the range of 7-25%) for Douglas-Fir (Straube, Onysko, & Schumacher, 2002).

$$Log_{10}(MC_u) = 2.99 - 2.113\left(log_{10}(log_{10}(R_w))\right) \qquad (22)$$

where,

   MC_u= Douglas-Fir moisture content [%mass]
   R_w= electrical resistance returned from MC pins [Ohms]

Different species have different structures, chemical compositions, and pore networks. Further compounding the problem is variations that temperature may play on the moisture content readings. Thus, moisture contents returned from electrical resistance pins must be calibrated for the wood species and temperature. Many authors have found species and temperature correlations for moisture content. Using research done by Garrahan (Garrahan, 1988) the Equation 24 was derived:

$$MC = \left[\frac{R_s + 0.567 - 0.0260x + 0.000051x^2}{0.881(1.0056)^x} - b \right] \div a$$

where,

      R_s= meter scale reading
      x= temperature of the wood [°C]
      a,b= species correction regression coefficients (calibrated at 22.8 °C)

For the four wood species provided, the three sets correction regression coefficients used are presented in Table 4.6.:

Table 4.6: Correction Regression Coefficients for Wood Species (Garrahan, 1988)

Species Type	a coefficient	b coefficient	Corrected Reading[1]
Eastern white pine	0.821	0.556	11.48
Western white pine	0.969	-0.391	10.02
Western Hemlock	0.838	0.693	11.22

[1]Corrected value for original reading of 10% MC at 21.5 °C

As the wood species are not known, it was assumed that E-SPF corresponds to an eastern white pine, W-SPF as a western white pine, Hem-Fir as being Western Hemlock. The European species was assumed to be sufficiently close to Eastern White Pine.

As all the testing occurring at isothermal conditions, the effects of temperature are minimal. Technically, localized temperature depressions will occur at the surface of the wood samples due to evaporation, but this temperature effect is very small and can be ignored.

The moisture content pins used in this experiment were created by using stainless steel nails coated in a ceramic coating. The tips remained uncoated as well as the topmost portion of the shank- to enable connection to the electric circuit. For consistency, the pins were installed perpendicular to the wood grain at various locations in the wood panels. Such locations include the board edges, bottom and top of the panels, and at various depths. Typically, MC pins were installed at the quarter and halfway point of the first board, and 5mm past the adhesive edge into the second layer. Three types of pins were used depending on the required depth of penetration. Figure 4.9 demonstrates the depths of penetrations used (all units in millimeters).
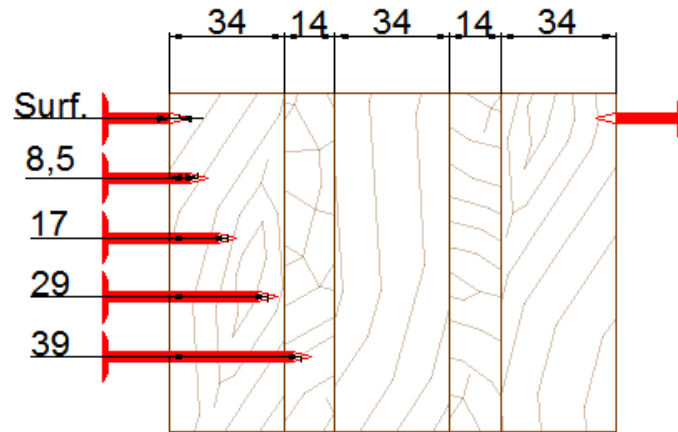
Figure 4.9: Moisture Pin Depth on 5-Ply Sample

Moisture content pins were installed at a depth of 8.5mm, 17mm, and 39mm on all the 5-ply samples- these depths correspond to the quarter depth points in the outer layer, whereas the 39mm pin is 5mm into the second layer of the panel. Extra pins were installed on some other panels to collect extra data- near the edge of edge lamina, at the bottom of the CLT panel, and at a depth of 29mm. The intent of the positioning of these extra pins is to determine any edge effects, the effects of gravity on redistribution, and to obtain a further understanding of the adhesive layer in the panel.

Similarly, on the 3-ply sample, moisture content pins were installed on the first two quarter points, and 5mm beyond the glue layer: a pin at 7.5mm, 15mm, and 35mm, respectively. Extra pins were installed at the middle of the second and third lamina on Er-3 (at 42mm and 79mm), and on Er-2, a moisture content pin was installed at 25mm depth, 5 mm within the first glue-line. It is common to assume an error of ±2% moisture content with electric resistance pins.

4.2.3. Procedure

The procedure used to determine the water absorption coefficient is divided into three-parts: 1) preparation, 2) wetting, and 3) drying.

4.2.3.1. Preparation Phase

Prior to wetting, each sample was photographed and documented- observations on the existence of cracking, checks, and pitch pockets were noted. The samples were measured using a Delmhorst meter to quantify their surface moisture content and their masses were taken.

Three types of water and vapour impermeable membrane systems were used. The types, explanation, and positive and negative consequences are discussed below.

Table 4.7: CLT Sample Preparation Information

Series	CLT Panel	Material	Installation	Notes
1	W1, W2, H2, H1	Bakor Blueskin TWF, Aluminum Foil tape	Aluminum tape was first used to wrap the edges, corners, and location of SAM joints. The SAM was installed on top of the Aluminum tape.	SAM=Self-Adhering Membrane. Edges peeled away as wood swelled and became saturated with water.
2	E1, E2, E3	Bakor Aquabloc 770, Bakor Blueskin TWF	SAM was used to cover the back of the CLT panel. Liquid applied membrane was used to seal the edges and wrapped on to the SAM.	Significant solvent loss, but very tight bond with the wood substrate. Samples were left to dry for a period of 6 months to ensure minimal impact on test results.
3	W3, H3, Er1, Er2, Er3	Bakor Blueskin, Staples/Simpson Strongtie Metal Strapping	SAM was used to wrap the samples. Staples or metal strapping was used to clamp down the edges of the SAM.	Minor peeling of the SAM along the edges of the panels. No Aluminum tape was used. Edge effects from nail/staple penetration is unknown, but assumed to be small.

Figure 4.10 depicts the process in which the Series 1 membrane system was installed.

Step 1- Seal Corners with Al Tape

Step 2- Apply Al Tape along Joint

Step 3- Apply first half of self-adhering membrane   **Step 4-** Finish membrane application

Figure 4.10: Preparation Procedures for Series 1 Membrane Application

Finally, the moisture content pins and a lag-eye screw were installed into the panels, as seen in Figure 4.11.

Figure 4.11: Fully Prepared CLT Sample

The samples were weighed one last time before starting the wetting phase.

4.2.3.2. Wetting Phase

Once the panels were prepared, they were placed in a soaking pool such that they imbibe water with minimal hydrostatic forces. The water level was maintained at a level no greater than 2-3mm above the bottom surface of each panel, using angled metal shelving to obtain the desired height. The panels were weighed periodically while imbibing water for a period of approximately 10 days. Figure 4.12 is a picture of Eastern SPF, Western SPF, and Hem-Fir samples placed in the soaking pool.

Figure 4.12: Imbibition Pool with Eastern SPF, Western SPF, and Hem-Fir samples

Once the samples reached fibre saturation, as determined by the innermost MC pin showing a MC nearly 28%, the samples were removed from the pool, weighed, and then hung on the scales.

4.2.3.3. Drying Phase

The drying phase consists of hanging each sample in the weighing apparatus. Figure 4.13 depicts four samples drying in the weighing apparatus. The laboratory was maintained at about 21 °C and 50%RH during the drying period.

Figure 4.13: Samples in Gravimetric Weighing Apparatus

The data were collected every five minutes. An averaging equation was utilized and provided an averaged value every 30 minutes. From the data collected during the wetting and drying phases, the absorption values were calculated for three wood species samples.

Previously, each load cell was calibrated such that the equivalent voltage read-out could be converted into units of mass. The mass loss was subtracted from the sample mass prior to drying and was converted into a moisture density flux ($kg \cdot m^{-2} \cdot s$).

4.2.4. Results

The results are divided into two distinct phases, as mentioned above. The results from wetting provide the water absorption coefficient, whereas the drying phase provides an estimate on the mass loss due to evaporation. Figures 4.14 to 4.16 graphically present the per unit area mass gain and loss from the wetting and drying phases for the various sample types.

These graphs were generated by plotting the change in mass relative to the initial water content. This was achieved by calculating the difference between two readings and adding it to the total water content of the sample. The same approach was utilized with the drying data and was concatenated to the data from the wetting phase. The exception is that the initial state for drying would be the saturated sample. Some slight modifications were made to account for changes in the counterweight mass.
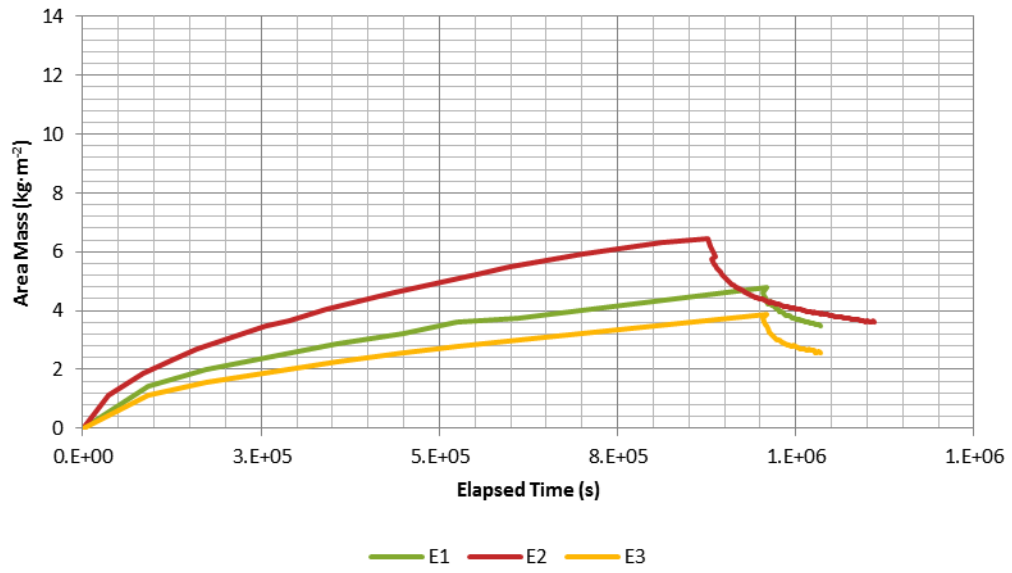
Figure 4.14: Moisture Uptake and Initial Drying for Eastern SPF CLT Samples
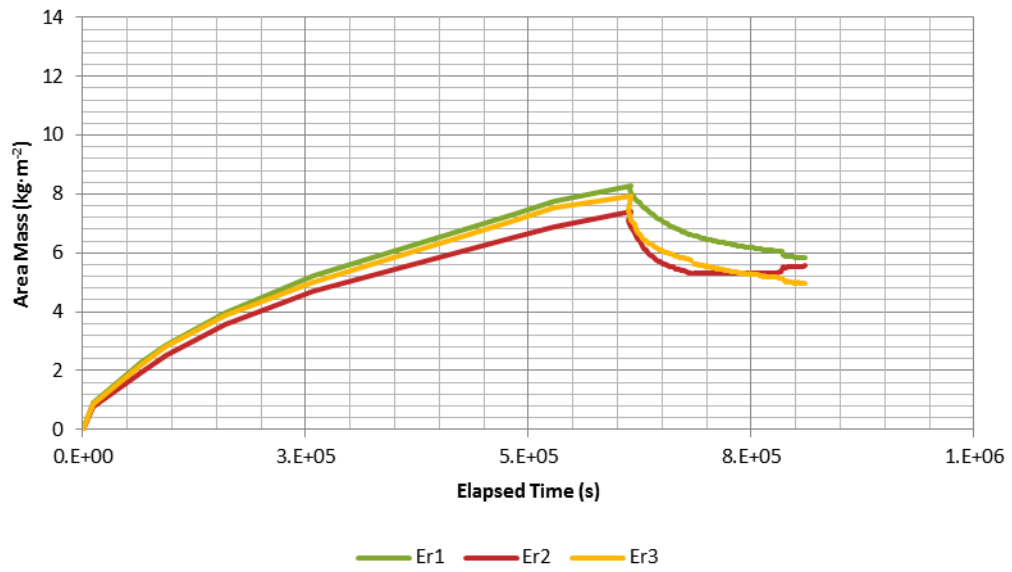
Figure 4.15: Moisture Uptake and Initial Drying for European CLT Samples
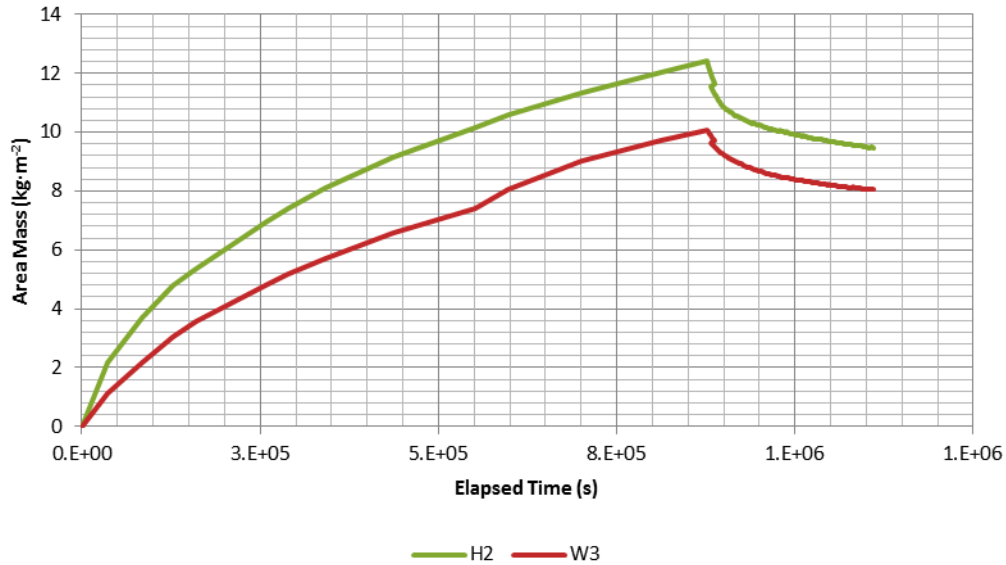
Figure 4.16: Moisture Uptake and Initial Drying of Hem-Fir and Western SPF CLT Samples

It should be noted that the first series of tests, which did not obtain sufficient data for the wetting phase, were not included in these plots. The data from the first series of experiments is provided in Appendix 2.

It can be observed that the grouping from all the European samples, and the two Eastern SPF samples which were tested together, seem to have similar ranges for total moisture uptake. Confounding factors in the wetting or preparation phase may invariably generate deviations to the results. Possible sources of error include different hydrostatic forces or weighing procedures. Nonetheless, testing all the species together at the same time would not have provided this revelatory bit of information.

When the uptake data are plotted against the square root of time, a straight line is formed. The slope of this line is the A-value, or absorption coefficient. Figures 4.17 to 4.19 plot such lines for the CLT samples.
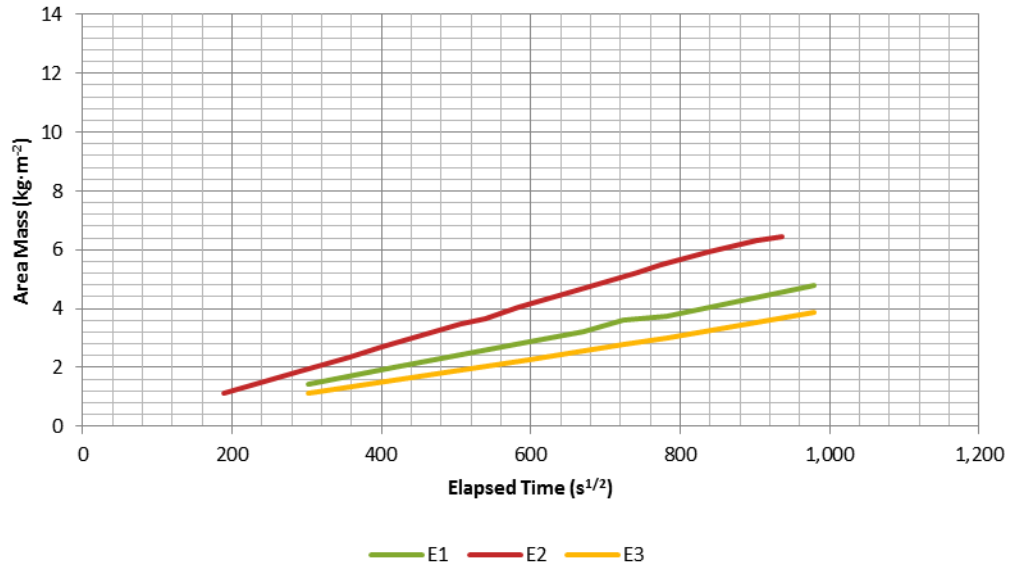
Figure 4.17: Mass v. Root Time for Eastern SPF CLT Samples
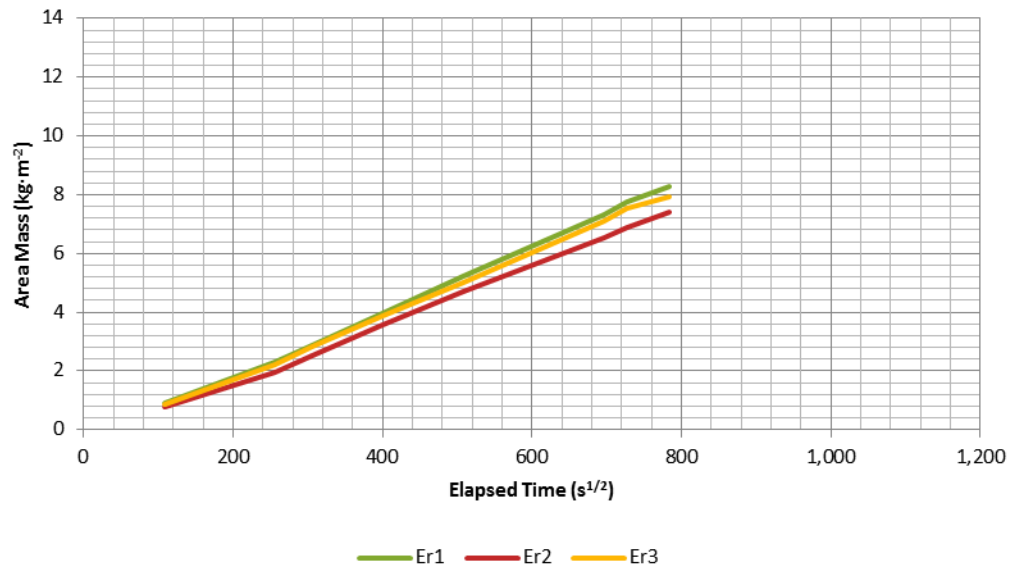
Figure 4.18: Mass vs. Root Time for European CLT Samples

57
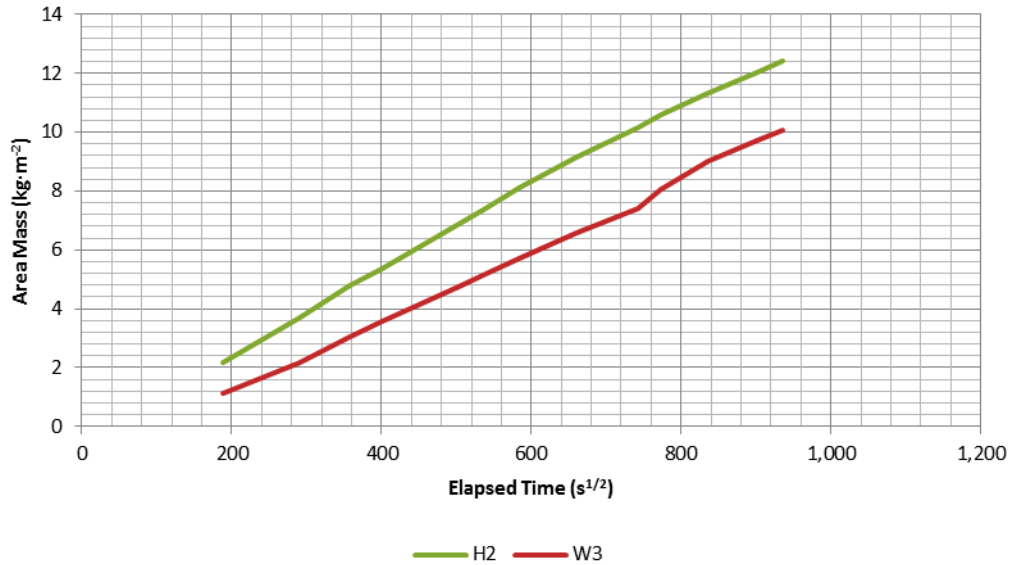
Figure 4.19: **Mass vs. Root Time for Hem-Fir and Western SPF CLT Samples**

The results for the A value are summarized in Table 4.8.

Table 4.8: Water Uptake Coefficients

Sample Type	Sample Code	A Value ($kg/m^2s^{1/2}$)	R^2 Value
Eastern SPF	E1	0.007	0.999
	E2	0.005	0.999
	E3	0.004	0.999
European	Er1	0.011	0.999
	Er2	0.010	0.999
	Er3	0.011	0.999
Western SPF	W3	0.012	0.998
Hem-Fir	H2	0.014	0.997

From the above plots, it can be seen that despite the European samples having roughly similar A-values as the Western SPF and Hem-Fir samples, the total moisture uptake between these two groups is not the same. It is possible that the different thicknesses between the two samples may be the parameter causing such variances. However, the resistance readings indicate near full saturation of the first and secondary lamina, with the last lamina not experiencing any observable moisture gain, on both 3-ply and 5-play panel types. It is unlikely that the saturated water content of the different wood species vary with any major significance. Consequently, it is possible that the adhesive layer between the boards requires a certain moisture content before bridging may occur. Alternatively, it is possible that the vapour impermeable membrane utilized may throttle upward moisture ingress due to increased pore pressure.

For comparative purposes, Table 4.9 provides published A-values for various woods.

Table 4.9: Published A-values for Wood Species

Species Name	A-Value (kg/m^{2}s$^{1/2}$)
Pine-Transverse (Krus, 1993)	0.0040
Pine- Longitudinal	0.0163
Softwood- Longitudinal (Candenado & Dérome, 2005)	0.0121
Softwood- Tangential and Radial (Candenado & Dérome, 2005)	0.0047

As can be seen in the previous tables, the A-values from the CLT panels correspond roughly with published A-values for different wood types. However, the A-values from the panels are all slightly above their corresponding counterparts. From the previous testing, the cracks between the boards in the laminae likely slightly increase the absorption rates of the CLT panels.

As the primary component of the panels is wood, the agreement between the obtained A-values indicates generally good agreement in using data from transverse wood species in the modelling.

When considering the moisture profile throughout the sample, plotting the electric resistance against time for the various depths can provide insight into the transient moisture content profile through the sample. The maximum recordable moisture content is 30%- actual moisture contents may exceed 30% MC. The following plots were produced with this data during the wetting and drying phase for an Eastern, Western, Hem-Fir, and European samples. The remaining plots for the other samples are provided in Appendix 3.
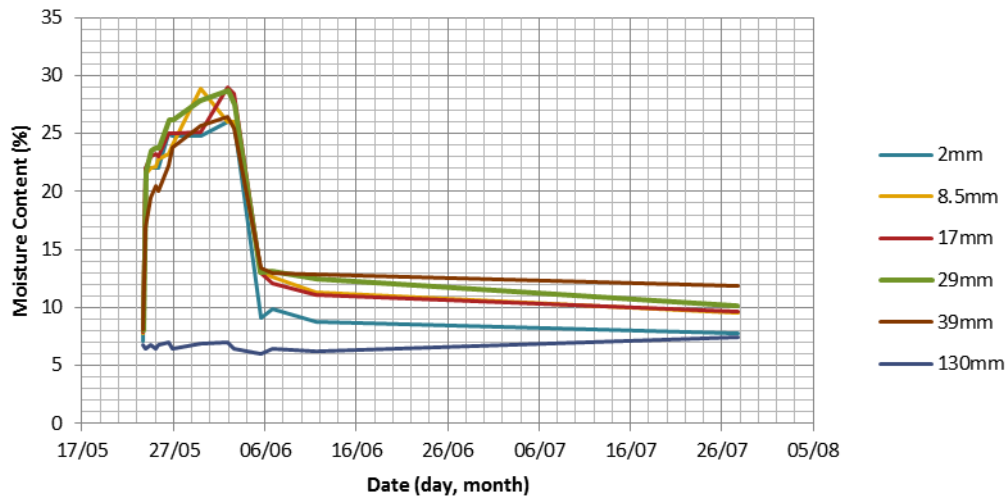
Figure 4.20: Moisture Profile of CLT Sample W2

MC Profile: E3
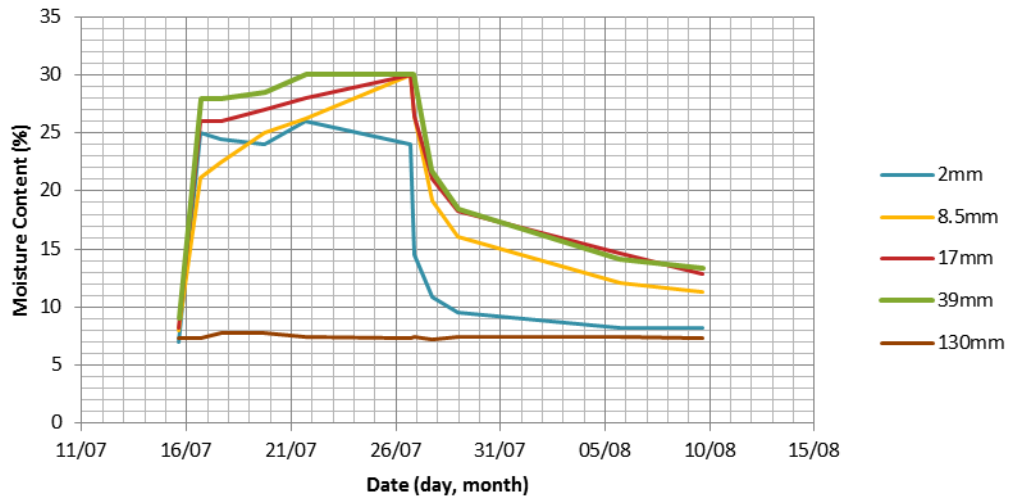
Figure 4.21: Moisture Profile of CLT Sample E3

MC Profile: H2
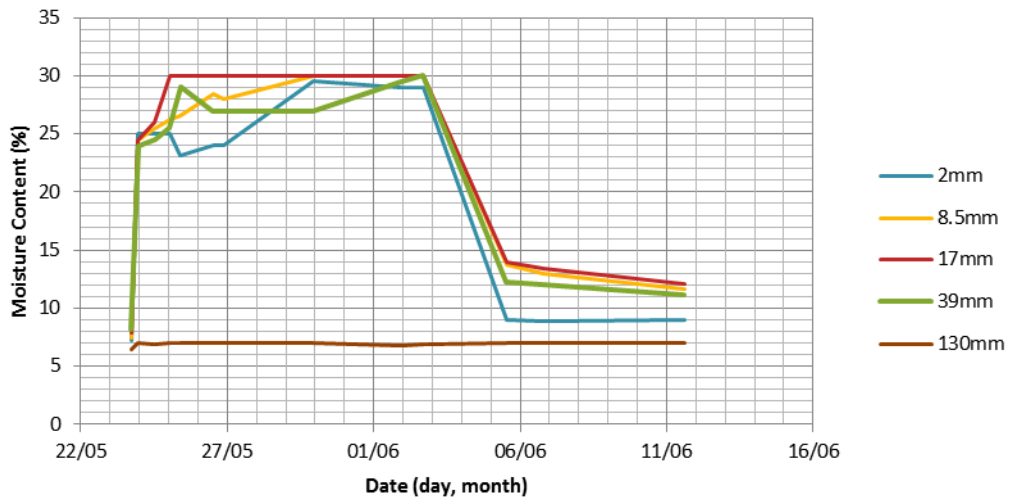
Figure 4.22: Moisture Profile in CLT Sample H2

MC Profile: Er3
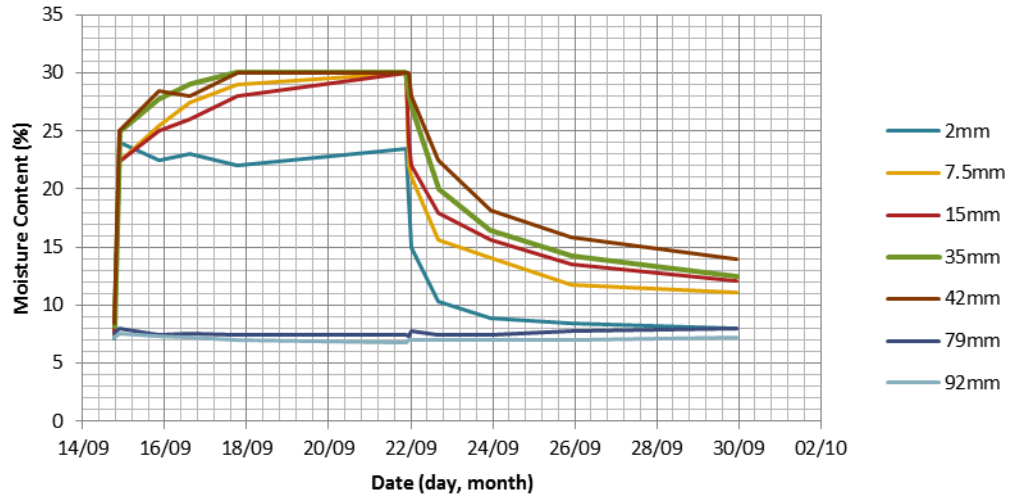
Figure 4.23: Moisture Profile in CLT Sample Er3

Moisture profile plots for the four select samples show the moisture content rapidly rises in not only the outermost layer, but that the inner layers also experience quick absorption during imbibition. However, as the samples are hung to dry, the moisture contents rapidly drop from their saturated moisture content levels down to below 15% MC in the span of less than 3 days.

Chapter 5- Analysis and Calibration

To assess the durability performance capacities of CLT panels without building a multitude of field exposure experiments across various climates, a modelling approach must instead be used. However, as a material property database of CLT panels has yet to be compiled, an analogue in the hygrothermal software must instead be used and modified accordingly. This calibration, based on experimental observations, is crucial to ensuring representative behaviour of the CLT in an in-situ scenario.

5.1. WUFI

The hygrothermal numerical program chosen to analyse the moisture flows in the wall assemblies was WUFI. Current moisture flow theory has difficulty in properly accommodating for the inhomogeneity, transient temperature and moisture characteristics, and anisotropic properties of wood- this is a limitation of some software. However, WUFI was programed with the underlying equations being calibrated and based upon macroscopic empirical behaviour of organic and inorganic materials (Künzel, 1995). This precludes the detailed testing required to generate topological material properties (e.g. pore size distribution, frequency of checks and cracks, etc.). The accuracy of the WUFI simulations have been verified by the Fraunhofer Institut Bauphysik in Holzkirche, Germany, against numerous full-scale field studies of enclosures over a number of years.

WUFI possess the capacity to properly account for water vapour adsorption and the absorption/redistribution of liquid water. The simulation is run for a given period, with the most common time step being 1 hour, considering the effects of sun, rain, temperature, and humidity. The quality of the results is extremely dependant on the veracity of the input material and condition data.

5.2. Procedures

The procedure used to calibrate WUFI to the data collected during the experiment was to first start with a simplified model and then conduct a parametric study on the various properties of this said model. Once an understanding of the relative influence of each property and characteristic is obtained, then new layers of complexity are added to the simplified model.

Initially, WUFI was used to model Sample #7 from the clear section test- sample #7 was selected due to the increase number of data points collected during the first round wetting phase, that it had one of the lower absorption coefficients of all the samples (it provides a lower bound to the problem), and because this sample was not used to test the effects of a cut in later rounds. Once the WUFI model closely matched the results from #7, the same calibrating procedure was applied to Sample #8, another sample which was not cut in subsequent testing rounds, and any modifications were made as required.

Once good agreement was found between modelling the clear section test samples to WUFI, the next step was to attempt to model the CLT panels. The European samples were selected first due to the decrease number of glue layers in the sample, its lower mass (a larger moisture response), and the higher quality of materials and manufacturing. Due to the different topographical nature of the CLT panels to pristine wood samples, another parametric study was undertaken to ascertain the influence of the various modelling properties in order to match the observed behaviour of the panels. Lastly, the discoveries learned from the parametric study were applied to the remaining 5-ply CLT panels.

5.3. Modelling

The approach taken towards modelling was to first model a clear sample wood sample to understand the relative effects of the various phenomena acting upon the sample.

5.3.1. Climate File

To replicate the wetting process, a climate file was designed using the included Excel climate file generator. The excel weather file is created by assigning the salient hygrothermal properties to every hour throughout the climate file period. The minimum parameters that must be included in the weather file are air temperature and air humidity- if no others are included; WUFI assumes the values are zero. The other conditions are radiation, precipitation, air pressure, wind direction, wind speed, and cloud index.

The lab is maintained at a constant temperature of 21°C and 50% RH using a PID controller. To replicate the samples being placed in a pool of water, the amount of precipitation, in $L \cdot m^{-2} h^{-1}$, was set to 99.9, as measured on the surface. This occurred for the entire period in which the samples were placed in the wetting pool. Afterwards, the rain value was set to 0.

The file was exported as a .WAC file and uploaded into the climate category in WUFI.

5.3.2. Boundary Conditions

As discuss above, the exterior side of the WUFI model was characterized by the climate file- exposure to air temperature, relative humidity, and rain. The interior side was set to a constant temperature of 21°C and relative humidity of 50%. Since the samples were wrapped with peel and stick across the back of the membrane, a vapour impermeable layer (Sd=100) was set on the indoor side of the model. The surface heat transfer coefficient was set to interior conditions.

5.3.3. Material Properties

The empirical tests only provided the basic material properties of volume, mass, absorption coefficient, and a transient moisture content profile through the samples. Many other properties had to be inferred from existing materials that are analogous to CLT panels- primarily, softwood lumber. The salient material properties that deal with moisture movement characteristics are density, porosity, reference moisture content (u_{80}), saturated moisture content, absorption coefficient, sorption isotherm, liquid moisture diffusivity, liquid moisture redistribution diffusivity, and the vapour diffusion coefficient. Again, because the tests were held at isothermal conditions, properties such as specific heat and thermal conductivity were neglected.

The base material utilized to broach the first cut analysis was a *Spruce, radial*, from the Fraunhofer-IBP-Holzkirchen; Germany source. The base properties are listed in Table 5.1:

Table 5.1: Baseline Spruce, Radial, Material Properties

Property	Value
Bulk Density	455 (kg·m^{-3}) °
Porosity	0.73 (m^3·m^{-3})
Diffusion Resistance Factor	130
Reference Moisture Content	80 (kg·m^{-3})
Saturated Moisture Content	600 (kg·m^{-3})
Water Absorption Coefficient	0.0004 (kg·m^{-2}·s$^{-1/2}$)

Bulk Density

The bulk density is the dry mass density of the material. Since wood can typically contain up to roughly 200% MC, the density plays an important role in characterising the sorption isotherm of the various wood products out there.

Porosity

The porosity determines the maximum amount of water that is capable of being held within the material pores. If this value exceeds the saturated moisture content, then this implies that bulk water is being held within voids in the material.

Diffusion Resistance Factor

The diffusion resistance factor sets the upper limit to the vapour diffusion resistance through the material. However, WUFI enables this factor to be dependent on the normalized water content of the sample. As wood increased in moisture content, its diffusion resistance decreases, due to opening of some of the pits and what is known as the "island effect"- pockets of water that are caught within a pore structure that effectively shortcut the path that a water molecule must take by unleashing a bound water molecule at the other end of the saturated pore network.

Reference Moisture Content and Saturated Moisture Content

These two values dictate two points in the suction and redistribution curves that WUFI generates as part of the liquid diffusivity of the material. The reference moisture content is the moisture content at a relative humidity of 80%, and the saturated moisture content is the maximum amount of water that can be held within the pore network through capillary forces.
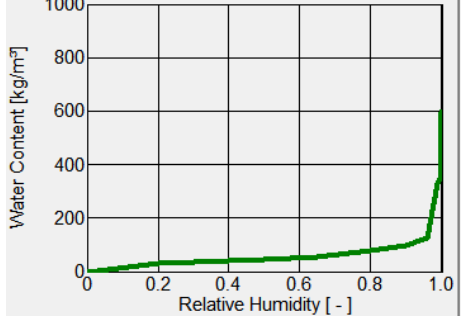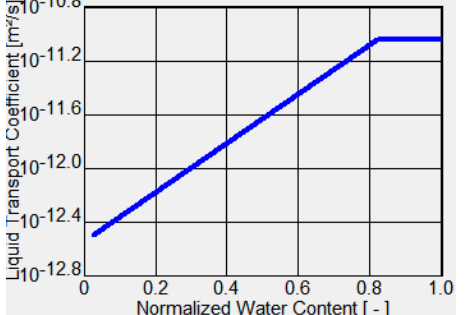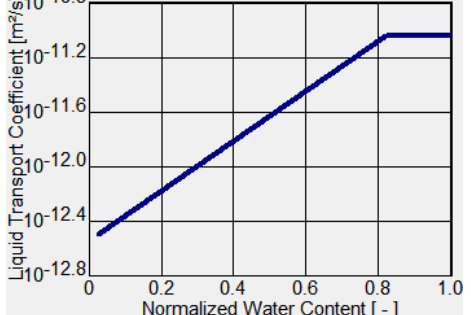
Water Absorption Coefficient

The water absorption coefficient determines the rate of moisture uptake via suction mechanisms. It also indirectly affects the redistribution values- unless otherwise modified, WUFI assumes that the liquid redistributive forces are a tenth of the suction values.

The following figures are graphs that WUFI utilizes to determine moisture flow through a material where the properties vary based on the normalized water content. The three most important ones are the **sorption isotherm**, **liquid transport coefficient- suction**, and **liquid transport coefficient- redistribution**. The moisture dependant water vapour diffusion resistance factor also plays a role in water movement

through the materials, due to the propensity of liquid water in the sample tests; its relative influence is decreased.

Table 5.2: Water Content Dependant Variables for Spruce, Radial, in the WUFI Database

Property	Plot
Sorption Isotherm	
Liquid Transport Coefficient- Suction	
Liquid Transport Coefficient- Redistribution	

5.4. Calibration

To assess the relative impact of the above mentioned properties, a parametric study was conducted. First, a baseline WUFI model was generated for the pristine sample experiment by calibrating it to the results from the experiment, using the collected data. Then, the procedure utilized was to hold all the values to those given in the WUFI database and modify one variable at a time to plus or minus 10% of the given value. Alternatively, a range of plus or minus 30% will be used for values in which insufficient response is observed using the former range. The values which were subjected to the parametric study are: sorption isotherm, absorption coefficient, liquid water diffusivity for redistribution, the porosity, and the vapour diffusion resistance. The primary metric for comparison is the total moisture uptake as compared to the empirical samples. Once the relative impacts of these properties were determined, the same procedure was applied to the 3-ply and 5-ply CLT specimens.

For the values important to redistribution, engineering judgment was used to compare the transient moisture content simulation with the moisture profiles collected from the moisture content pins.

5.4.1. Clear Wood Sample Test Calibration

As previously discussed, the clear wood sample consists of 38mm of spruce softwood given in the WUFI database. However, as the only data accumulated was related to moisture uptake, and not the drying process, the pristine wood sample tests were utilized to calibrate the moisture uptake- the redistribution values (D_{ww}) were not considered as part of this parametric study.

The baseline WUFI model was generated by comparing the results piece meal with the obtained data from sample #7. Sample #7 was selected due to the increased number of data points collected during the uptake test- this is due to it having a lower absorption coefficient. Consequently, using sample #7 as a baseline, it should provide a reasonably conservative lower bound value for all the other tests.

The first step was to model the sample using the data provided from the WUFI database. The following plot depicts the WUFI simulated total water uptake versus that of sample #7.
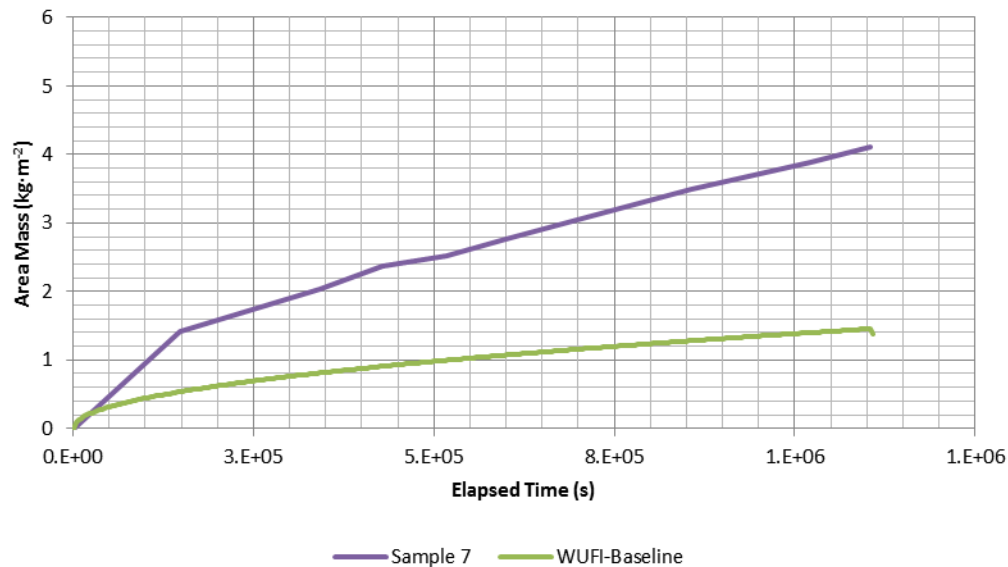
Figure 5.1: WUFI Baseline Result vs. Sample #7 Total Moisture Uptake

As can be seen in the previous plot, the total amount of moisture uptake is far greater in the sample that what is captured in the WUFI simulation. But this simulation was run utilizing the database A-value: 0.0004 $kg \cdot m^{-2} \cdot s^{-1/2}$. By changing this to the measured value of 0.00457 $kg \cdot m^{-2} \cdot s^{-1/2}$, the following plot is obtained.
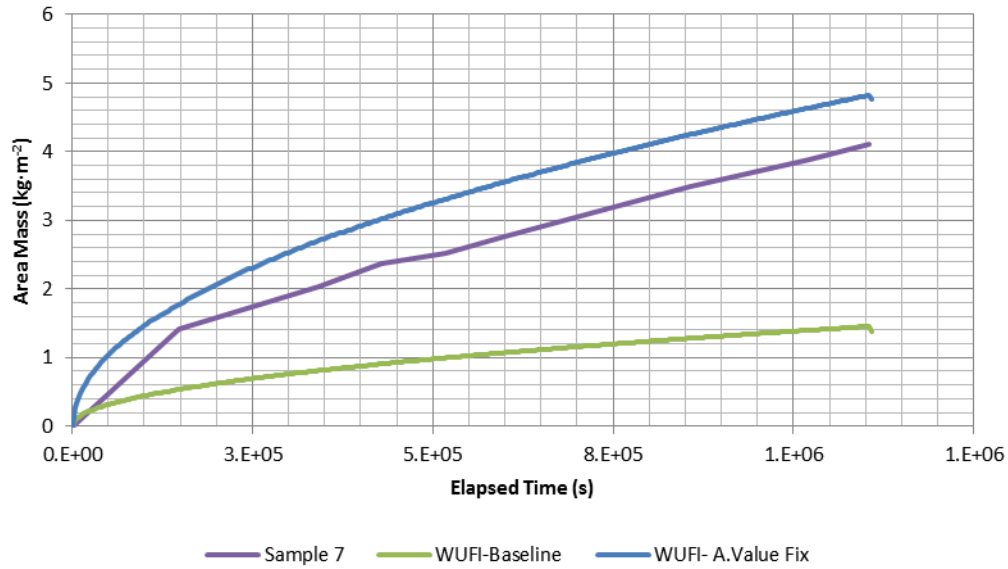
Figure 5.2: WUFI A-value Corrected vs. Sample #7 Total Moisture Uptake

Thus, it is apparent that modifying the A-value by an order of magnitude has a significant impact on the total water uptake in the sample. However, the simulation overestimates the actual water content absorbed by sample. As wood generally has a maximum moisture content of roughly 200%, the sorption isotherm must also be modified to more accurately reflect the actual sample. Since the WUFI database has the density, and consequently the sorption isotherm, set for a bulk density of 455 kg·m^{-3}, and the sample density was only 378 kg·m^{-3}, it was hypothesized that reducing the sorption isotherm by the ratio of the two densities, a total of 17%, that the total uptake would more closely match the results obtained from sample #7. The following is the result of that modification:
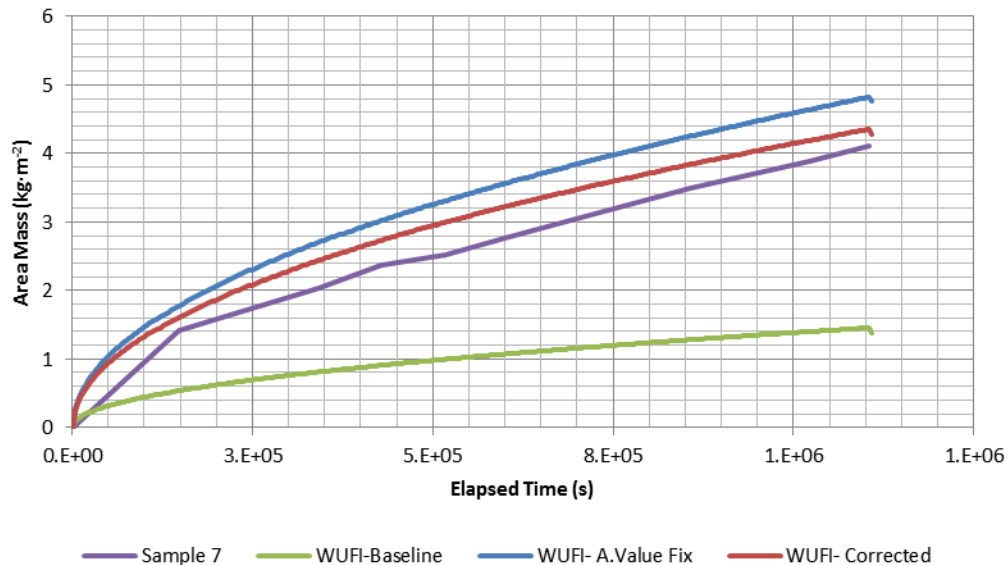
Figure 5.3: WUFI A-value and Sorption Isotherm Corrected vs. Sample #7 Total Moisture Uptake

67

As can be seen, the corrected model closely matches the total uptake from sample #7 from the experiment. Thus, the results of this comparative analysis are that the appropriate A-value and density corrected sorption isotherm seem to approach the observable behaviour of the samples. This same technique will be utilized for all the other models. However, as no data were collected on the effects of vapour diffusion resistance, sorption isotherm, porosity, or other properties, out of prudence, these values were left to those given in the WUFI database. Instead, they were subjected to a parametric study, as listed below.

5.4.2. 3-Ply CLT Calibration

In applying the knowledge gathered from the modelling of the clear sample tests, the same routines were applied to the three ply CLT samples. The exception in this case is that now redistribution values were obtained from empirical testing- moisture properties related to redistribution must now also be considered.

Within the WUFI database resides a model for a CLT material provided by the German Society for Wood Research. This material was utilized as a baseline for calibration with the 3-ply CLT panels. The results from the simulation, plotted with the results from European sample #1(Er1) is as follows:
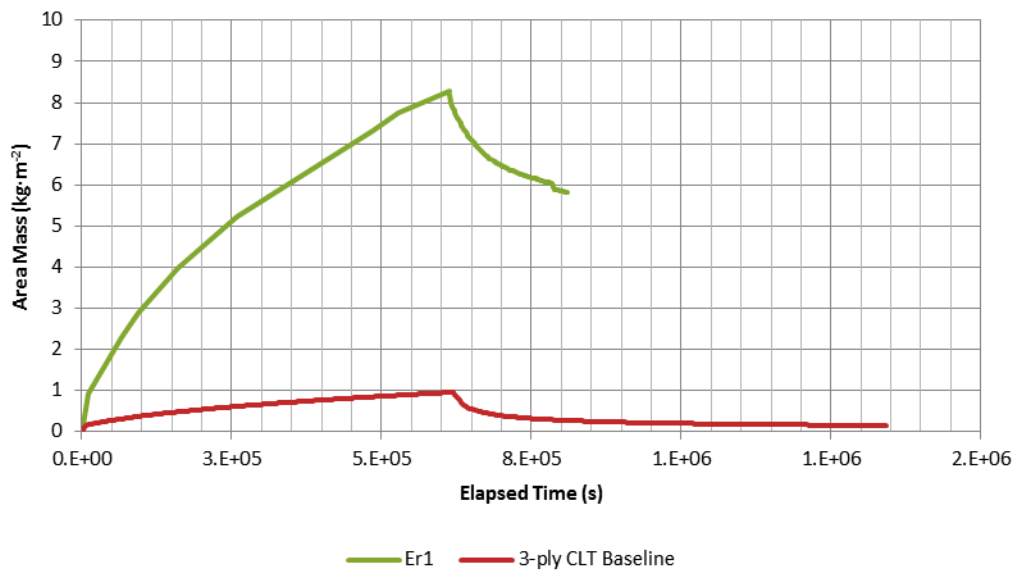
Figure 5.4: Baseline CLT material plotted with Er1 CLT Sample

Following the same strategies discovered in the previous testing, corrective measures were made to the A-value and to the density of the material. The new results still does not provide a sufficiently high area density, as seen in Figure 5.5.
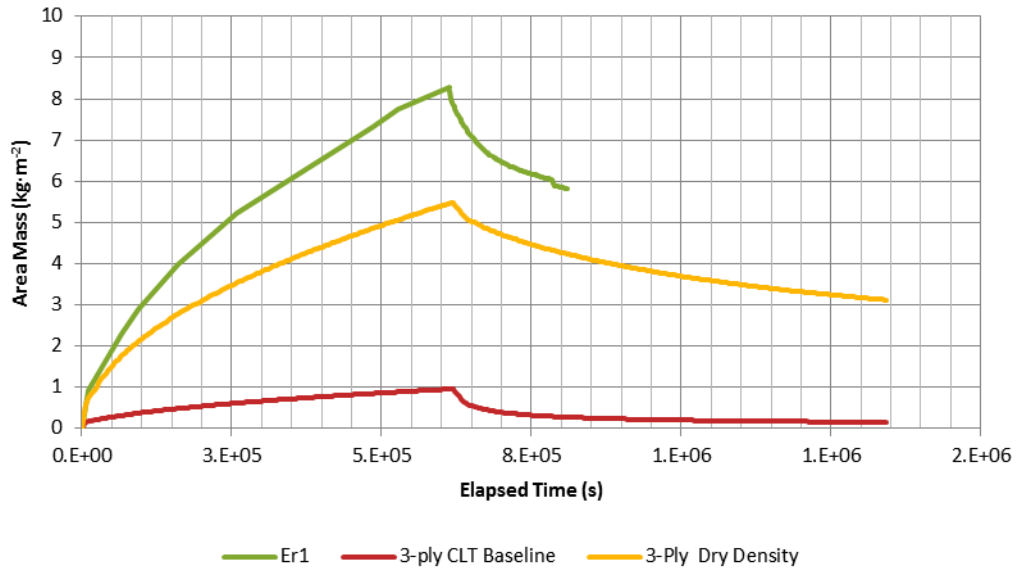
Figure 5.5: 3-Ply Density and A-value Corrected plotted with Er1 and Baseline Data

The density used to create the 3-Ply Corrected curve subtracted the equivalent moisture content of the sample to obtain the dry bulk density. However, by including the equivalent moisture content as part of the bulk density of the panels, a more representative curve is obtained. It is likely that the same problem was encountered in determining the dry mass of the samples- that drying to near 0% MC would result in structural damage to the panels.
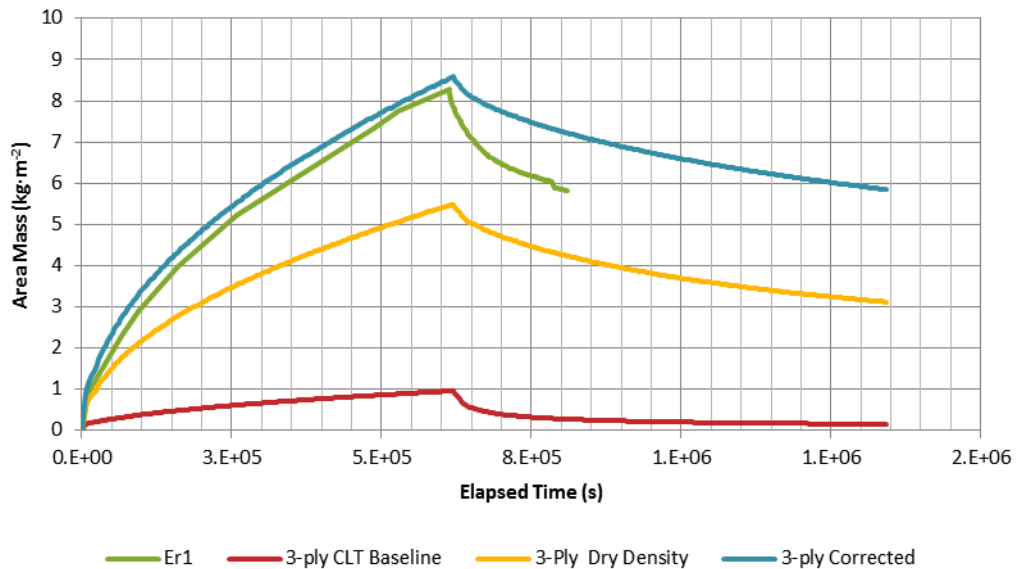
Figure 5.6: 3-Ply with EMC Density plotted against Baseline and Bulk Density Data

It can be seen that there is generally good agreement between the 3-ply corrected plot and the Er1 sample. However, a discrepancy still exists in matching the drying values between the simulated and empirical values. As the drying process is a very complex phenomenon and little research exists in the way of creating appropriate models, the matching process is a matter of trial and error of matching not

only the area mass of the samples, but also the moisture profile front, as collected by the moisture content pins.

The plot for redistribution contained within the WUFI data file is shown in Figure 5.7.
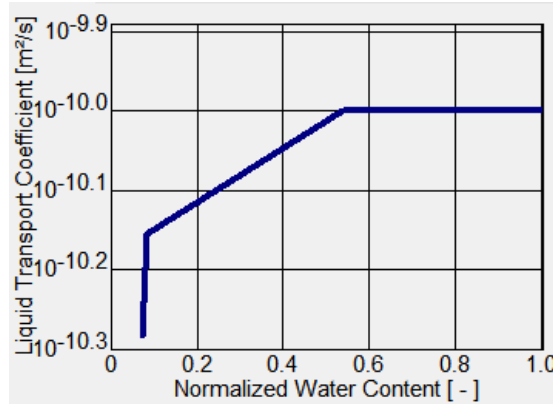
Figure 5.7: Liquid Transport Coefficient for Redistribution of CLT Sample

For reference, the liquid diffusivity of the CLT material in the WUFI database is listed below, in Table 5.3. However, these values are corrected for the density. The normalized water content is based on a material porosity of 0.56.

Table 5.3: Liquid Diffusivity for Suction and Redistribution for WUFI Database CLT-Density Corrected

Normalized Water Content	Water Content ($kg \cdot m^{-3}$)	Liquid Diffusivity, Suction ($m^2 \cdot s^{-2}$)*	Liquid Diffusivity, Redistribution ($m^2 \cdot s^{-2}$)
0	0	0	0
0.09	53	7.6E-12	5.2E-11
0.11	60	-	7E-11
0.70	393	3E-9	1E-10

*These values were generated from the A-value

However, a disparity still exists in the drying rates between the simulation and the test results. Data by Krus and Vik (Krus & Vik, 1999) suggest that in the saturated regime, a liquid diffusivity of 100 may be used for wood. In doing so, it may be observed that a quicker drying rate occurs within the regime- not to the same magnitude as in the test sample, but much more closely modelled than the simulation without the highest redistribution factor.
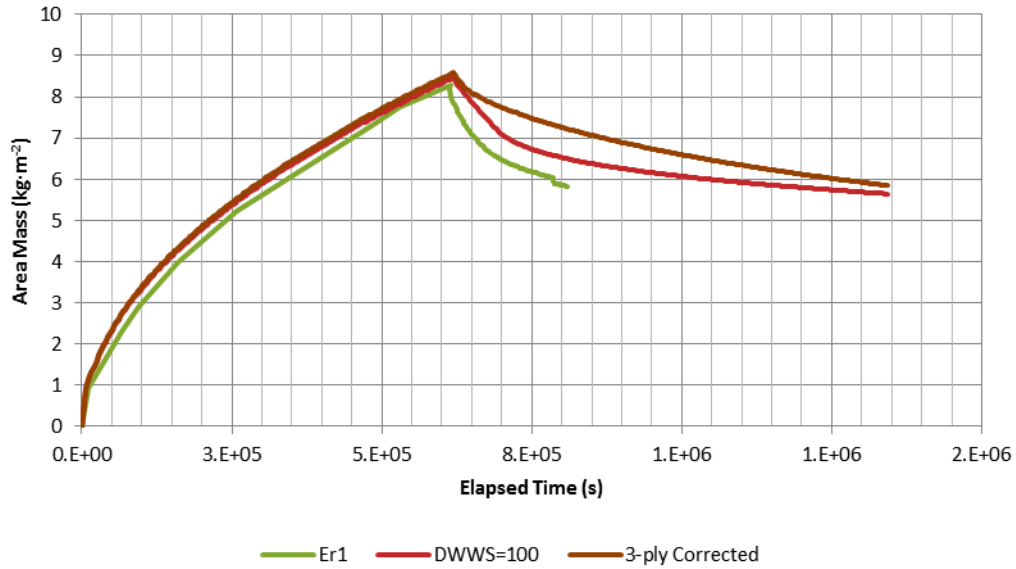
Figure 5.8: Drying rates with Dwws set to 100 Compared to WUFI Data

Intuitively, increasing the liquid diffusivity should result in faster drying rates. However, the degree of drying is noticeably less than when the saturated diffusivity is set to 100. At the initial drying phase, it can be seen that the rate of change of the slope is constant. This suggests that another factor is limiting the drying of the panels. As a fan was located above the drying racks, it was posited that changing the heat transfer coefficient, and thus the moisture transfer coefficient, from 0.125 $m^2 \cdot K \cdot W^{-1}$ (preset for "partition wall" in WUFI) to 0.0588 $m^2 \cdot K \cdot W^{-1}$ (preset value for "external wall") could possibly help to steepen the slope in the drying rate.
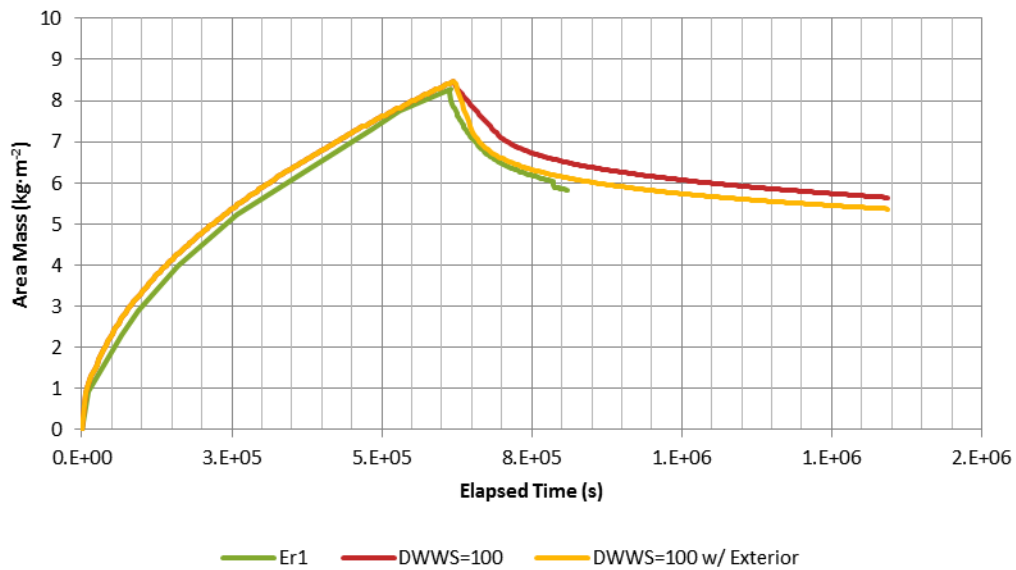
Figure 5.9: Boundary Condition Change to Enhanced Surface Transfer Coefficient

While the total uptake now approaches that of the sample, problems still persist with the transient moisture profile through the sample. A higher liquid diffusivity in the saturated regime necessitates a high inward redistribution as well, thus increasing the overall time to drying due to elevated water penetration into the sample. Collected data indicates that no such rapid redistribution occurs. By trial and error, it was found that one of the biggest influences is not the maximum value of the liquid diffusivity, but the rate of change of the liquid diffusivity that affected the overall rate of mass loss. Thus, a value of 100 $m^2 \cdot s^{-1}$ was kept and an arbitrary data point was selected such that the rate of drying closely matched the actual sample.

Near saturated water contents, the boards swell to such a point that the cracks between them were closed shut. After a short period of drying however, the cracks re-emerged. This results in a noticeable increase in surface area- approximately 70%. However, the effective surface area would be much less than that, due to constriction of air flow and degree of swelling of the boards. To represent the shrinkage of the boards, the arbitrary corrective value was selected at 10kg·m^{-3} less than saturated (383 kg·m^{-3}) and, through trial and error, a liquid diffusivity of 1E-4 $m^2 \cdot s^{-1}$ was found to provide generally good agreement in terms of water content density as well as transient moisture profile.
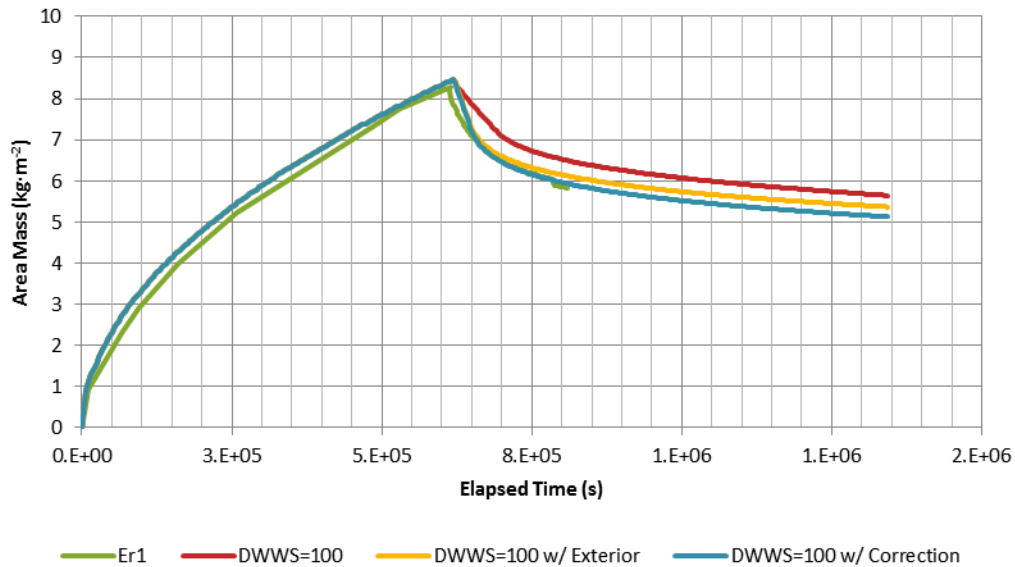
Figure 5.10: Modified Redistribution Values for Simulated Model

As can be seen in the above figure (Figure 5.10), good agreements are achieved not only in the rate of drying, but also in the magnitude of the water content. Further, the transient moisture profile of the simulated model is in generally good agreement with the results from the moisture content pins. The following table lists the values used for the liquid diffusivity in redistribution and the justification for its use.
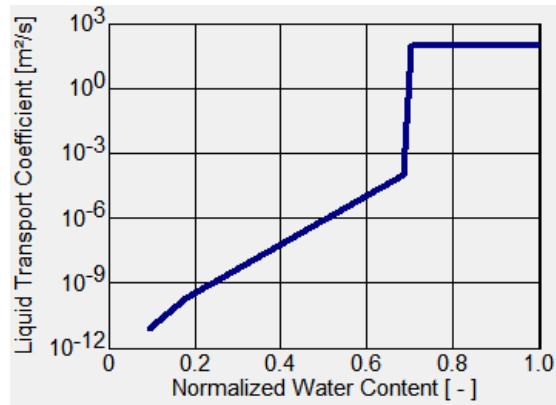
Figure 5.11: Liquid Transport Coefficient for Redistribution- Effective Plot

Table 5.4: Liquid Diffusivity Values for Redistribution for Modified WUFI Model

Normalized Water Content	Water Content (kg·m^{-3})	Liquid Diffusivity, Redistribution (m^2·s^{-1})	Justification
0	0	0	-
0.09	53	7.6E-12	Same value for the liquid diffusivity for suction
0.18	100	2E-10	(Krus & Vik, 1999)
0.68	383	1E-4	This value was obtained by trial and error.
0.70	393	100	(Krus & Vik, 1999)

5.4.3. 5-Ply CLT Calibration

The calibration of the 5-ply CLT panels follows a similar procedure as those used in the 3-ply CLT calibration experiment. A summary of the more important lessons learned from the previous two calibration experiments can be found below:

- Calibrate the sorption isotherm to the sample density- set the saturated and reference content values equal to those provided in the sorption isotherm
- Set absorption coefficient to empirically derived values
- Set the interior surface heat transfer coefficient to the predefined outdoor value
- Set the saturated liquid diffusivity for redistribution to 100 m^2·s^{-1} and calibrate the slope at a value at 10 kg·m^{-3} less than saturated
- Set the saturated liquid diffusivity for redistribution to 2E-10 m^2·s^{-1} at 30% MC
- Verify transient moisture profile with data collected from the moisture content pins

To validate the procedures utilized in calibrating the material properties in WUFI for the European and the clear section samples, the guidelines listed above should provide good estimates for the remaining CLT samples. The results are shown in Figure 5.12.

73
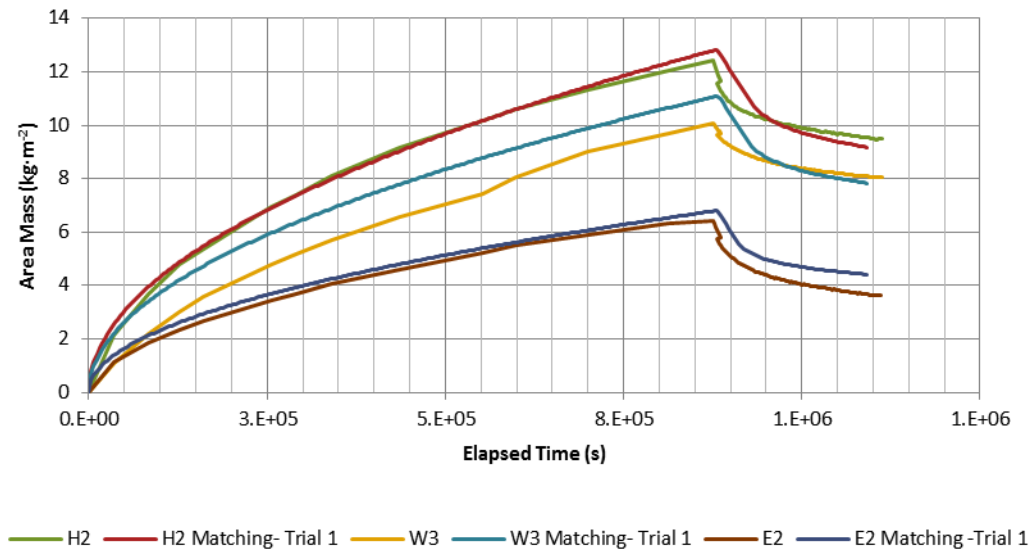
Figure 5.12: Preliminary Matching of WUFI Simulations to Empirically Obtained Data

As can be seen above, the agreement between the modelled and experimental set of curves are in generally good agreement, thus validating the process used in calibrating the WUFI model. The exception is the W-SPF 3 sample. It is possible that sample W-SPF 3 was not in full contact with the water at the beginning of the wetting process- this would invariably lead to a water deficit at after a period of time, despite the problem being rectified. However, as the steps used to quantify the uptake in the Hem-Fir and European SPF sample provided good modelling of the uptake, it will be assumed that the uptake portion of the Western SPF simulation would similar approach actual conditions.

In all of the above WUFI plots, it can be seen that the redistribution curve does not match the actual samples. However, as one of the data points in the redistribution curve was obtained through trial and error, the same process was applied to H2, W3, and E2. The results may be found in Figure 5.14.
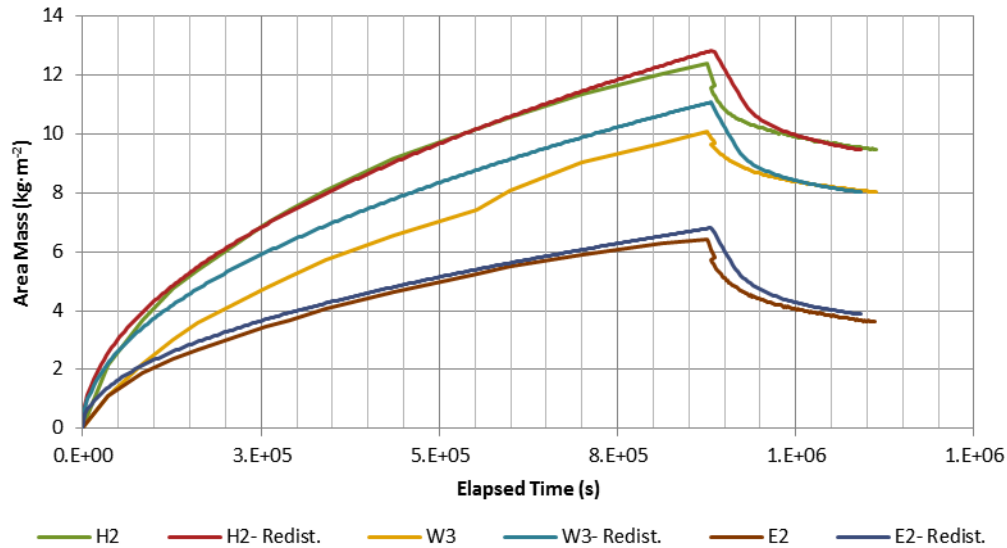
Figure 5.13: Redistribution Modified Plots for CLT Samples H2, W3, and E2 Samples

Some slight deviations from actual conditions still exist, but the differences are slightly overestimated (thus providing an upper bound limit on possible moisture contents in simulated walls). With the completion of the calibration for the four samples, modelling of wall assemblies in various climates may now be undertaken.

5.5. Parametric Study

Using the baseline WUFI model calculated above, a parametric study was employed to assess the relative impact of the various components used in the WUFI model. The sorption isotherm, absorption coefficient, porosity, liquid diffusivity for redistribution, and vapour diffusion resistance were all modified in an attempt to set an upper and lower limit which would bound most of the experimental samples. For simplicity, only the clear sample simulated model was subjected to the parametric study-the results should equally apply to the 3-ply and 5-ply CLT models as well.

Density

Modifying the density does not directly change any of the water content results. Changing the density only alters the water content dependant variables, such as the reference and saturated water content. As such, to appropriately conduct the parametric study, only the variables which directly affect the water content results will be modified.

Porosity

The porosity determines the maximum amount of water which can be held within the material. However, as the saturated moisture content of the wood samples is set to 200% of the density, WUFI does not allow any extra moisture to be absorbed by the sample. Thus, modifying the porosity to 0.63 or 0.83 does not change the water uptake curves.

75

Vapour Diffusion Resistance

The vapour diffusion resistance set in the WUFI database is 130. Modifying this value by 10% does not cause a noticeable difference in the change in the water content. Intuitively, as there is a large influx of liquid water, a more dominant moisture transport mechanism, this makes sense. The greatest impact of the vapour diffusion resistance would likely result in the redistribution aspect of the samples- which will be tested in the 3 and 5 ply CLT sample parametric study. Since insufficient resolution is obtained by providing a plot of the difference in vapour diffusion resistance, Table 5.5 summarizes the peak moisture content in the sample for various levels of the vapour resistance.

Table 5.5: Effect of Modifying Vapour Diffusion Resistance

Vapour Diffusion Resistance (m)	Percent Difference	Peak Water Content (kg·m^{-3})
195	+50%	4.33
169	+30%	4.34
143	+10%	4.35
130	0%	4.36
117	-10%	4.37
91	-30%	4.39
65	-50%	4.43
4	-97%	5.35

By decreasing the vapour resistance, it can be seen that the peak water content increases. A low resistance enables water vapour to progress deeper within the sample than a higher vapour resistance would otherwise allow. A value of four was selected as this was a value reported by Krus and Vik (Krus & Vik, 1999). However, all of these values assume that the vapour diffusion resistance remains constant across the entire water content range. It is known that the properties of wood are moisture dependant and thus, these results are a conservative simplification.

Sorption Isotherm

Modifying the sorption isotherm not only changes the time at which the various moisture dependant rates change, but also limits the maximum water capacity of the samples. Without modifying the density (which would change the automatically generated moisture dependant variables), but maintaining the reference and saturated water content, which are density related properties, the following plot was generated.
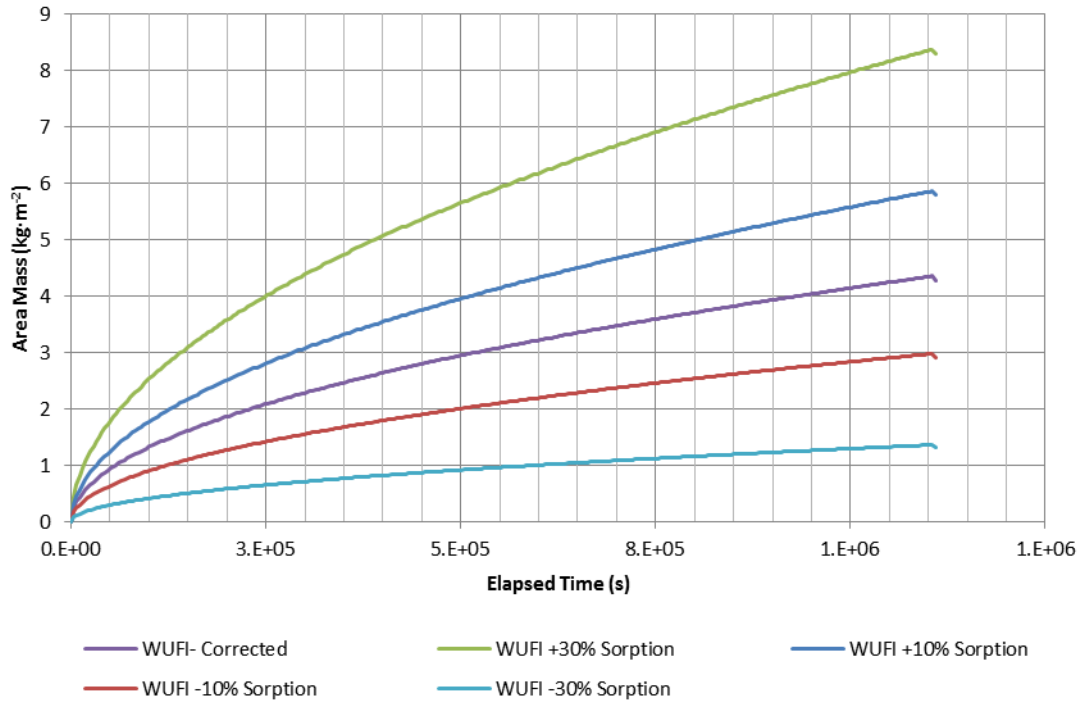
Figure 5.14: Impact of Parametric Modification of Sorption Isotherm on Total Moisture Uptake

The cause for such large difference is due almost exclusively to the difference in saturated water content. As the samples are exposed to near limitless supply of water, the sample rapidly approaches the saturated water content, regardless of the value of the liquid diffusivity, as seen in Table 5.6.

Table 5.6: Diffusivities for Different Sorption Isotherm Regimes

Curve	Saturated Water Content ($kg \cdot m^{-3}$)	Water Content ($kg \cdot m^{-3}$)		Diffusivity ($m^2 \cdot s^{-1}$)
+30% Sorption	648	Reference (u_{80})	66	3.1 E -13
		Saturated (u_f)	648	1.5E -10
Normal	498	Reference (u_{80})	66	6.4 E -13
		Saturated (u_f)	498	2.6 E -10
-30% Sorption	349	Reference (u_{80})	66	1.9 E -12
		Saturated (u_f)	349	5.2 E -10

As the saturated water content decreases, the diffusivity increases non-linearly. For comparison, the following plots provides the total water content for the outer 4mm of the sample (in red), and the remaining 32mm of the sample (in blue) over the modelled test period.
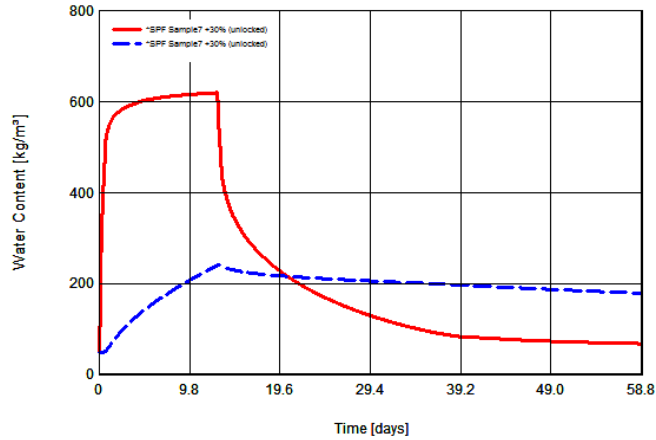
Figure 5.15: Water Content Profile for Outer 4mm Layer (Red) and Rest of CLT Sample (Blue) on +30% Sorption Isotherm Curve.
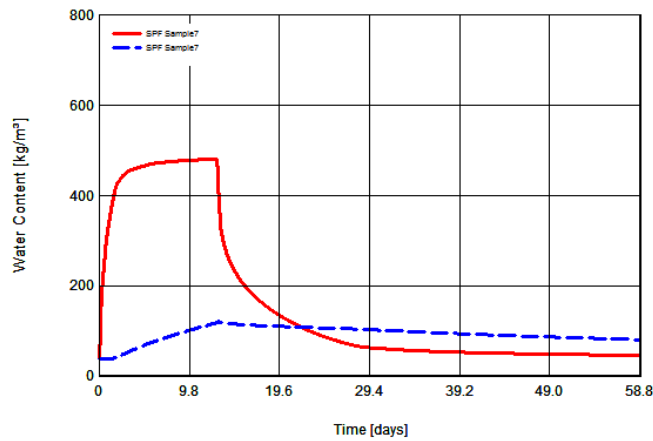
Figure 5.16: Water Content Profile for Outer 4mm Layer (Red) and Rest of CLT Sample (Blue) on Sample #7
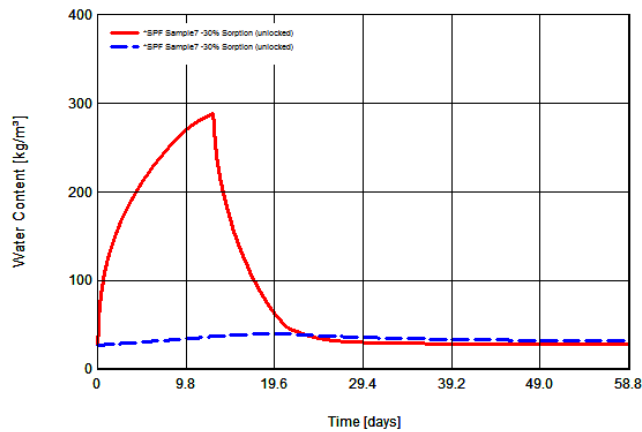
Figure 5.17: Water Content Profile for Outer 4mm Layer (Red) and Rest of CLT Sample (Blue) on -30% Sorption Isotherm Curve

A-value

The absorption coefficient holds an important role in the determination of the liquid diffusivity in suction. Compared to the other parameters that were modified, the a-value has a much more significant

78

role in determine the quantity of moisture absorbed in the simulation. The impact, as seen by a 10% and 30% range from the original A-value from sample #7, may be seen in the following plot.
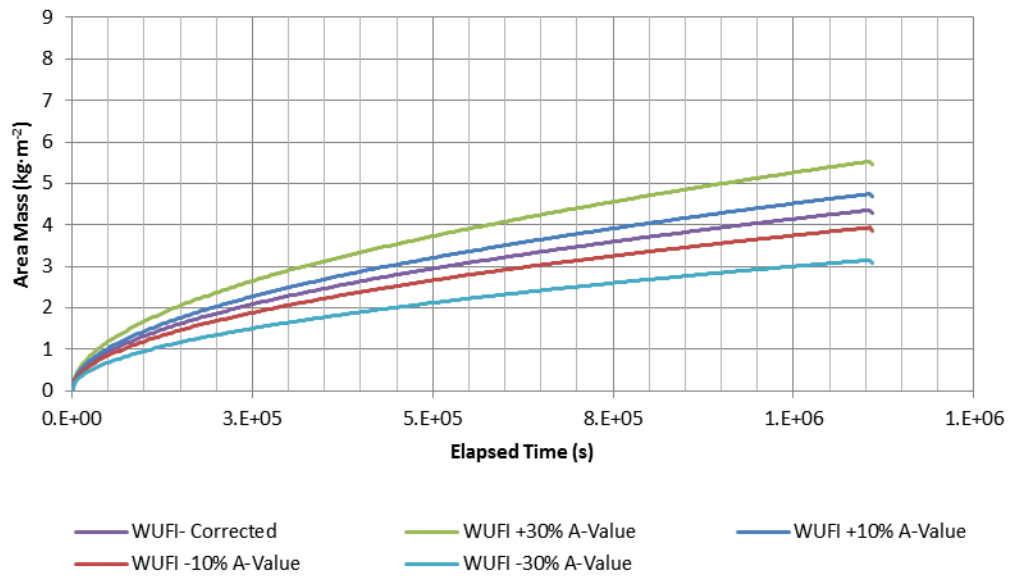
Figure 5.18: Impact of A-value on Moisture Uptake

It should be noted that in the pristine sample experiment, a range of ±30% of the A-value was observed in the 10 samples. All the samples came from the same piece of lumber.

Chapter 6- Modelling

The practical goal of this thesis is to provide recommendations for the use of CLT panels in the construction of enclosure wall assemblies that will have little or no risk of moisture damage in the Canadian climates.

The physical measurements documented in the previous chapter provide an initial snapshot of CLT material characteristics. Using assumed and measured properties, it was shown that it was possible to estimate the moisture performance of CLT panels using the WUFI hygrothermal modeling software.

Given this modeling capacity, this chapter presents work that extrapolates the performance to a number of different wall assemblies for a range of Canadian climates in which CLTs may be considered as a viable building material.

6.1. Climates

A total of six cities were considered in the hygrothermal modelling program. The primary metric for comparison between each city's climate is the heating degree day (HDD18.3). This metric is determined by summing the difference between the reference temperature of 18.3°C and the daily average outdoor air temperature, for the days in which it falls below the reference temperature. The HDD is generally considered to be proportional to the amount of heating required for a given building. However, other metrics were also considered in the selection of the sample cities. Relative humidity, precipitation, and drying capacity (i.e., the Scheffer index), combined with considerations for prospective CLT markets, were also considered in the selection of the cities. Considering all of the above factors, the following cities (shown by black dots on Figure 6.1, and described in Table 6.1) were chosen as representative climates.

<div align="center">Table 6.1: City Selection for Hygrothermal Modelling</div>

City	Köppen Climate Zone	Justification
Vancouver, British Columbia	Oceanic Climate (Cfb)	Situated in a saturated wood market. Local interest in green building. Possesses a high moisture load during the winter.
Edmonton, Alberta	Humid Continental (Dfb)	Rapidly developing infrastructure. Poses challenging cold climate conditions.
Winnipeg, Manitoba	Extreme Humid Continental (Dfb)	Very humid summers and cold, dry winters.
Ottawa, Ontario	Humid Continental Climate (Dfb)	Cold winters and hot and humid summers. Representative climate for many Ontario cities.
Québec City, Québec	Subarctic Climate (Dfc)	Very cold dry winters, cool dry summer. Reflects conditions that may be experienced in other logging communities in Northern Québec.
St. John, New-Brunswick	Humid Continental Climate (Dfb)	Located near logging communities. Possesses typical Atlantic province climate.
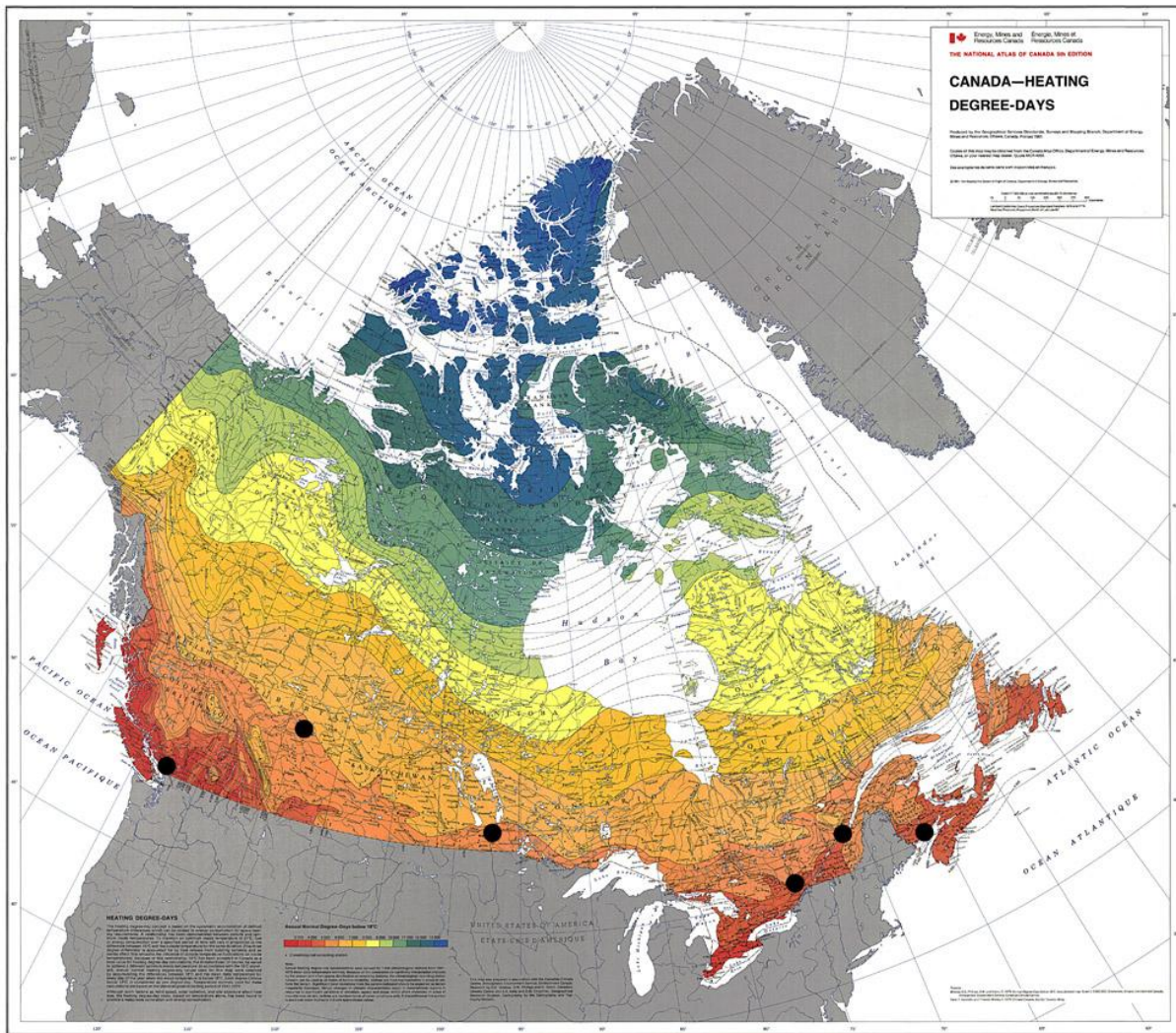
Figure 6.1: Canadian Map of Heating Degree Day Zones marked with Select Cities for Climate Modelling (Environment Canada, 2011)

Summary climatic information may be found in Table 6.2. The climatic data is sourced from the ASHRAE weather files or from the WUFI 'cold year' weather files included with that software. Included in Table 6.2 is the Scheffer index, an index utilized to characterise the relative drying capacity of the local climate. It is an aggregate product of rain fall and temperature throughout the year. The Scheffer indices were taken from Forestry Chronicles (Setliff, 1986).

Table 6.2: Weather Data on Select Cities Across Canada

Locations	Vancouver	Edmonton	Winnipeg	Ottawa	Québec	St. John
HDD <18.3°C	2932	5708	5750	4563	5094	4771
HDD <10°C	801	2947	3552	2517	2891	2419
Mean Temperature(°C)	10.4	4.1	3.0	6.5	4.7	5.3
Max. Temperature (°C)	28.3	31.4	34.0	33.2	31.8	29.6
Min. Temperature (°C)	-9.1	-31.7	-35.4	-27.3	-29.7	-26.4
0.4%. Dew Point Temperature (°C)	16.8	16.3	21.0	21.5	21.3	18.6
99.6%. Dew Point Temperature (°C)	-13.9	-34.7	-37	-31	-33.1	-29.4
Normal Rain (mm/year)	1155	365	416	732	924	1148
Scheffer Index	52.3	32.5	34.9	41.2	48.2	40.4*

*The Scheffer index was not available for St. John. Therefore, the value for Moncton, New Brunswick, was used.

More detailed climate information, such as wind rosettes, solar irradiation, and temperature profiles, and other detailed meteorological data for each city, may be found in Appendix 2.

6.2. Interior Climate

The interior environment of a building is inter-related with the outdoor environmental conditions. Although a buildings heating and cooling system may control the temperature, the interior humidity conditions are strongly dependent on the moisture content of the exterior air. Consequently, using a single interior climate for all the cities listed above would be inappropriate, as the interior conditions of a building in Vancouver in January would be different than for one in the city of Québec.

Further compounding the issue are the building characteristics (air leakage rates, mechanical ventilation rates, etc.) and occupant behaviour (clothes drying, shower usage, etc.), both of which may have significant impacts on the interior moisture load. Given the uncertainty around the above mentioned factors, three humidity regimes will be considered: low, medium, and high moisture load. Each humidity regime is governed by a sinusoidal wave, with the peak occurring on the first of August.

Table 6.3: Indoor Humidity Regimes for WUFI Simulations

Moisture Regime	Low	Medium	High
Relative Humidity	30-55%	40-60%	50-60%
Explanation	Air-leaky buildings New buildings with mechanical ventilation Low occupancy activities Building located in a colder climate	Air tight construction High humidity loads from cooking, frequent washing, or firewood storage Operation of a mechanical humidifier	Very air-tight construction without mechanical ventilation Interior environment maintained at higher humidities (pools, green house, retirement homes, etc.) Building located in a humid climate

The interior temperature was assumed to vary sinusoidally around a mean of 21°C, peaking on the 1st of August. The final result, for a low humidity regime in Vancouver, is plotted in Figure 6.2.
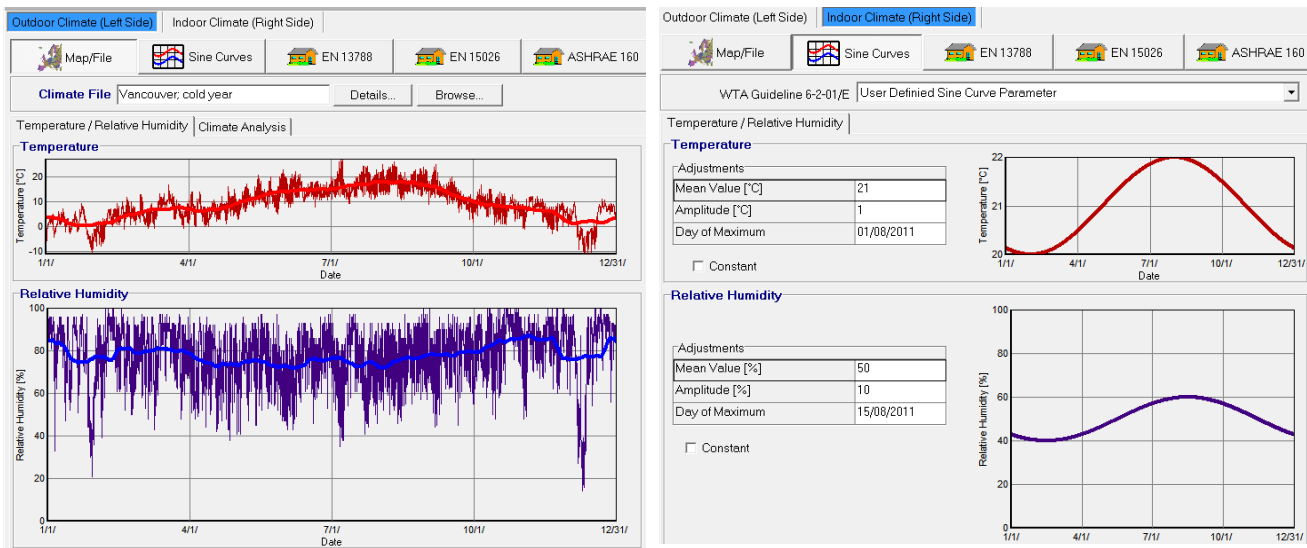
Figure 6.2: Outdoor (left) and Indoor (right) Climate Settings

6.3. Wall Component

The following section discusses the various components associated with the wall being simulated. The components extend beyond just the wall assembly; they also include information such as surface transfer coefficients and orientation.

6.3.1. Orientation and Surface Transfer Coefficients

The orientation and surface transfer coefficients play an important role in determining the boundary conditions of the simulated wall. The orientation determines the effects of wind-driven rain as well as drying capacity due to solar radiation. The surface transfer coefficients help determine the rates of drying of the outer and innermost surfaces of the wall assembly. The exterior surface film coefficient was set to 0.0588 m^2·K·W^{-1} ("external wall" setting in WUFI), and the interior surface film coefficient was

set to 0.125 m²·K·W⁻¹ ("partition wall (inner)" setting in WUFI. No vapour resistance coating was applied to the exterior; however it was assumed that the interior surface of the wall assembly would have latex paint. Consequently, an Sd-Value of 0.3 (equivalent to a vapour permeance of about 10 US perms or 570 metric perms), was applied. The following figure summarizes the surface transfer coefficients.

Figure 6.3: Surface Transfer Coefficient Settings Screen

As one of the emerging market applications for CLT panels is in midrise buildings, the rain load calculation should be chosen to represent this type of building. WUFI uses the Equation 25 to calculate the rain load on a vertical surface.

$$Rain\ Load = Rain \cdot FE \cdot FD \cdot 0.2 \left[\frac{s}{m}\right] \cdot Wind\ Velocity \tag{24}$$

Where the coefficient FE, is the rain exposure factor, and FD, is the rain deposition factor. Data by Straube suggests that a rain deposition factor of 0.9 to 1+ may be appropriate for the edges of a tall building.
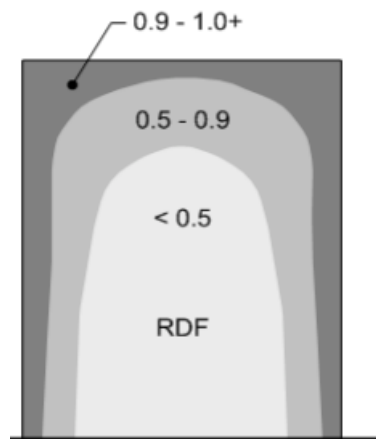
Figure 6.4: Rain Deposition Factor Values for Tall Buildings (Straube J. F., 1998)

With respect to the rain exposure factor, the urban terrain exposure, when combined with a height factor (wind velocities increase at higher elevations) can be used to develop an estimate.
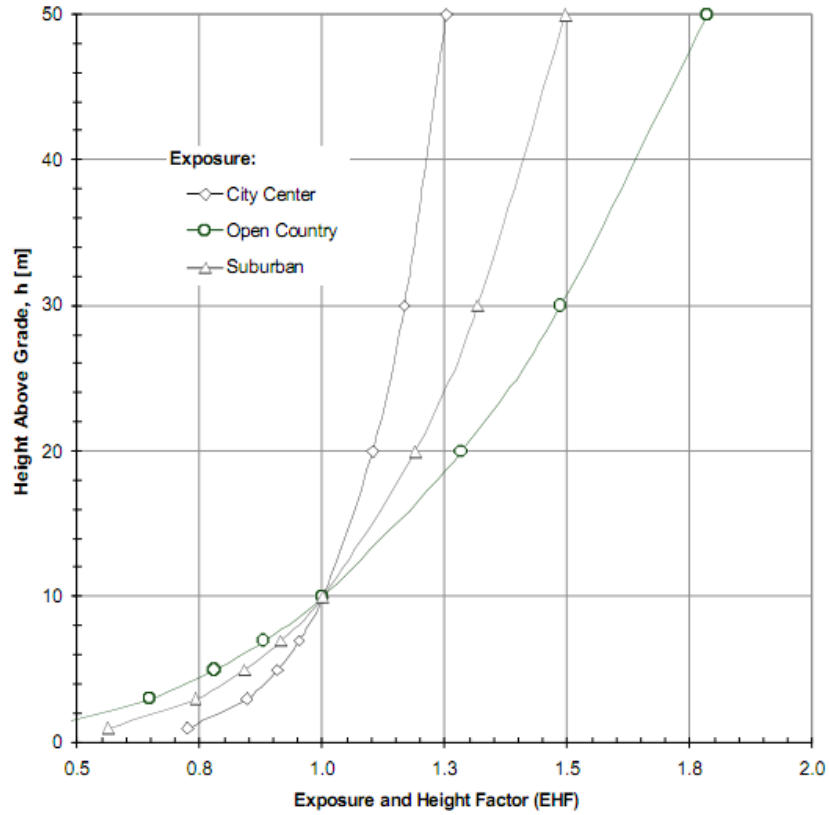
Figure 6.5: Rain Exposure and Height Factor (Straube, 1998)

Based on Figure 6.5, for a building of a height of approximately 20m in an urban environment, a rain and height exposure factor of 1.28 should be used.
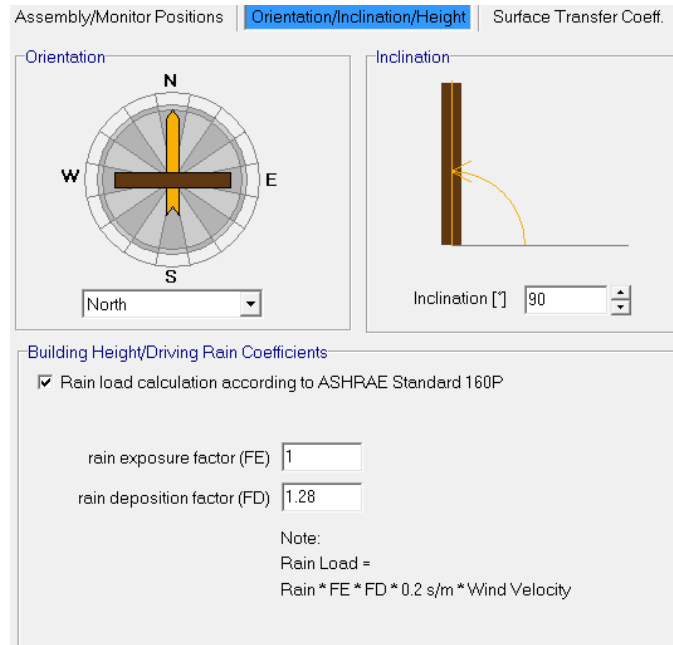
Figure 6.6: WUFI Screenshot of Orientation and Rain Exposure Screen

While these values may be slightly elevated for a mid-rise building, as the moisture sensitive material of concern is also the primary structure of the building, a larger rain load would yield an upper-bound on the possible moisture effects on the building. Further, a rain adherence factor was assumed to be 0.7. This value represents the fact that not all precipitation will remain adhered to a building's surface- some may splash or drip off.

6.3.2. Wall Assembly

A total of three wall assembly types were considered for simulations. These include two with outboard insulation of varying vapour resistance and one with interior insulation. Table 6.4 and Table 6.5 summarize the possible permutations and the codes used throughout the remainder of this thesis to identify specific simulations. Figure 6.7: Section of SXPAN- Storage Cladding, Drainage Cavity, XPS Insulation, Permeable Membrane, CLT, Air Space, and GWBFigure 6.7 and Figure 6.8 are sectional views of possible wall assemblies of CLT construction.

Table 6.4: Wall Assembly Code

Wall Component	Code	Definition	Notes
Cladding	S	Storing	Moisture storing wall cladding (i.e. brick)
	N	Non-Storing	Non-moisture storing wall cladding (i.e. metal siding)
Exterior Insulation	X	XPS	Vapour resisting insulation
	R	Mineral Fibre	Vapour permeable insulation
	N	None	No exterior insulation
Water Resistance Barrier and Air Barrier System	P	Vapour Permeable	More than 10 US-perms (i.e. vapour permeable self-adhering membrane)
	I	Vapour Impermeable	Less than 1 US perm (i.e. polyethylene faced bituminous membrane)
Service Space	A	Air	
	B	Fibre Glass Batt	
Vapour Control	Y	Yes	Less than 1 US-perm vapour control (i.e. polyethylene sheeting)
	N	No	

Table 6.5: Boundary Condition Data Code

Component	Code	Definition	Notes
Climate	Van	Vancouver, B.C.	
	Edm	Edmonton, Alberta	
	Wng	Winnipeg, Manitoba	
	Ott	Ottawa, Ontario	
	QbC	Québec, Québec	
	StJ	St. John, New-Brunswick	
Humidity Regime	H	High	50-60% RH
	M	Medium	40-60% RH
	L	Low	30-55% RH
Direction	N	North	
	R	Wind Driven Rain	Direction that presents the greatest combined effect of wind driven rain and solar irradiance.
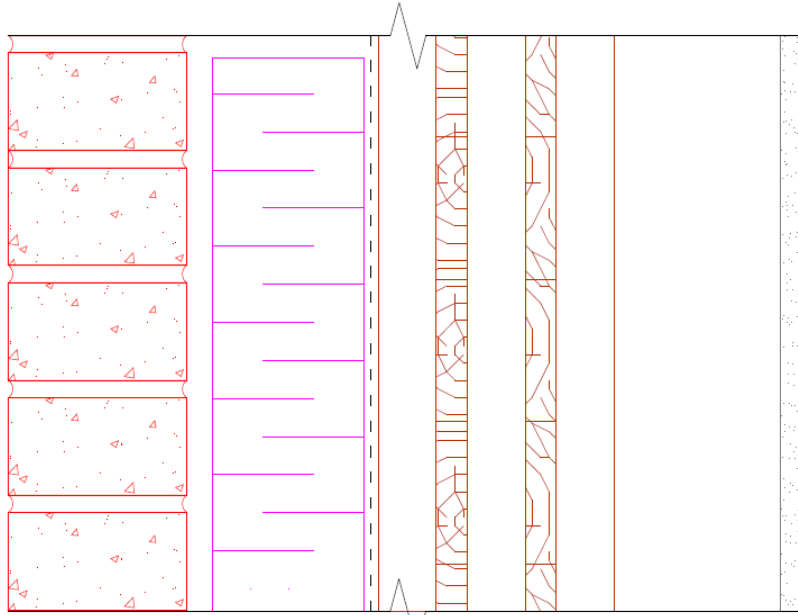
Figure 6.7: Section of SXPAN- Storage Cladding, Drainage Cavity, XPS Insulation, Permeable Membrane, CLT, Air Space, and GWB
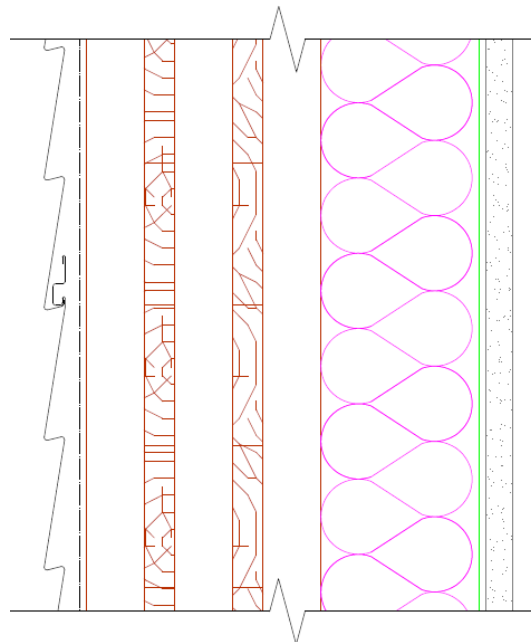
Figure 6.8: Section of NNIBY- Non-Storage Cladding, Drainage Cavity, No Insulation, Impermeable Membrane, CLT, Batt Insulation, Vapour Control Membrane, GWB

The walls with the outboard insulation were designed to comply with current best enclosure design practices- that is, to be in conformance with the principles of the "perfect wall". The wall with the interior insulation was selected to demonstrate an alternative insulation strategy proposed by others (this does not represent a design approach that would be recommended by building science).

The naming convention utilized in the simulation follows upon the assembly and climate type. For instance, a wall assembly with a mass storing cladding (S), with extruded polystyrene insulation (X), and a vapour permeable water and air barrier (P), with an air space (A) and no interior vapour control layer (N) in Vancouver (Van) with a medium humidity regime (M) facing North (N) would be labelled SXPAN-MN-Van. The simulation schedule utilized may be found in Table 6.6.

Table 6.6: WUFI Simulation Schedule

Cladding		Exterior Insulation			WRB		Int. Cavity		Int. V.B.		Direction	
S	N	X	R	N	P	I	A	B	Y	N	N	R
•		•			•		•			•	•	
•			•		•		•			•	•	
•			•		•		•			•		•
•		•				•	•			•	•	
	•	•			•		•			•	•	
	•		•		•		•			•	•	
•				•		•		•	•		•	

6.4. Modelling Procedure

The panels (131mm thick) were divided in to 7 layers in the simulation model. The outermost layer, as previously mentioned, was set at 4 mm thick. The subsequent layers were 10mm, 30mm, and 43mm- the panels were symmetric about the 43mm central layer. The metric for comparing the moisture performance of the CLT panels was the moisture content of the 4mm layer on the interior and exterior of the panel. This 4mm sliver, if at elevated moisture contents, is a good indicator of the propensity for mould growth. The next 10mm layer, if at elevated moisture contents, is a good gauge of the capacity of the CLT panel to dry out- elevated moisture contents in this layer suggest restricted drying capacities.

The hygrothermal models were all run with an initial temperature 21°C and with typical construction moisture contents- the moisture content of the CLT panels was set to 12% MC. The model was run until an apparent annual equilibrium was achieved, as seen in Figure 6.9.
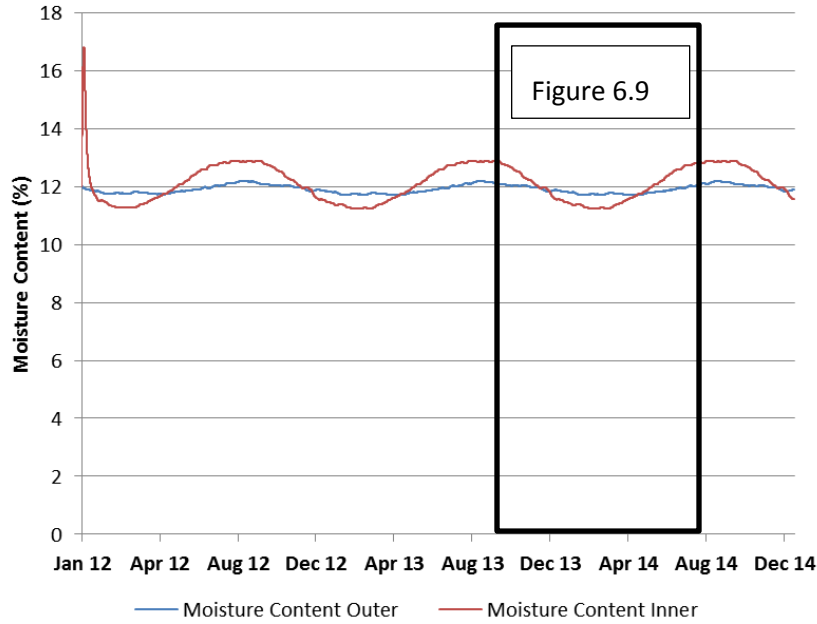
Figure 6.9: Moisture Content of the Outer and Innermost CLT Layer in SXPAN-Van-MN

Similar plots are produced for the temperature of the outer and inner layer of CLT.
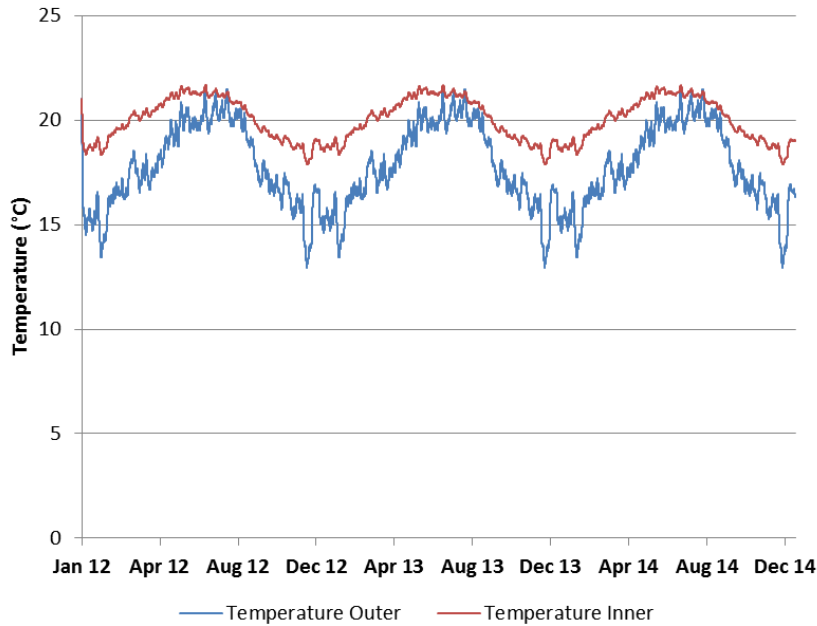
Figure 6.10: Temperature of the Outer and Innermost CLT Layer in SXPAN-Van-MN

As can be seen in Figure 6.9 and Figure 6.10, equilibrium is reached rather quickly in this specific wall assembly in this selected climate. A more detailed view of the moisture content on an annual basis may be found in Figure 6.11.

90
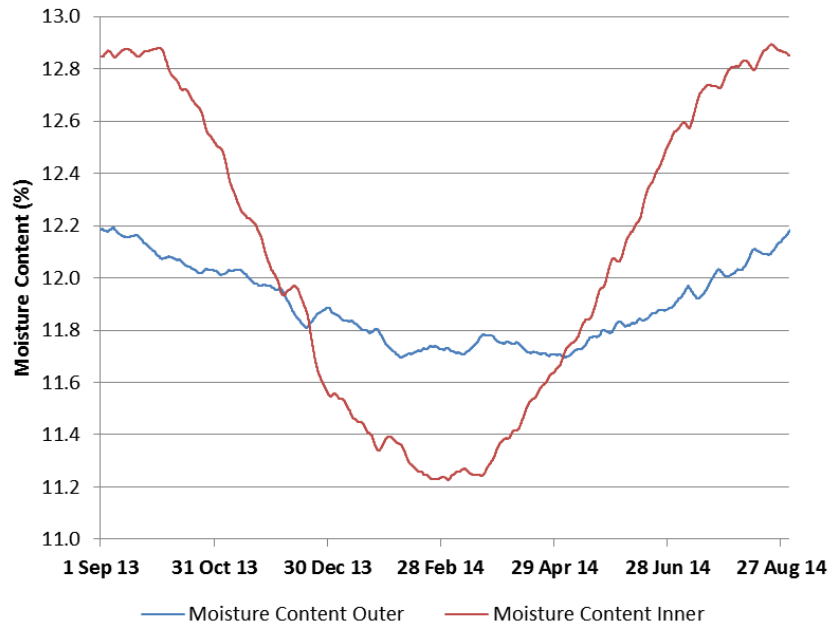
Figure 6.11: Moisture Content of the Outer and Innermost CLT Layer in SXPAN-Van-MH from Sept 1 to Aug 31

The data was analyzed from September 1st to August 31st. This range was selected because typically, moisture contents in wood products rise during the colder months. This is both a result of condensation of water vapour, and due to the rise of moisture content by adsorption from air with higher relative humidity (the higher RH due to cooler temperatures). However, as can be seen in the above plot, the CLT panel tends to dry in the winter, as opposed to gain moisture.

6.4.1. Construction Moisture

Modelling was also conducted to investigate the impact of CLT panels with higher levels of construction moisture. To create the baseline moisture conditions, a simulation was conducted in which the CLT panel was exposed to the worst three months of rainfall for each respective climate (worst being characterised by the most average rainfall), facing the most severe wind driven rain orientation.

The panels were assumed to have been erected and the WUFI simulation only accounted for vertical walls. Any horizontal panels which have been installed, for instance, in floor assemblies, would likely be covered by subsequent floor installations and thus protected from precipitation. Furthermore, these panels will experience interior climates and will thus have the capacity to dry out in time. It is for this reason that the simulation only considered vertical CLT panel walls.

To appropriately reflect construction environments, the exterior climate was set to the identical climate file as used in the non-construction-moisture simulation files. However, during the construction wetting period the interior conditions were also set to match the exterior climate, less the precipitation. While this is not entirely true, as the enclosure will provide a modicum of environmental separation, from reducing wind velocity and providing a level of insulation, the difference in reality is both difficult to predict and small.

After running the model for the period of 3 months, a water content profile plot is obtained (see
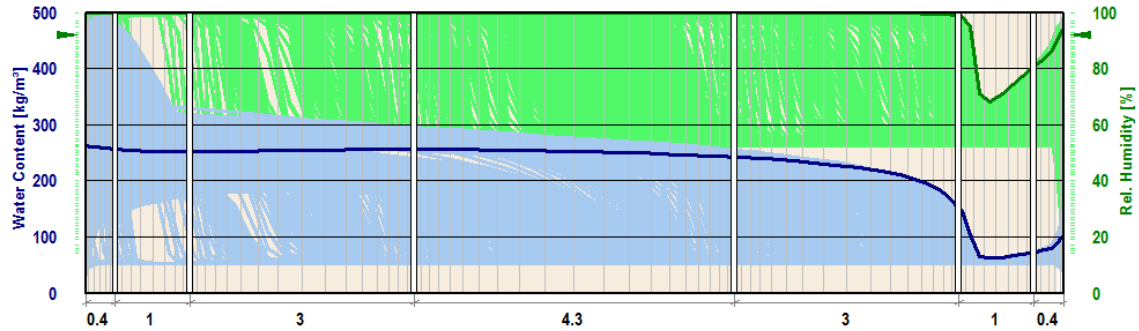
Figure 6.12: Water Content and Relative Humidity Profile after 3 Month of Exposure in Vancouver Climate

The results of this three month simulation were converted to an average water content for each layer. The resulting initial conditions used to start the subsequent WUFI simulation are summarized in Table 6.7.
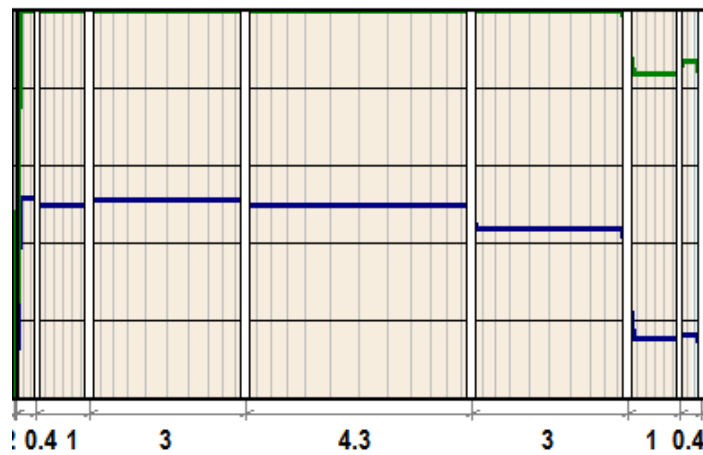
Figure 6.13: Averaged Water Content in CLT Layers for Simulating Construction Moisture

Table 6.7: Initial Averaged Moisture Content for CLT Layers due to Construction Moisture

City	Period	Direction	Moisture Content at Specified Layer (%) (Layers in mm)						
			4	10	30	45	30	10	4
Vancouver	Nov 1 – Feb 1	SE	57	55	56	55	48	17	18
Edmonton	June 1 – Sept 1	NW	36	44	47	35	13	13	16
Winnipeg	June 1 – Sept 1	W	15	24	20	13	12	13	14
Ottawa	July 1 – Oct 1	NE	54	54	37	13	12	13	14
Québec City	July 1 – Oct 1	E	44	44	36	20	16	16	18
St. John	Sept 1 – Dec 1	SE	33	46	51	45	24	17	18

Cells shaded in red indicate moisture contents in excess of the fibre saturation point (assumed to be 30% MC).. As can be seen, construction moisture wetting can be a serious concern in some climates, especially Vancouver (in winter), Ottawa (in summer), and St John (in the Fall).

6.5. Modelling Results

The salient output provided by WUFI is the water content of the CLT layers. The water content is converted into a moisture content by dividing the result by the bulk density of the material. It is known that elevated moisture contents may cause wood bio-deterioration; therefore this will be the metric of comparison between assemblies, humidity regimes, and climates.

The full schedule of simulations was run for the Vancouver climate. The data summarized in Table 6.7 is the moisture content of a 4mm layer in the outermost and innermost lamina in the CLT panel. As can be seen, for CLT panels that start at 12% M.C., very little moisture gain occurs throughout the year once equilibrium is reached.

Table 6.8: Moisture Content in Various Wall Assemblies and Humidity Regimes in a Vancouver Climate

Wall Assembly Code	Moisture Content (%)					
	Low Humidity		Medium Humidity		High Humidity	
	Outer	Inner	Outer	Inner	Outer	Inner
SXPAN-N	12.1	12.3	12.2	12.9	12.3	13.1
SRPAN-N	13.3	12.3	13.3	13.0	13.3	13.2
SRPAN-R	13.3	12.3	13.3	13.0	13.4	13.2
SXIAN-N	12.1	12.3	12.3	12.9	12.4	13.1
NXPAN-N	12.2	12.3	12.2	12.9	12.3	13.1
NRPAN-N	13.7	12.3	13.7	13.0	13.8	13.2
SNIBY-N	12.7	12.3	12.7	12.6	12.7	12.7
SNPBY-N	15.3	12.4	15.3	12.6	15.3	12.8

In analysing The full schedule of simulations was run for the Vancouver climate. The data summarized in Table 6.7 is the moisture content of a 4mm layer in the outermost and innermost lamina in the CLT panel. As can be seen, for CLT panels that start at 12% M.C., very little moisture gain occurs throughout the year once equilibrium is reached.

Table 6.8, some patterns emerge. The first observation to make is that all of the samples remain very dry throughout the entire simulation period. The second observation is that the outer moisture content of the CLT panel is not particularly impacted by the interior humidity levels. Similarly, a higher exterior moisture load does not seem to affect the interior moisture content much either. This corroborates well with the parametric testing conducted in previous sections- that CLT panels themselves perform well as vapour retarders.

Another pattern that can be seen is that the XPS outboard insulation functions as a vapour retarder against both moisture storing and non-storing cladding systems. The difference is further emphasised when compared with a permeable outboard insulation- SXPAN-NM has an outer MC of 12.2% whereas SRPAN-NM has an MC of 13.3%. Similarly, a difference is seen between vapour permeable and impermeable water resistance and air barrier system; the vapour permeable membrane enables inward moisture ingress. It should however be noted that this is for samples with a starting moisture content of 12%. The implications of a vapour impermeable WRB/ABS will be further discussed in the construction moisture section.

To minimize unnecessary simulation work, only the more significant wall assemblies and humidity regimes were tested for the other climates: these are highlighted in red in Table 6.8: SRPAN-RH, SXIAN-NH, NRPAN-NH, SNIBY-NH, and SNPBY-NH. SRPAN-NH was highlighted in green to represent one of the wall assemblies which is hypothesized to perform best in all climatic conditions- it was included in the testing to confirm that hypothesis. The results of the simulations for each city may be found in Table 6.9. The maximum and minimum moisture contents for each wall were taken in the 3rd year of simulation, to minimize the influence of any initial moisture re-profiling.

Table 6.9: Maximum MC for Outer and Inner CLT Layer in Select Wall Assemblies

Code	Vancouver		Edmonton		Winnipeg		Ottawa		Québec		St. John	
	Out	In	Out	In	Out	In	Out	In	Out	In	Out	In
SRPAN-NH	13.3	13.2	12.9	13.4	14.3	13.4	13.8	13.2	14.2	13.2	13.5	13.1
SRPAN-RH	13.4	13.2	12.9	13.4	14.3	13.4	13.8	13.2	14.2	13.2	13.5	13.1
SXIAN-NH	12.4	13.1	12.4	13.3	12.4	13.2	12.4	13.1	12.5	13.1	12.5	13.1
NRPAN-NH	13.8	13.2	13.1	13.4	14.7	13.5	14.3	13.3	14.7	13.3	14.0	13.2
SNIBY-NH	12.7	12.7	16.3	17.5	16.2	18.0	16.2	17.4	16.5	17.3	16.5	16.8
SNPBY-NH	15.3	12.8	14.7	15.3	14.5	15.7	14.5	15.1	15.7	15.1	15.9	14.8

The cells highlighted in red represent somewhat elevated moisture contents, however these are still below 19% MC, the typical maximum recommended safe moisture content for wood studs (established to limit swelling/shrinkage, and not for reasons of decay). In general, the vapour permeable wall assemblies are typically drier in all climates.

6.5.1. Construction Moisture Drying Results

To approach the problem of construction moisture, the average moisture content for each layer was inserted in the 'initial conditions' page in WUFI (see

Table 6.7). While this does not generate a smooth moisture profile through the wall (it appears more like a step-function), the relevant information is that the total moisture content in the walls are comparable.

As the most pertinent question surrounding construction moisture is the rate of drying, only two walls will be considered for modelling- the most vapour permeable, and least vapour permeable walls, NRPAN-NH and SNIBY-NH, respectively. For comparison purposes, a third option is considered, a CLT wall exposed to environmental conditions, less any precipitation, named "Environment".

Table 6.10: Moisture Content in CLT Layers in 3 Wall Assemblies in All Simulated Climates

City/Code	Moisture Content (%)						
	4mm	10mm	30mm	43mm	30mm	10mm	4mm
Vancouver	58	57	57	56	49	48	47
NRPAN-NH	11	13	18	21	18	14	13
SNIBY-NH	49	49	49	49	48	21	16
Environment	14	18	22	24	22	18	15
Edmonton	36	44	47	35	13	13	16
NRPAN-NH	9	11	15	19	13	13	13
SNIBY-NH	32	32	31	31	13	13	14
Environment	11	15	21	23	13	13	13
Winnipeg	15	24	20	13	12	13	14
NRPAN-NH	8	10	14	14	14	12	12
SNIBY-NH	14	14	11	13	14	12	12
Environment	11	13	14	12	12	13	13
Ottawa	54	54	37	13	12	13	14
NRPAN-NH	9	11	13	14	12	13	13
SNIBY-NH	27	27	11	14	17	14	12
Environment	11	14	17	14	12	13	13
Québec	44	44	36	20	16	16	18
NRPAN-NH	9	11	14	17	15	14	13
SNIBY-NH	27	27	12	16	20	20	16
Environment	12	16	20	20	16	14	13
St. John	33	46	51	45	24	17	18
NRPAN-NH	9	11	27	27	27	20	16
SNIBY-NH	33	37	14	20	24	25	23
Environment	14	20	24	25	23	17	16

The general conclusions to be drawn from the summarized results in Table 6.10 is that vapour permeable construction is preferable to vapour impermeable construction as it allows any construction moisture to dry out over a period of several years. This is further demonstrated by comparing the moisture density of each wall assembly. The moisture area density is the amount of water that enters, or leaves, the entire wall assembly, in units of kg·m^{-2}.
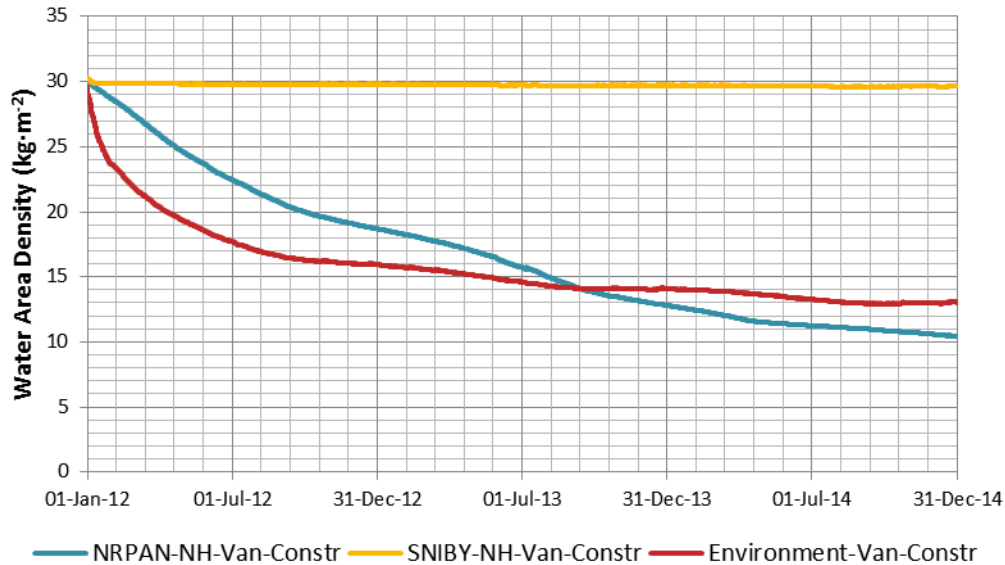
Figure 6.14: Water Area Density for Construction Moisture in NRPAN-NH, SNIBY-NH, and Environment-NH in Vancouver

Figure 6.14 shows that after a brief period of time, the water content in the CLT panel exposed to the ambient environment decays to the equivalent moisture content of the local climate. After approximately two years, the NRPAN-NH wall dries to a greater degree than the exposed CLT wall. This is due to the insulation and vapour control strategy that was selected for this wall assembly- the exterior insulation keeps the CLT panel at warmer temperatures while the vapour permeable insulation and water and air resistant membranes enable the panel to dry out to its equilibrium moisture content. The vapour impermeable strategy, SNIBY-NH, does not allow any drying to occur, only redistribution. Therefore, an impermeable strategy may work only if the wall is built without excess construction moisture (that is, if the moisture content upon closing in is less than 20% M.C. throughout the entire wall) and that the wall is free from defects causing leaks. Similar plots for the other walls and climates may be found in Appendix 3.

It should be noted that the approach taken towards modelling the construction moisture (averaged water content for each layer), resulted in some computation errors in WUFI, known as convergence errors. These occur typically for extremely high moisture fluxes (for instance, drying of construction moisture in the middle of an Edmonton winter) and for unusual material properties. Convergence errors may result in errors in the reported water content of the various layers in the wall assembly. However, in these simulations, these errors predominantly occur at the initial phases as the water content adjusts itself to the micro-environments; the values listed in Table 6.10 are the long-term minimum moisture content values and so should not be particularly impacted by any initial problems in reaching a state of moisture equilibrium. The following table lists the number of convergence errors for each associated wall assembly in each climate.

Table 6.11: Convergence Errors for Construction Moisture Simulated Walls

City	Number of Convergence Errors		
	NRPAN-NH	SNIBY-NH	Environment
Vancouver	78	48	1

Edmonton	561	130	0
Winnipeg	599	1697	0
Ottawa	599	51	0
Québec	611	101	0
St. John	27	55	0

In general, NRPAN walls experienced a high number of convergence errors, due to increase moisture flux through the wall assembly. Edmonton was a particularly difficult city to model with the standard start and end times (start of January 1, 2012). To minimize the significant moisture flux (from a wet CLT wall to the dry, cold Edmonton winter), the start and end dates were pushed back by 6 months, starting June 1st. This enabled WUFI to run the simulation, albeit with 561 convergence errors. The high number of convergence errors for Winnipeg, compared to the are unknown, but visual review of the WUFI film data suggest that the values provide in the Table 6.10 are reasonable. Under typical and less computationally intensive simulations, a range from 0-20 convergence errors is considered to be acceptable.

An alternative method to assess the effects of the convergence errors is to compare the moisture balance of the left side and right side of the samples. For instance, despite Winnipeg having 599 convergence errors, the moisture balance on NRPAN-NH goes from 2.1 to 2.4; an error of approximately 0.3 kg·m^{-2}, relatively small considering that the original water content is 9.3 kg·m^{-3}; an error of approximately 3%.

Table 6.12: Water Moisture Balance of WUFI Simulations

City	Moisture Balance (kg·m^{-2})					
	NRPAN-NH			SNIBY-NH		
	Right	Left	Error (%)	Right	Left	Error (%)
Vancouver	19.5	20.1	2.0	0.6	0.6	<0
Edmonton	9.6	10.4	4.2	0.2	0.2	<0
Winnipeg	2.1	2.4	3.2	0.3	0.6	3.1
Ottawa	5.9	6.4	3.4	0.5	0.5	<0
Québec	6.1	6.7	4.1	0.4	0.4	<0
St. John	7.4	10.1	17	0.5	0.4	0.2

The error related to the moisture balances are all very small, with the exception of St. John (discussed below). When compared to the starting water content, the greatest error occurs with 17% for St. John, due to many rain absorption failures (55), but all the second highest is 4.2% in Edmonton.

The results from the St. John simulations are likely a product of a rapidly drying wall.
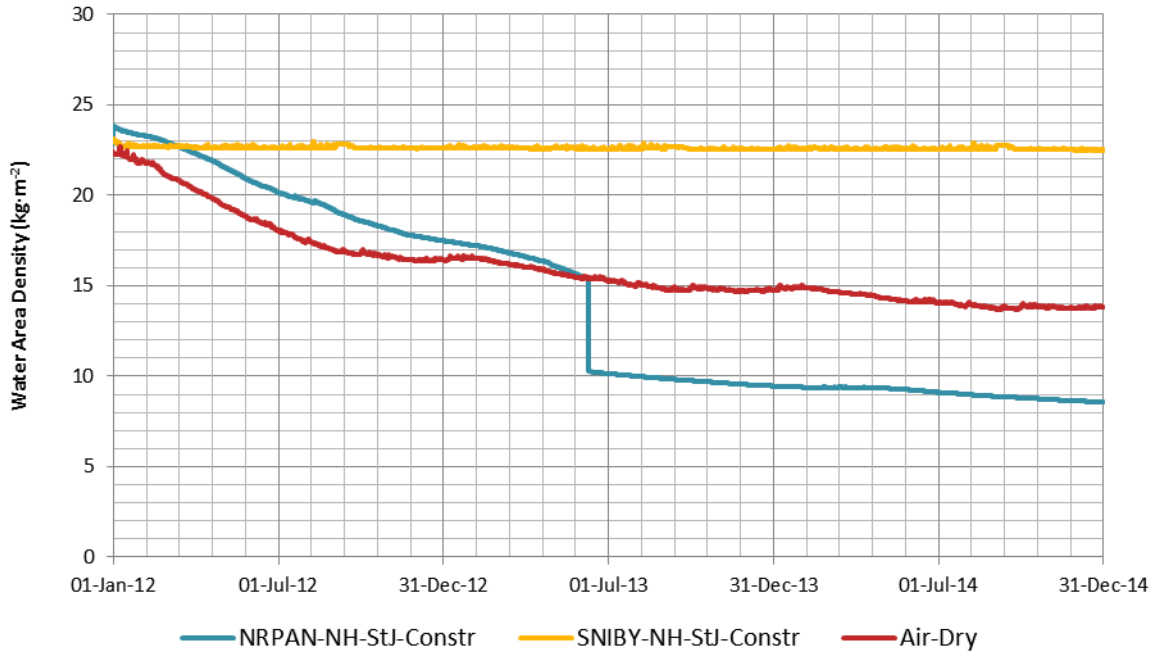
Figure 6.15: Water Area Density for Construction Moisture in NRPAN-NH, SNIBY-NH, and Environment-NH in St. John

The cause for the 17% error can be seen in the NRPAN-NH-StJ-Constr series in Figure 6.15, a rapid drop in the total water content of the wall. This likely represents an extreme rapid drying event which precipitated in calculations errors in the hygrothermal software. Despite this, the NRPAN-NH-StJ-Constr line trends downwards, drying out more than the exposed CLT panel. As a result, the moisture contents provided in Table 6.10 are likely no greater than the 17% calculated error. Reliance on the computed error for the series does not always explain the circumstances.

Chapter 7- Recommendations

This section is divided in to two portions- a section on recommendations for design and construction for the implementation of CLT panels in the built assembly for cold climates in Canada, and second, a section for further research.

7.1. Recommendations for Design and Construction

With respect to construction moisture, the simulations found that the water content may become dangerously high if uncovered CLT panels are exposed to prolonged periods of precipitation (e.g., months). Concerns of mould and rot may consequently arise. However, should these panels be installed in a vapour permeable system, the walls will have the capacity to reach a safe equilibrium moisture content over the period of a few years by drying to the exterior and the interior. On the other hand, wall assemblies built with wet CLT panels and vapour impermeable membranes (either interior or exterior) will experience high moisture contents for prolonged periods, and hence likely experience some form of bio-deterioration. This is not likely a concern for panels exposed to only a few days of wetting.

One simple and practical solution to reducing construction moisture (other than covering the CLT panels until they are clad) includes installing water and air barrier membrane systems on the CLT while still in the factory that become parts of the finished wall assembly. Alternatively, a temporary, low-cost hydrophobic coating (which could acts as a primer for subsequent membrane application) could be used. This approach not only reduces the exposure to moisture during erection of the structure, but also ensures superior quality control of the application of the membrane and reduces delays on the construction site.

7.2. Recommendations for Further Research

A literature survey revealed very little information directly related to the moisture properties and risks of CLT panels used in wall assemblies. Even less information is available for CLT panels when considered in wall assemblies in cold Canadian climates. The research reported here is just a beginning. Much remains unknown, and hence, further research in to CLT moisture performance and risk should be conducted. A very small number of samples and wood sources / species was considered in the experimental work. Much work should be conducted to provide a stronger statistical backing to the results.

The experimental aspect of this research consisted of a water uptake test, to determine the effective liquid diffusivity. A simulation study to assess the relative importance of liquid and vapour transport mechanisms in CLT was also undertaken. However, as both studies were conducted in the free water saturation range of the material, the vapour diffusivity used may not accurately represent the impact of vapour diffusion in the hygroscopic range of the material, as the effect of liquid diffusivity overwhelms and obscures any contributions from vapour diffusion. Further study should be conducted to assess the vapour diffusivity of CLT panels in the hygroscopic ranges.

At the time of publication of this document, research was being undertaken by other members of the NEWBuildS research network in to obtaining functional material properties of CLT, such as air permeance, vapour permeance, and sorption isotherm, among others. It is possible that further material

testing may be required to ascertain sub-assembly level effects of CLT panels (e.g. how checks and cracks in the CLT panel may affect sorption isotherms, capillary condensation, vapour flow, etc.).

During the simulation portion of this thesis, some aberrations were observed in the manner in which the liquid diffusivity for redistribution behaves compared to that of suction; as soon as the sample is removed from a source of water, rapid redistribution of the moisture occurs (much faster than if the sample was exposed to the water source). While the properties are modelled after experimental data, further research needs to be conducted in refining the process and understanding of the physical phenomenon.

Chapter 8- Conclusions

The primary goal of this research was to assess the moisture durability of wall assemblies of CLT construction and to specifically address concerns about construction moisture. The experimental approach utilized, that of a water uptake and drying test, was chosen to help calibrate a hygrothermal model that could be used to simulate typical wall assemblies in a range of Canadian climates. The results from the modelling may be inferred to indicate relative levels of moisture risk to the simulated wall assemblies.

A water uptake test was conducted on twelve 2'x2 ' (600 x 600 mm) CLT panels to obtain a sub-assembly level absorption coefficient; that is, an absorption coefficient which accounts for natural topological features of CLT panels, such as cracks, checks, and resin pockets. The absorption coefficients ranged from 0.004 to 0.014 $kg \cdot m^2 \cdot s^{-1/2}$. These values fall within the range of published data for the A-values of various wood species. Furthermore, an experiment was conducted to assess the effects of small cracks between the boards and lamina of the CLT panels. The results of this experiment suggest that cracks do play a small role in changing the A-value of the CLT panels, but further research is required to determine the significance of these cracks to moisture performance.

The calibration of the WUFI material data file generated several important discoveries. First and most importantly, utilizing the appropriate density and correlated sorption isotherm has a greater significance on the liquid water uptake than the effects of varying the A-value, liquid diffusivity, water vapour diffusion resistance, or the porosity. Difficulties were encountered in matching the water uptake and drying curves with the gravimetric values without large, and sometimes unrealistic, modifications to the parameters. The literature suggests that organic materials change their structure with varying relative humidity, and the changing structure makes it difficult for hygrothermal programs to model. This necessitates the use of unrealistic suction and redistribution diffusivity curves to try to reconcile the limitations of the software. Differences were also observed between the moisture profiles obtained by electric resistance measurements and the results of the simulations. However, as the total water content of the samples was of greater concern, gravimetric readings were deemed more important.

The major conclusion drawn from this research is that CLT panels can be moisture durable in wall systems for Canadian buildings. This durability arises primarily due to the products high moisture storage capacity, inherent vapour resistance, and thermal properties. Despite this, prolonged exposure to certain damaging environmental conditions may result in elevated moisture contents (that is, exceeding the fibre saturation point). This poses risks of fungal decay, mould growth, and construction service problems, such as difficulty of bonding of adhesives or paints and swelling of the CLT panels. The simulation results show that, provided the panels are delivered dry, and protected from extending rain wetting, all of the proposed wall assemblies should adequately accommodate a multitude of exterior Canadian climates and a range of interior conditions. Exceptional interior conditions (e.g., swimming pools, etc.) or exterior conditions (e.g. more than about 6000 HDD18.3C) should receive special analysis.

However, moisture risks can accrue if construction moisture is not considered. The drying capacity of the wall assembly, when considered in its respective climate, becomes very important for the moisture durability of the CLT panels. It was found that the use of vapour impermeable membranes on the exterior or the interior of the assembly increases the risk of moisture damage if installed on a wet CLT panel. Specifically, vapour impermeable layers installed outside of the CLT, were shown to result in

elevated moisture contents at the outer layer of the CLT panels- well in excess of the required moisture content for fungal degradation. To minimize construction moisture levels, the panels should either be protected from precipitation during construction, or an exterior insulated and vapour permeable wall assembly type should be utilized (to allow for drying). The installation of insulation and vapour barrier to the interior of the CLT panel also has significant performance limitations and entails moisture risk.

References

ASHRAE. (2009). *ASHRAE Fundamentals 2009 SI Edition.* Atlanta: American Society for Heating, Refrigerating, and Air-Conditioning Engineers.

Boise Cascade. (2011). *Boise Cascade*. Retrieved October 14, 2011, from www.bc.com

Candenado, L., & Dérome, D. (2005). Numerical Simulation of Wwater Absorption in Softwood. *Ninth International IBPSA Conference.* Montréal, Canada: International Building Performance Simulation Association.

Claesson, J. (1993). A Few Remarks on A Few Remarks on Moisture Flow Potentils; Heat, Air, and Moisture Transfer in Insulated Envelope Parts. *International Energy Agency Annex 24, Task 1: Modelling*.

Crespell, P., & Gagnon, S. (2010). *Cross Laminated Timber: a Primer.* Vancouver: FP Innovations.

Environment Canada. (2011). Atlas of Canada, 5th edition.

Esau, K. (1977). *Anatomy of the seed plants, 2nd ed.* New York: John Wiley and Sons.

FP Innovations. (2011). *CLT Handbook: Cross-Laminated Timber.* Vancouver: FP Innovations.

FPL. (2010). *Wood Handbook, Wood as an Engineering Material, Centennial Edition.* Madison: Forest Products Laboratory.

Franks, F. (1984). *Water.* Royal Chemistry Paperbacks.

Galbraith, G. H., McLean, R. C., & Guo, J. (1997). *Moisture Permeability Data Presented as a Mathematical Function Applicable to Heat and Moisture Transport Models.* Ottawa: International Building Performance Simulation Association.

Garrahan, P. (1988). *Moisture meter correction factors.* Ottawa, Canada: Forintek Canada Corp.

Hens, H. (1996). *Heat, Air, and Moisture Transport. Final Report, Vol 1, Task 1: Modelling.* Leuven, Belgium: International Energy Agency Annex 24.

Hiemenz, C. P., & Rajagopalan, R. (1997). *Principles of Colloid and Surface Chemistry, 3rd ed.* New York: Marcel Dekker.

Hoadley, R. B. (2000). *Understanding wood a crasftman's guide to wood technology. Revised.* Newton, C.T.: Taunton.

Hutcheon, N. B. (1963). *CBD-48 Principles Applied to an Insulated Masonry Wall.* Ottawa: National Research Council.

Hutcheon, N. B. (1964). *CBD-50. Principles Applied to an Insulated Masonry Wall.* Ottawa: National Research Council of Canada.
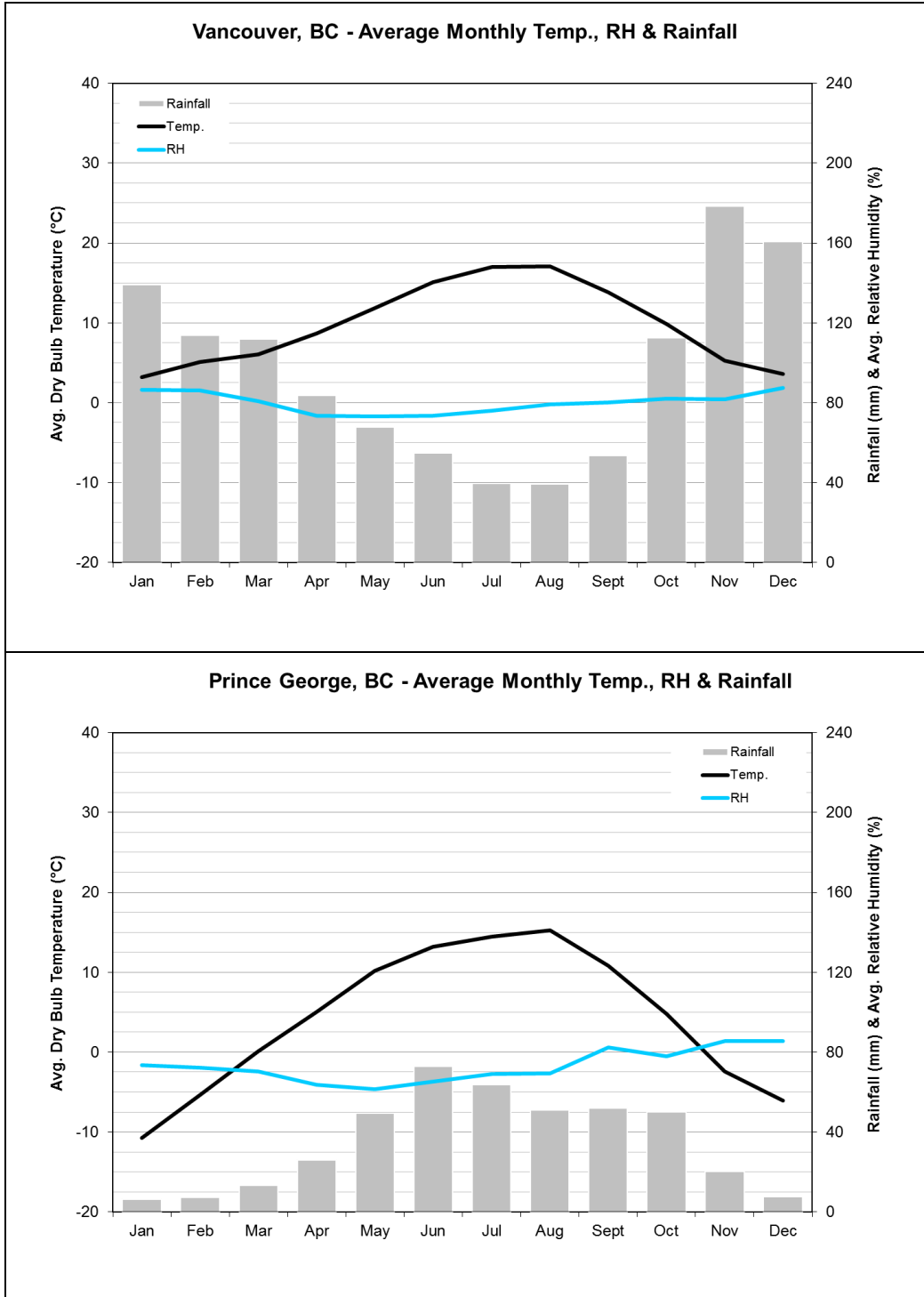
Hutcheon, N. B., & Jenkins, J. H. (1967). CBD-85 Some Basic Characteristics of Wood. In D. o. Research, *Canadian Building Digests.* Ottawa: Division of Building Research, National Research Council of Canada.

KLH. (2011). *KLH*. Retrieved September 9, 2011, from http://www.klh.at/en/kreuzlagenholz/verleimung.html

Kretschmann, D. E., Alden, H. A., & Verill, S. (1998). Variations of microfibril angle in loblolly pine: comparison of iodine crystallization and X-ray diffraction techniques. In B. Butterfield, *Microfibril angle in wood* (pp. 157-176). Canterbury, New-Zealand: University of Canterbury.

Krischer, O. (1963). *Die wissenschaftlichen Grundlagen der Trocknungstecknik.* Berlin, Germany: Springer Verlag.

Krus, M. (1995). *Feuchtetransport-und Speciherkoeffizienten poröser mineralischer Baustoffe. Theoretische Grundlagen und neuue Mebtechniken, Lehrstuhl Konstrktive Bauphysik.* Holzkirchen, Germany: Fraunhofer Institute for Building Physics.

Krus, M., & Künzel, H. M. (1993). Determination of Dw from A-value. *IEA Annex XXIV Report T3-d-93/02*.

Krus, M., & Künzel, H. M. (1995). Flüssigtransport im Übersättigungsbereich. *IBP-Mitteilung 22*, Nr. 270.

Krus, M., & Vik, T. A. (1999). Determination of Hygric Material Properties and Calculation of the Moisture Balance of Wooden Prisms. *Proceedings of the 5th Symposium Building Physics in the Nordic Coutnries* (pp. 313-320). Gotebord, Sweden: Chalmers University.

Künzel, H. M. (1995). *Simultaneous Heat and Moisture Transport in Building Components. One- and two-dimensional calculation using simple parameters.* Stuttgart, Germany: IRB Verlag.

LP Corp. (2011). *LP Corp*. Retrieved October 14, 2011, from www.lpcorp.com

Lstiburek, J. (2008, May 20). *BSI-001: The Perfect Wall.* Retrieved October 2, 2011, from Building Science Corp: http://www.buildingscience.com/documents/insights/bsi-001-the-perfect-wall

NBC. (2010). *National Building Code of Canada.* Ottawa: National Research Council of Canada.

Nordbord. (2011). *Norbord*. Retrieved October 14, 2011, from www.nordbord.com

OBC. (2006). Ontario Building Code. Queen's Printer for Ontario.

Panshin, A. J., & deZeeuw, C. (1980). *Textbook of wood technology, 4th ed.* New York: McGraw-Hill.

Raven, P. H., Evert, R. F., & Eichhorn, S. E. (2003). *Biology of Plants, 6th ed.* New York: WH Freeman and Company.

Sedblauer, K. (2004). *Predication of mould fungus formation on the surface of and inside building components, PHD Thesis.* Munich, Germany: Fraunhofer Institute for Building Physics.
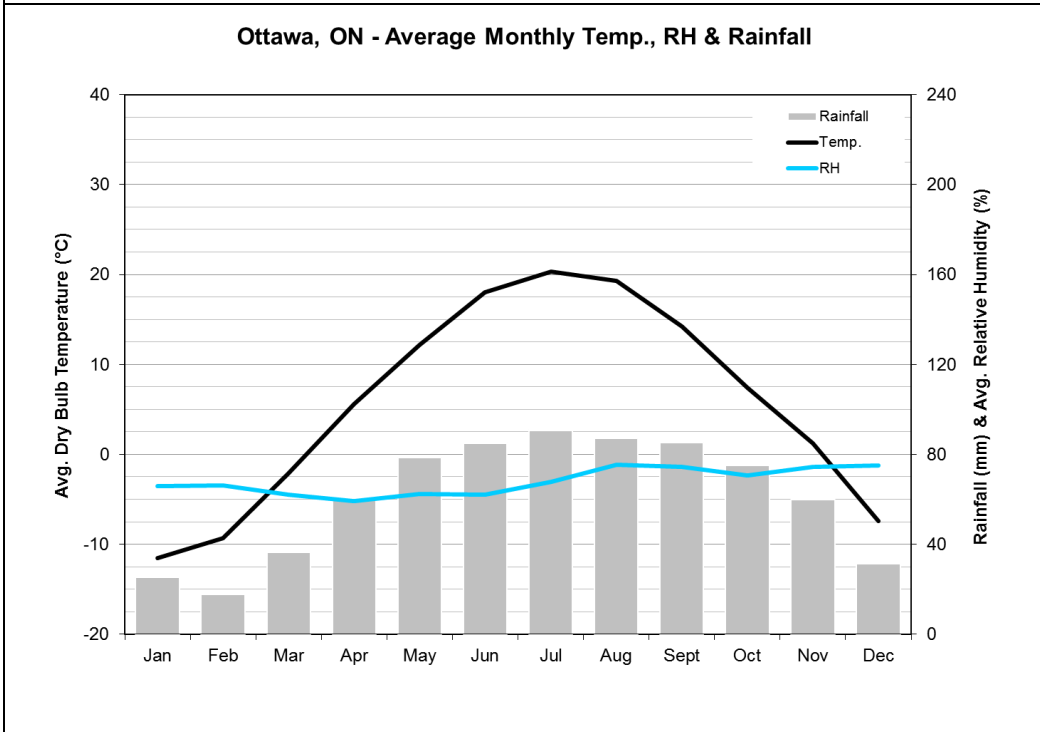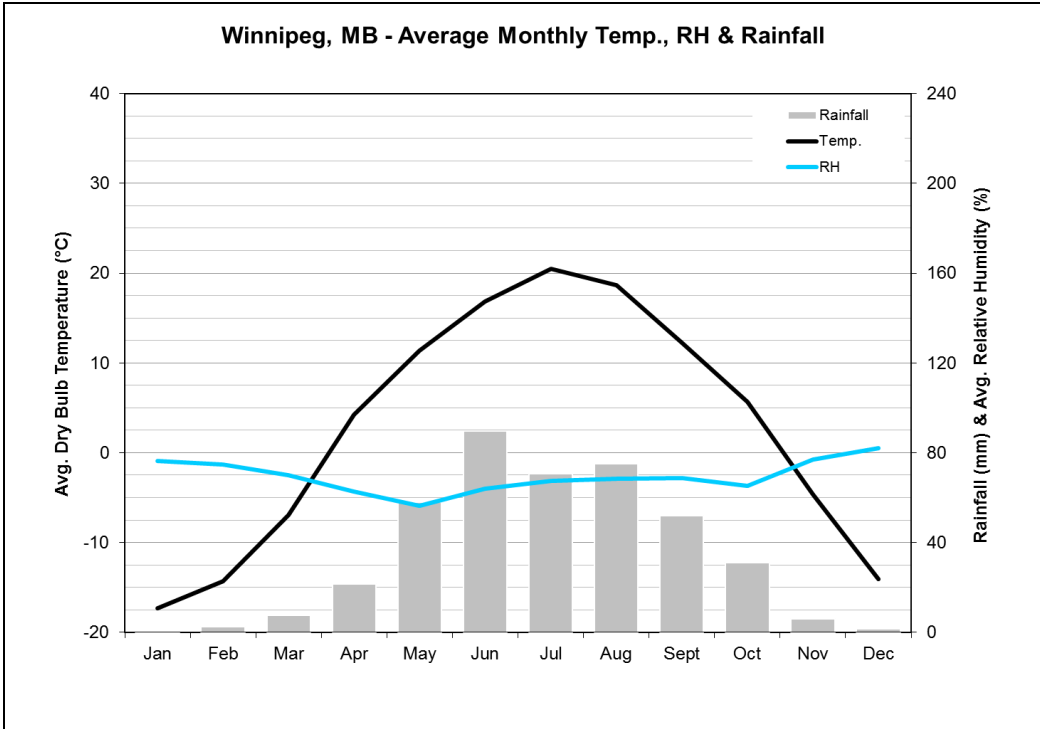
Setliff, E. C. (1986). *Wood Decay Hazard in Canada Based on Scheffer's Climate Index Formula.* Thunder Bay: The Forestry Chronicles.

Straube, J. F. (1998). *Moisture Control and Enclosure Wall Systems, Ph.D. Thesis.* Waterloo, Canada: University of Waterloo.

Straube, J. F., Onysko, D., & Schumacher, C. (2002). Methodology and Design of Field Experiments for Monitoring the Hygrothermal Performance of Wood Frame Enclosures. *Journal of Thermal Environment and Building Science, Vol 26, No. 2*, 123-151.

Straube, J., & Burnett, E. (2005). *Building Science for Building Enclosures.* Westford, Massachussets: Building Science Press Inc.

Viitanen, H. A., & Paajanen, L. (1988). *The critical moisture and temperature conditions for the growth of some mould fungi and the brown rot fungus Coniohora puteana on wood.* Stockholm, Sweden: International Research Group on Wood Preservation.

Wang, J. (2011, November 18). Personal Conversation.

Wang, J., Clark, J., Symons, P., & Morris, P. (2010). Time to Initiation of Decay in Plywood, OSB, and Solid Wood Under Critical Moisture Conditions. *International Conference on Building Envelope Systems and Technology.* Vancouver: ICBEST.

Waugh Thistleton. (2011). *Projects*. Retrieved 2011, from Waugh Thistleton Architects: http://www.waughthistleton.com/project.php?name=murray&img=4
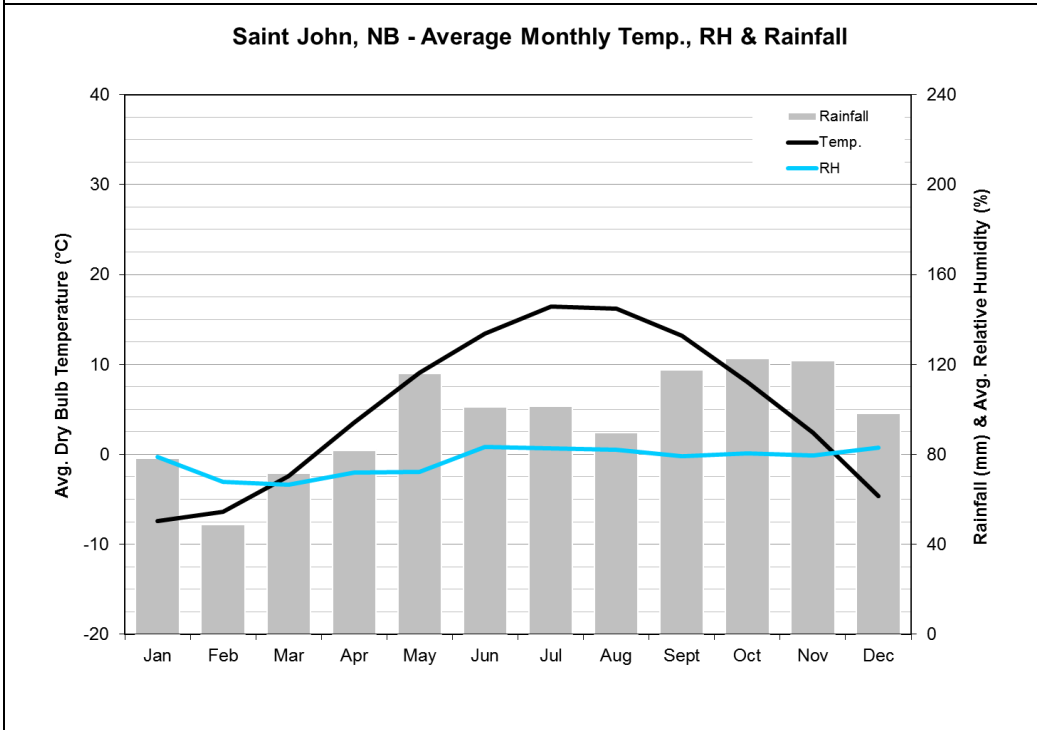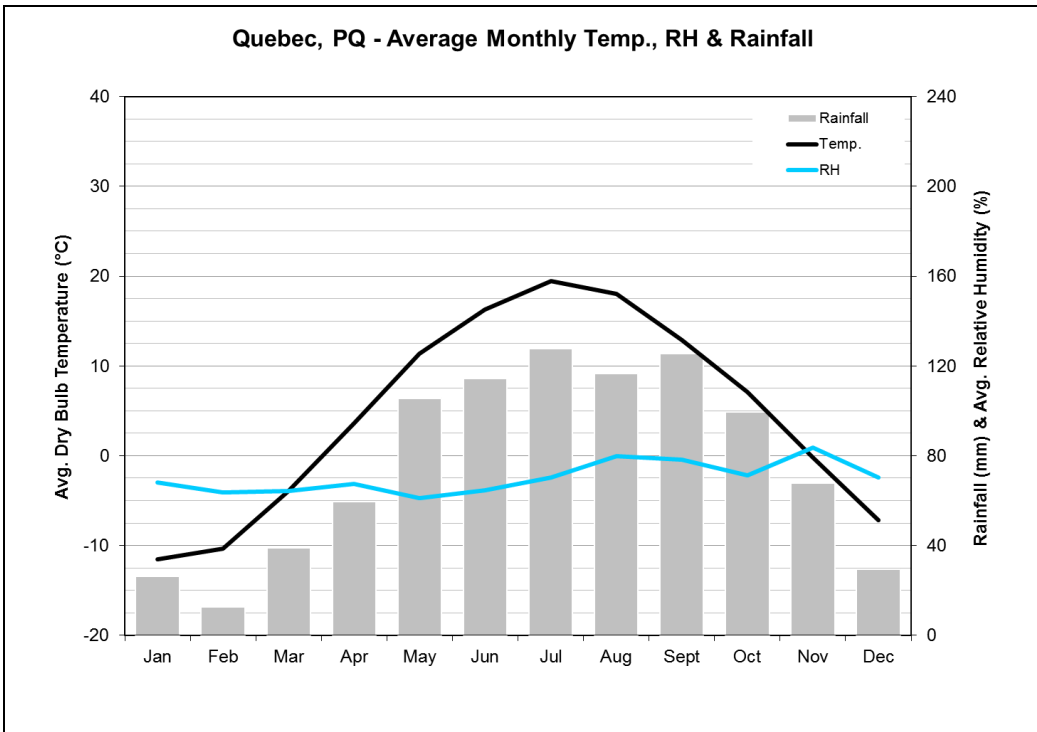
Appendix 1- Climatic Data

The following pages include the climatic data utilized in the hygrothermal simulations. The data is courtesy of Building Science Consulting, Inc.

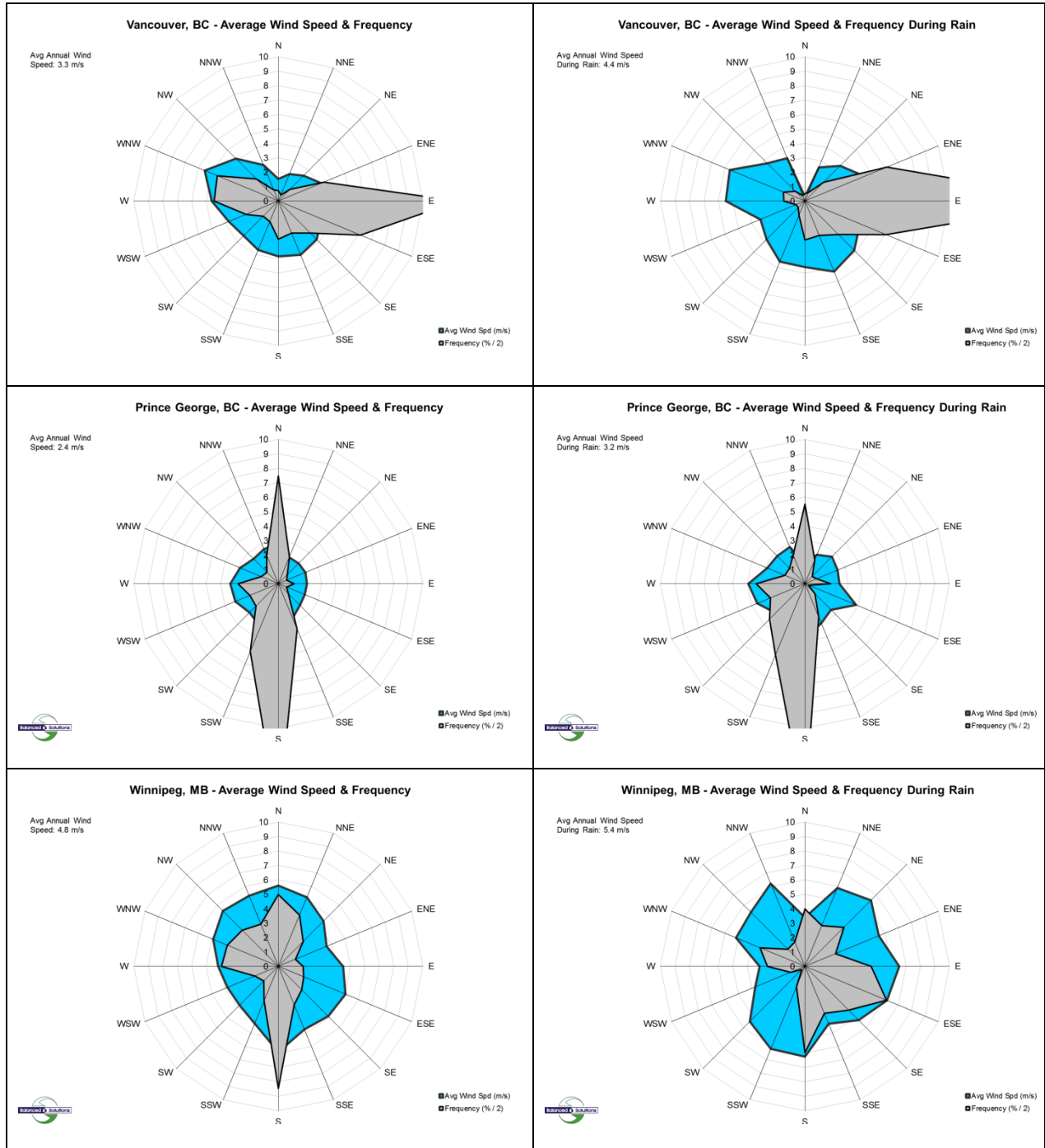**Monthly Average Temperature, RH, and Rainfall**

Winnipeg, MB - Average Monthly Temp., RH & Rainfall

Ottawa, ON - Average Monthly Temp., RH & Rainfall

Quebec, PQ - Average Monthly Temp., RH & Rainfall

Saint John, NB - Average Monthly Temp., RH & Rainfall
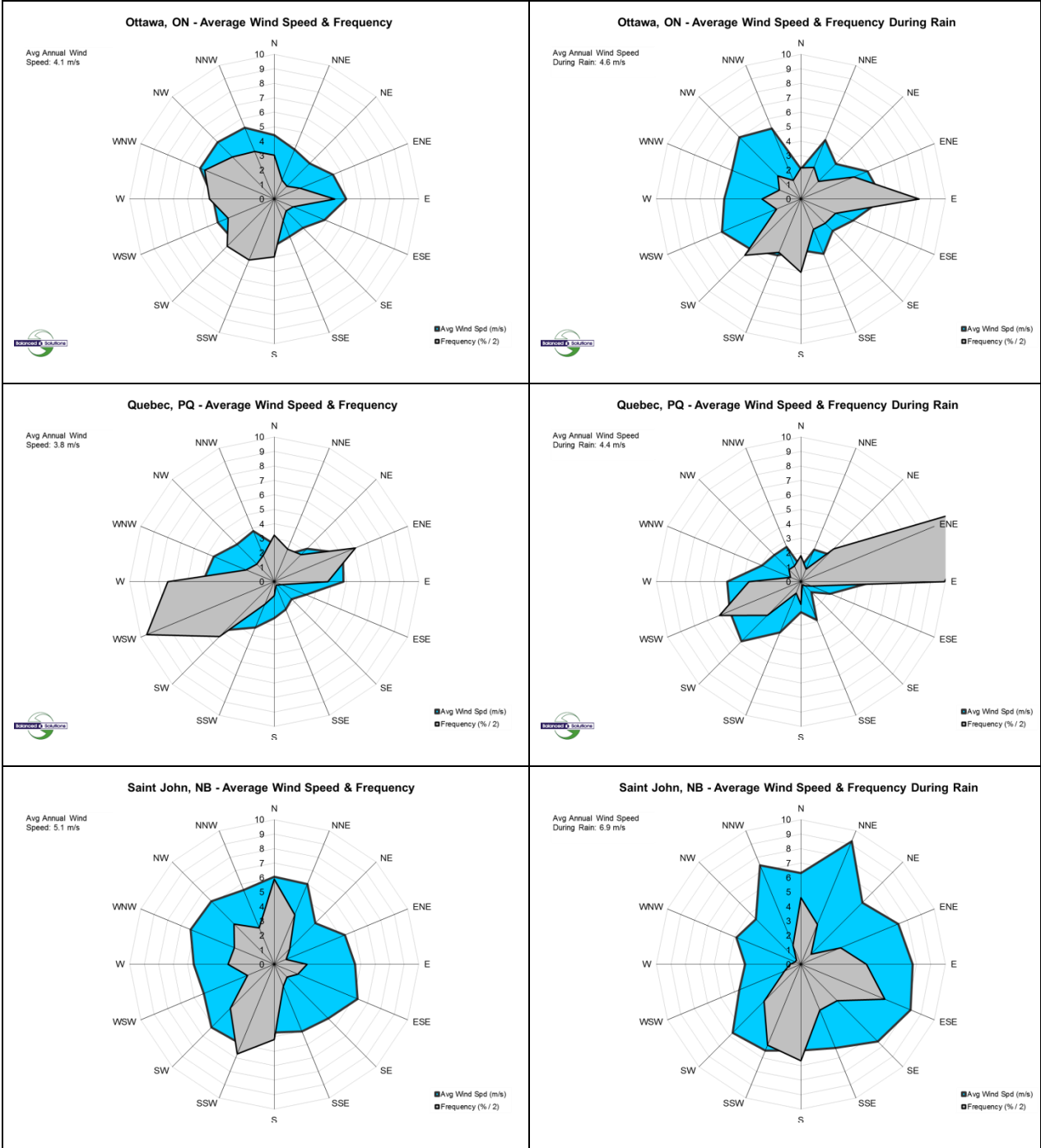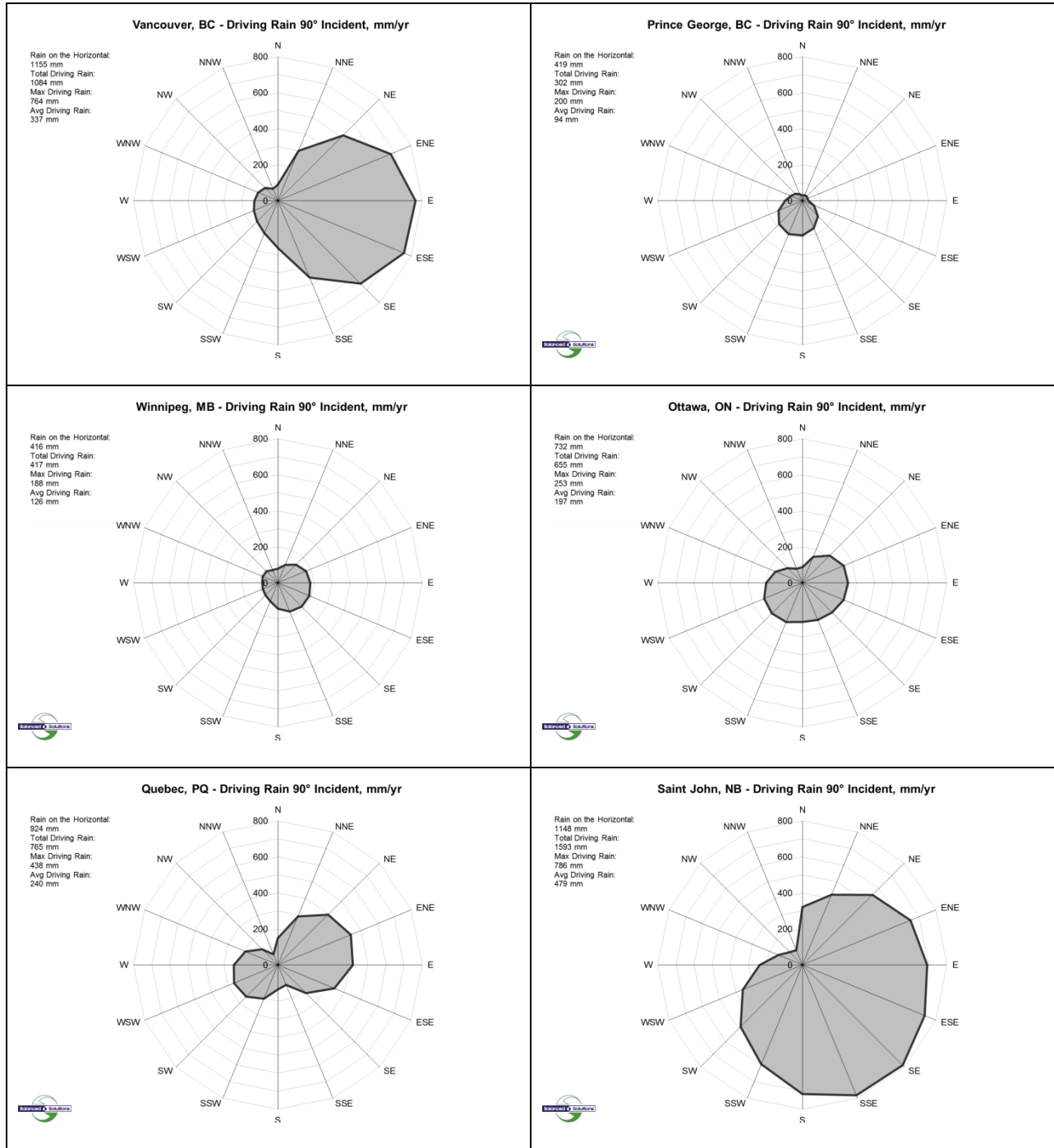
109

Wind Speed and Frequency With and Without Rain

Vancouver, BC - Average Wind Speed & Frequency

Vancouver, BC - Average Wind Speed & Frequency During Rain

Prince George, BC - Average Wind Speed & Frequency

Prince George, BC - Average Wind Speed & Frequency During Rain

Winnipeg, MB - Average Wind Speed & Frequency

Winnipeg, MB - Average Wind Speed & Frequency During Rain

Ottawa, ON - Average Wind Speed & Frequency

Avg Annual Wind Speed: 4.1 m/s

Ottawa, ON - Average Wind Speed & Frequency During Rain

Avg Annual Wind Speed During Rain: 4.6 m/s

Quebec, PQ - Average Wind Speed & Frequency

Avg Annual Wind Speed: 3.8 m/s

Quebec, PQ - Average Wind Speed & Frequency During Rain

Avg Annual Wind Speed During Rain: 4.4 m/s

Saint John, NB - Average Wind Speed & Frequency

Avg Annual Wind Speed: 5.1 m/s

Saint John, NB - Average Wind Speed & Frequency During Rain

Avg Annual Wind Speed During Rain: 6.9 m/s

111

Wind Driven Rain Rosette

Vancouver, BC - Driving Rain 90° Incident, mm/yr

Rain on the Horizontal:
1155 mm
Total Driving Rain:
1084 mm
Max Driving Rain:
764 mm
Avg Driving Rain:
337 mm

Prince George, BC - Driving Rain 90° Incident, mm/yr

Rain on the Horizontal:
419 mm
Total Driving Rain:
302 mm
Max Driving Rain:
200 mm
Avg Driving Rain:
94 mm

Winnipeg, MB - Driving Rain 90° Incident, mm/yr

Rain on the Horizontal:
416 mm
Total Driving Rain:
417 mm
Max Driving Rain:
188 mm
Avg Driving Rain:
126 mm

Ottawa, ON - Driving Rain 90° Incident, mm/yr

Rain on the Horizontal:
732 mm
Total Driving Rain:
655 mm
Max Driving Rain:
253 mm
Avg Driving Rain:
197 mm

Quebec, PQ - Driving Rain 90° Incident, mm/yr

Rain on the Horizontal:
924 mm
Total Driving Rain:
765 mm
Max Driving Rain:
438 mm
Avg Driving Rain:
240 mm

Saint John, NB - Driving Rain 90° Incident, mm/yr

Rain on the Horizontal:
1148 mm
Total Driving Rain:
1593 mm
Max Driving Rain:
786 mm
Avg Driving Rain:
479 mm

Solar Irradiance

Vancouver, BC - Monthly Total Incident Solar Radiation

Prince George, BC - Monthly Total Incident Solar Radiation

113

Winnipeg, MB - Monthly Total Incident Solar Radiation

Ottawa, ON - Monthly Total Incident Solar Radiation

114

Quebec, PQ - Monthly Total Incident Solar Radiation

Saint John, NB - Monthly Total Incident Solar Radiation

115

Appendix 2- Preliminary CLT Water Uptake Test Results

CLT Samples H1, H3, W1, and W2

The first series of testing was conducted on samples H1, H3, W1, and W2. However, the testing for these samples experienced numerous problems- only 3 data points were collected on the water uptake, some of the scales jammed during testing, data loss occurred for some periods of time, and significant jumping occurred when the counterweight mass was changed. The mass gain and loss from the first series of tests may be found in the following figure. Unfortunately, due to limited number of data points, the A-value could not be properly obtained for these samples.
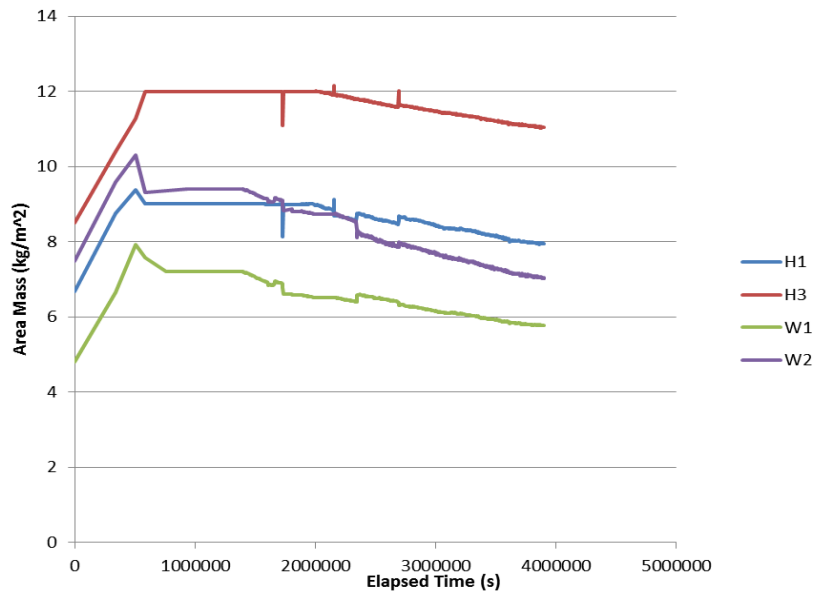
The following series of tests improved upon the mistakes and errors discovered in the first round. The code for the data logger was modified such that gaps in the data did not occur due to overflow, the counterweights were set such that no changes would be required (or such that it only occurs once during the mass loss), data was collected much more frequently during water uptake, and the scales were checked to ensure that the bearing joint did not get stuck.
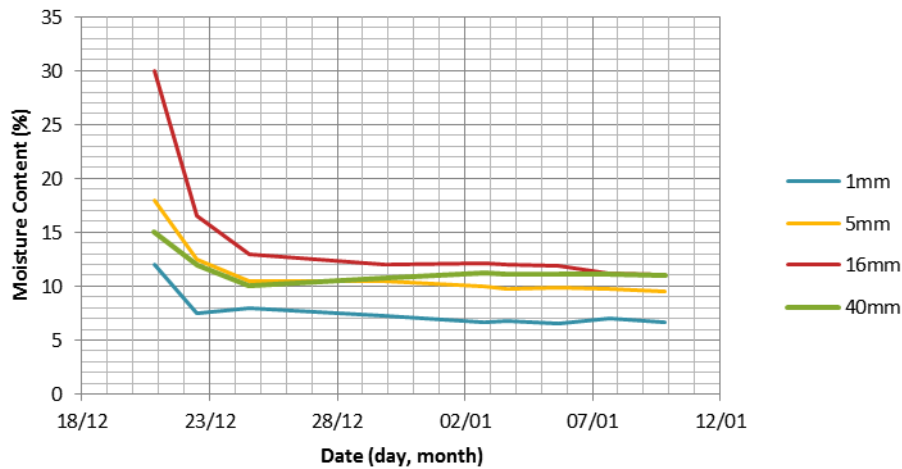
Appendix 3- CLT Testing- Moisture Profiles

This section includes the moisture profile plots collected by the moisture content pins installed at depths through the CLT panels that were not included in the body of the thesis. The plots for CLT Samples W1, H1, H3, Er1, and Er3 follow.
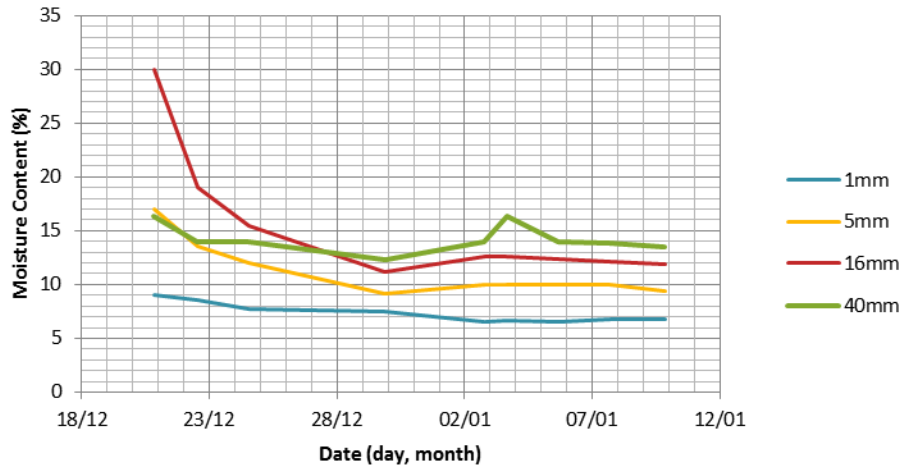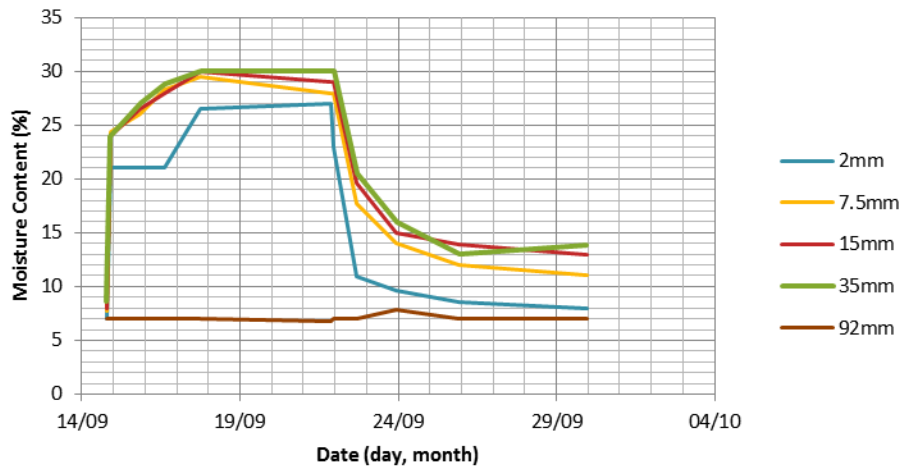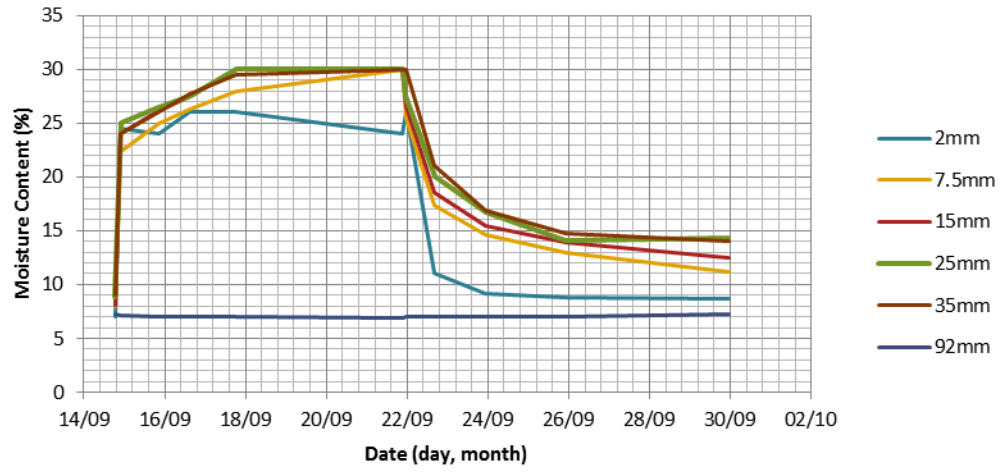
MC Profile: W1
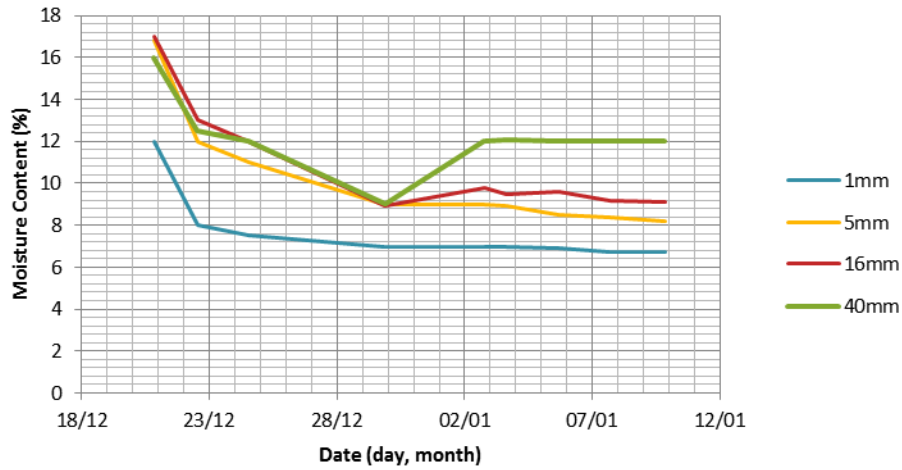
MC Profile: H1

MC Profile: H3

MC Profile: Er1

120

MC Profile: Er2

Legend: 2mm, 7.5mm, 15mm, 25mm, 35mm, 92mm

Appendix 4- Simulation Results- Construction Moisture

This section contains the plots for the total construction water content loss for the NRPAN, SNIBY, and Environment wall assembly series for the remaining 4 climates.